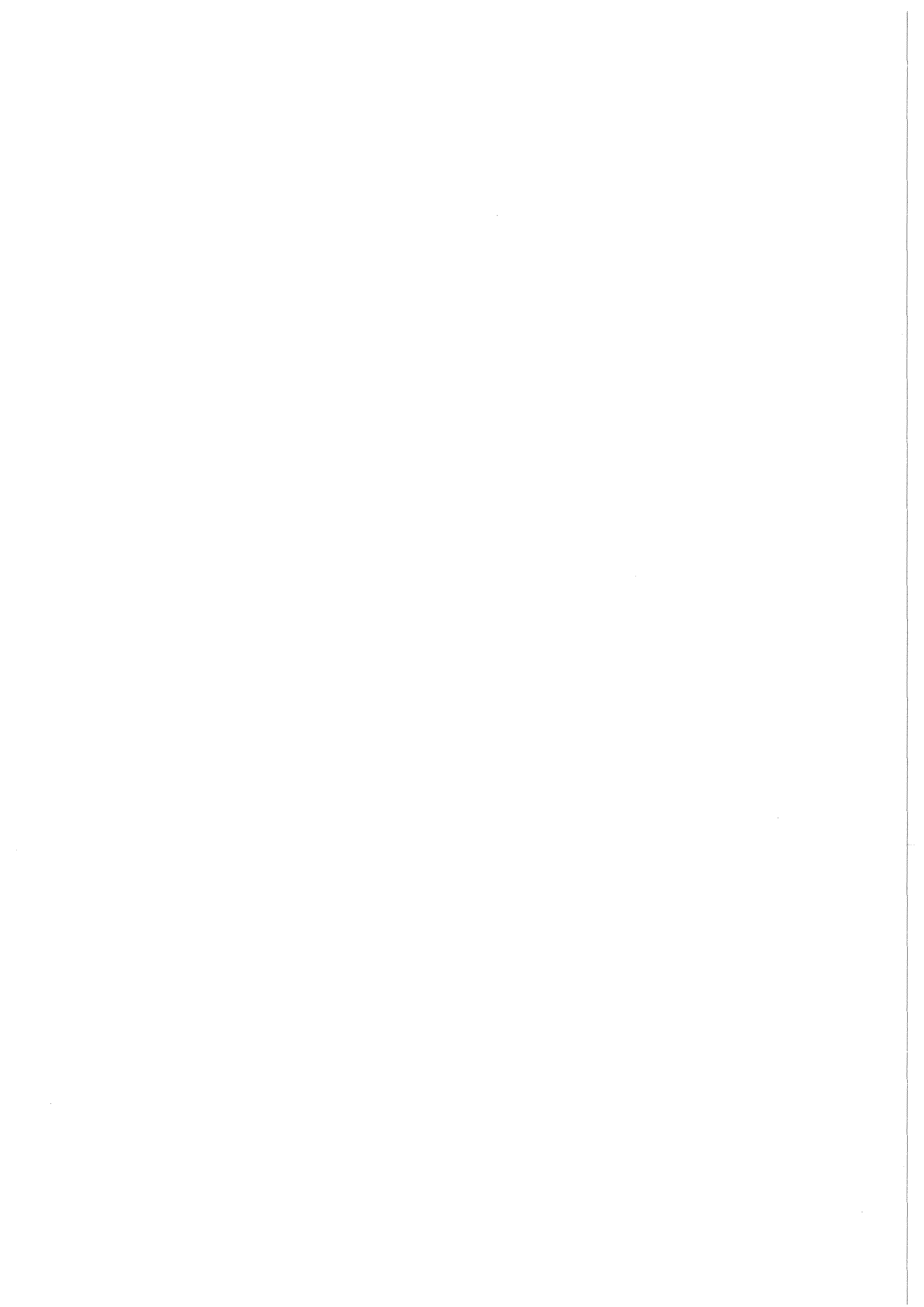# The Charged Particle Transport Module CIRCE as Part of the KATACO Code System

K. Küfner, J. Ligou, T. M. Tran

Institut für Neutronenphysik und Reaktortechnik

Kernforschungszentrum Karlsruhe

KERNFORSCHUNGSZENTRUM KARSLRUHE
Institut für Neutronenphysik und Reaktortechnik

KfK 4581

THE CHARGED PARTICLE TRANSPORT MODULE CIRCE
AS PART OF THE KATACO CODE SYSTEM

K.Küfner, J.Ligou[1], T.M.Tran[1]

[1] Laboratoire de Génie Atomique,École Polytechnique Fédérale de Lausanne

i

Abstract

The CIRCE code solves the time dependent slowing down of suprathermal ions in a one dimensional (spherical or plane) medium. This module has been coupled to the one dimensional plasma hydrodynamics code MEDUSA-KA in the frame of the KATACO code system. The energy deposition (to plasma ions and electrons) is calculated by CIRCE using a given hydro state provided by MEDUSA-KA. These deposition profiles are then used in MEDUSA-KA to replace the local deposition approximation used so far in the standard version. This report describes the CIRCE code and the coupling procedure between MEDUSA-KA and CIRCE. The last chapter contains a comparison between the Fokker-Planck equation used in CIRCE and the time dependent particle tracking method for the burn phase of a HIBALL target.

MODELLIERUNG DES TRANSPORTS GELADENER TEILCHEN MIT DEM MODUL CIRCE ALS TEIL DES KATACO CODESYSTEMS

Zusammenfassung

CIRCE löst die zeitabhängige Transportgleichung, die das Abbremsen suprathermischer Ionen in einem eindimensionalen (sphärische oder ebene Geometrie) Plasma beschreibt. Dieser Modul wurde mit dem eindimensionalen Hydrodynamik Programm MEDUSA-KA im Rahmen des Programmsystems KATACO gekoppelt. Die Energiedeposition (für die Plasma-Ionen und -Elektronen) wird von CIRCE berechnet auf der Grundlage des von MEDUSA-KA berechneten hydrodynamischen Zustandes des Plasmas. Diese Depositionsprofile werden dann in MEDUSA-KA benutzt um die bisher in der Standardversion verwendeten lokalen Energiedepositionsprofile zu ersetzen. Dieser Bericht beschreibt das Programm CIRCE und die Koppelungsprozedur zwischen MEDUSA-KA und CIRCE. Das letzte Kapitel vergleicht die in CIRCE benutzte Fokker-Planck Gleichung und die zeitabhängige sogen. 'particle tracking' Methode für die Abbrandphase eines HIBALL Targets.
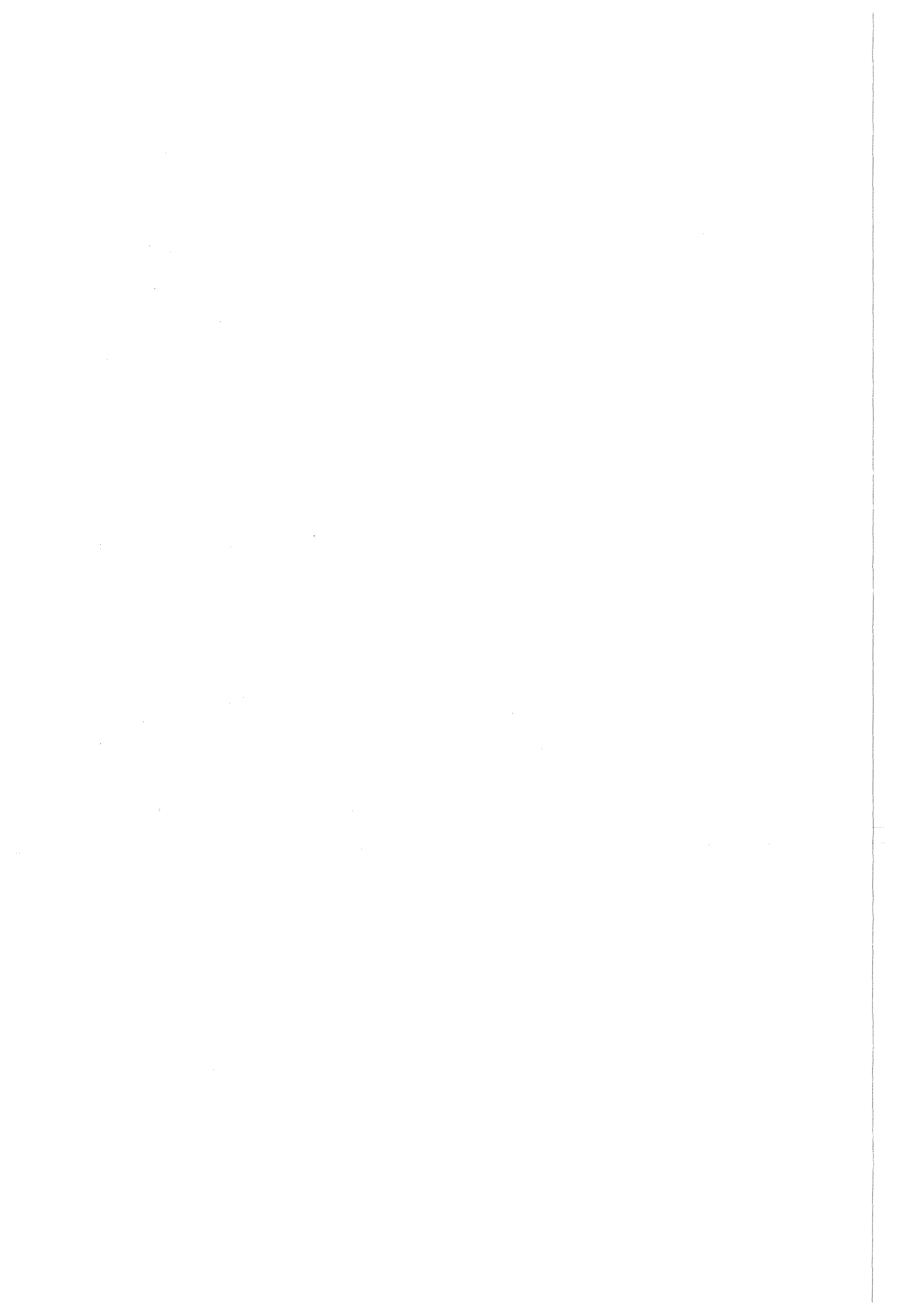
Table of Contents

List of Illustrations

List of Tables

PART A : Description of the Method

Chapter 1. Introduction

At the Nuclear Research Center Karlsruhe, the KATACO /1/ code system is used to simulate the compression and burn phase of ICF targets for ion beam drivers. It contains the one-dimensional, two temperature, Lagrangian hydrodynamics code MEDUSA-KA based on the MEDUSA-1 code /2/ developed originally at Culham Laboratory, England and improved at KFK.

In its standard version, MEDUSA-KA assumes local energy deposition of fusion generated charged particles, i.e., they deposit their energy instantaneously at the place of their birth. This approach neglects both, time and space dependence of the energy deposition process, thus overemphasizing the self-heating of the fuel.

A more accurate treatment of suprathermal charged particle transport and thermalization may be based on the time dependent Fokker-Planck equation /3/ in one-dimensional Lagrangian form. Recently, the CIRCE code /4/ has been developed by T.M.Tran and J.Ligou to solve this equation. This report describes how CIRCE has been coupled to MEDUSA-KA. and implemented in the KATACO code system.

In the following, only α-particle transport is described, though the code may also be used for the transport of other types of charged particles or the energy deposition of an incoming ion beam. "Chapter 2. Accurate Charged Particle Transport Equation" describes the Fokker-Planck formalism and the collision coefficients used. The next chapter deals with the numerical solution scheme. This is followed by a chapter on coding details, containing also the coupling procedure between CIRCE and KATACO. An input description is provided in "Chapter 5. Input Description and User Information" . Then we show effects of α-particle transport on the burn process found in recalculations of a 4 mg HIBALL target /5/ and estimate the influence of an adiabatic approximation to charged particle transport. The last chapter deals with a comparison between the CIRCE solution method and the time dependent particle tracking method /6/ .

Chapter 2. Accurate Charged Particle Transport Equation

2.1 Fokker-Planck Equation for Charged Particles

Slowing down of fast ions in an ICF plasma can be modeled with good accuracy by the linear time dependent Fokker-Planck equation which takes account of continuous slowing down and angular diffusion mechanisms /3/ . In the following it is assumed that the direction of the particles is defined by only one variable, μ, the deflection cosine. This means, in practice, that only 1d geometries with an axis of symmetry are considered (slab and sphere). The equation for the angular flux ψ of charged particles then can be written /4/ as:

$$\frac{1}{qV} D_t (V\psi) + \vec{\Omega} \cdot \nabla \psi \;=\; \frac{\partial}{\partial E} (S + F)\psi + T D_\mu \psi + \frac{\partial}{\partial \mu} (1 - \mu^2) G \psi + Q \qquad [1]$$

$$\text{where}\quad D_\mu \;:\; = \; \frac{\partial}{\partial \mu}(1 - \mu^2)\frac{\partial}{\partial \mu} \quad\text{and}\quad D_t \;:\; = \; \frac{\partial}{\partial t} + \vec{u} \cdot \nabla \qquad [2]$$

with initial and boundary conditions:

$$\psi(r, \mu, E, 0) = \psi_0(r, \mu, E) \qquad [3]$$

$$\psi(R_{outer}, \mu, E, t) = f_{right}(\mu, E, t) \quad \text{if} \quad \mu < 0 \,,\, E_c < E < E_0 \qquad [4]$$

$$\psi(r, \mu, E, t) = 0 \quad \text{if} \quad E < E_c \;\text{or}\; E > E_0 \qquad [5]$$

$$\psi(R_{inner}, \mu, E, t) = f_{left}(\mu, E, t) \quad \text{if} \quad \mu > 0 \qquad [6]$$

where symbols are introduced as :

$\psi = \psi(r,\mu,E,t)$	angular flux of suprathermal (test) particles;
$Q = Q(r,\mu,E,t)$	spectral density of the particle source;
$S = S(r,E,t)$	stopping power coefficient;
$T = T(r,E,t)$	deflection coefficient due to ion-ion collisions;
$F = F(r,\mu,E,t)$	stopping power-like inertia coefficient arising as a consequence of the Lagrangian formulation;
$G = G(r,\mu,E,t)$	deflection-like inertia coefficient arising as a consequence of the Lagrangian formulation;
$V = V(r,t)$	plasma specific volume;
$q = q(r,t)$	$= \mid v(r,t) - u(r,t) \mid$ the relative velocity of the test particles, v and u being the velocity of the test particles and the drift velocity of the plasma, respectively;
$E = 1/2\, m\, q^2$	particle energy, m being the mass of the particle;
$\vec{\Omega}$	solid angle;
μ	the corresponding direction cosine in 1d geometry
r	the Lagrangian space coordinate;

The ranges of the variables r, μ, E, t are:

$$t > 0$$
$$R_{inner}(t) \leq r \leq R_{outer}(t)$$
$$-1 \leq \mu \leq +1$$
$$E_c \leq E \leq E_0$$

where R_{inner} and R_{outer} represent the coordinates of the inner and outer boundaries of the medium, while E_c and E_0 are minimum and maximum energy of the fast ion, respectively. E_c is representative for the energy of the thermal plasma.

The user-supplied function f_{right} in Eq. [4] may characterize an energy and angular distribution of an ion beam penetrating the plasma at its outer boundary. If there is no beam acting there, $f_{right} = 0$ (vacuum condition) is assumed in CIRCE. For Eq. [6] the function f_{left} is used differently for slabs and spheres. In slab geometry, $f_{left} = 0$ (vacuum condition) is assumed. In spherical geometry, $f_{left}(\mu,E,t) = \psi(R_{inner},-\mu,E,t)$. For $R_{inner} = 0$, this means that the net current is equal to zero; in the case of a hollow spherical plasma ($R_{inner} > 0$), we have void in the inner region.

The streaming term $\vec{\Omega} \cdot \nabla \psi$ has the explicit form (g = 1 for slab and g = 3 for spherical geometry; note that cylindrical geometry is not handled since it would require treatment of two angular variables):

$$\vec{\Omega} \cdot \nabla \psi = \frac{\mu}{r^{g-1}} \frac{\partial}{\partial r}(r^{g-1}\psi) + \frac{g-1}{r} \frac{\partial}{\partial \mu}((1-\mu^2)\psi) \qquad [7]$$

2.2 Calculation of Physical Coefficients

2.2.1 Collision Coefficients S and T

Stopping power is split into electronic and ionic part using averaged ion mass, ion charge and ion density defined by

$$m_{ion} = \sum_j m_k \frac{n_k}{n_{ion}} \quad , \quad m_{elec} = 0.9109534E - 30$$

$$Z_{ion} = \sum_j Z_k \frac{n_k}{n_{ion}} \quad , \quad Z_{elec} = -1.0$$

$$n_{ion} = \sum_j n_k \quad , \quad n_{elec} = n_{ion}$$

where all summations are taken over all ion species (excluding the electron contribution). Only θ_{ion} (ion temperature), θ_{elec} (electron temperature), ρ (mass density), m_{ion} (average ion mass), Z_{ion} (average ion charge) and n_{ion} (average ion mass number) as calculated by KATACO are used to calculate S and T in CIRCE. In the present version, the stopping power term, S, and the deflection term, T, are calculated in CIRCE using the asumption that the host medium is fully ionized and consists of a charge neutral mixture of electrons and ions and the particles to be transported are slowed down by coulomb interactions. If in a particular application these assumptions are not true, the corresponding subroutine (SIGMA1) has to be replaced by a new version which includes other effects (e.g., partially ionized

medium or collective interactions). The details of the derivation of the formulas used for these coefficients may be found in references /7/ and /4/ . Here we only summarize the formulas.

$$S_k = 2\pi Z^2 Z_k^2 e^4 n_k \frac{L_k}{\theta_k} \frac{g(y_k)}{y_k^2}$$ [8]

$$T_k = \frac{\pi}{2} Z^2 Z_k^2 e^4 \frac{m_k}{m} n_k \frac{L_k}{\theta_k} \frac{h(y_k)}{y_k^2} \frac{1}{E}$$ [9]

m_k , Z_k, θ_k and n_k are mass, charge number, temperature (in keV) and volume density of ions and electrons, respectively. m, Z and E are mass, charge number and kinetic energy (in keV) of the particle to be transported. $e^2 = 1.44E\text{-}10$ keVcm is the electron charge. The remaining terms are defined as follows:

$$y_k^2 = \frac{m_k}{m} \frac{E}{\theta_k}$$ [10]

$$g(y) = erf(y) - \frac{2}{\sqrt{\pi}} y e^{-y^2}$$ [11]

$$h(y) = (1 - \frac{1}{2y^2})g(y) + \frac{2}{\sqrt{\pi}} y e^{-y^2}$$ [12]

$$L_k = \frac{\ln(1 + \Lambda_k^2)}{2} \quad , \quad \Lambda_k = \frac{\lambda_D}{p_k}$$ [13]

$$\lambda_D^2 = 4\pi e^2 n_k \frac{Z_k^2}{\theta_k} \qquad (Debye\ length) \quad [14]$$

$$p_k = \frac{|Z_k|Ze^2}{\mu_k u_k^2} \qquad [15]$$

$$\mu_k = \frac{m_k m}{m_k + m} \qquad (reduced\ mass) \quad [16]$$

$$u_k^2 = \frac{3\theta_k}{m_k} + 2\frac{E}{m} \qquad (relative\ velocity) \quad [17]$$

2.2.2 Inertia Coefficients F and G

CIRCE is intended to be coupled with Lagrangian hydro codes. Therefore, the transport equation has to be written for a moving host medium. As shown in /8/, two additional coefficients show up then in Eq. [1] , a pseudo stopping power, F, and a pseudo deflection coefficient, G. They have the following analytic form:

$$F = m\mu \ (D_t u + \mu q \frac{\partial}{\partial r} u) \qquad (slab) \quad [18]$$

$$F = m\mu \ (D_t u + \mu q \frac{\partial}{\partial r} u) + m \frac{u}{r} q(1 - \mu^2) \qquad\qquad (sphere) \quad [19]$$

$$G = \frac{m}{2E} \ (D_t u + \mu q \frac{\partial}{\partial r} u) \qquad\qquad (slab) \quad [20]$$

$$G = \frac{m}{2E} \ (D_t u + \mu q(\frac{\partial}{\partial r} u - \frac{u}{r})) \qquad\qquad (sphere) \quad [21]$$

In addition to the hydro variables needed in Eq. [1] , Eq. [8] and Eq. [9] , the derivatives $D_t u$, $\frac{\partial}{\partial r} u$ of plasma velocity and the term $\frac{u}{r}$ are needed in Eq. [18 - 21] and have to be calculated before calling CIRCE.

2.3   Calculation of Energy Deposition

Once the angular flux $\psi(r,\mu,E,t)$ has been obtained by solving Eq. [1] , it is easy to calculate the energy deposited to electrons and ions during the slowing down of charged particles:

$$E_{elec}(r,t) \ = \ \int_{E_c}^{E_0} S_{elec}(r,E',t) \ \phi(r,E',t) \ E' \ dE' + E_c \ P_{elec}(r,t)$$

$$[22]$$

$$E_{ion}(r,t) \ = \ \int_{E_c}^{E_0} S_{ion}(r,E',t) \ \phi(r,E',t) \ E' \ dE' + E_c \ P_{ion}(r,t)$$

where

$$\phi(r,E,\ t) = \int_{-1}^{+1} \psi(r,\ \mu',E,t)d\mu' \qquad\qquad [23]$$

$$P(r,t) = S(r,\ E_c,t)\phi(r,\ E_c,t) \qquad\qquad [24]$$

E_{elec} and E_{ion} represent the energy deposited to electrons and ions, respectively, of the host medium per unit time and unit volume (for the definition of E_c and E_0 see "Fokker-Planck Equation for Charged Particles" on page 5).

Defining the quantities E_{supra} (suprathermal energy), E_{leak} (leaking energy), E_{input} (input energy) and E_{inert} (inertia term) as :

8

$$E_{supra}(r,t) = \frac{\partial}{\partial t} \int_{E_c}^{E_0} \frac{\phi(r,E,t)}{v} \, dE'$$

$$E_{leak}(r,t) = \frac{1}{r^{g-1}} \frac{\partial}{\partial r} \int_{E_c}^{E_0} \int_{-1}^{+1} \mu' \psi(r,mu', E',t) \, d\mu' \, dE'$$

$$E_{input}(r,t) = \int_{E_c}^{E_0} \int_{-1}^{+1} Q(r,mu', E',t) \, d\mu' \, dE'$$

$$E_{inert}(r,t) = \int_{E_c}^{E_0} \int_{-1}^{+1} F(r, \mu', E',t)\psi(r, \mu', E',t) \, d\mu' \, dE' + E_c \int_{-1}^{+1} F(r, \mu', E_c,t)\psi(r, \mu', E_c,t) \, d\mu'$$

[25]

the energy balance equation for each mesh cell is given by

$$E_{supra}(r,t) + E_{leak}(r,t) + E_{ion}(r,t) + E_{elec}(r,t) + E_{inert}(r,t) = E_{input}(r,t)$$

[26]

Integrating over the spatial domain a global balance useful for checking the accuracy of the soultion is obtained.

2.4 Simplifiying Approximations to Fokker-Planck Equation

Some simplified approximations can be obtained from Eq. [1] by dropping different terms.

Setting the time derivative term to zero one obtains the "adiabatic" equation. This means that suprathermal particles slow down completely within each hydro time step.

Neglecting the inertia terms, F and G, the equation is considerably simplified (even for the numerical treatment). This amounts to neglecting the motion of the host medium.

The time dependent particle tracking equation, described in /6/ is obtained by setting to zero the coefficients T, F and G in Eq. [1]. This amounts to neglecting the motion of the host medium and the angular diffusion.

In "Chapter 6. Effects of α-Particle Transport" on page 33 and "Chapter 7. Time Dependent Particle Tracking" on page 39 the effects of these simplifications are studied in more detail.
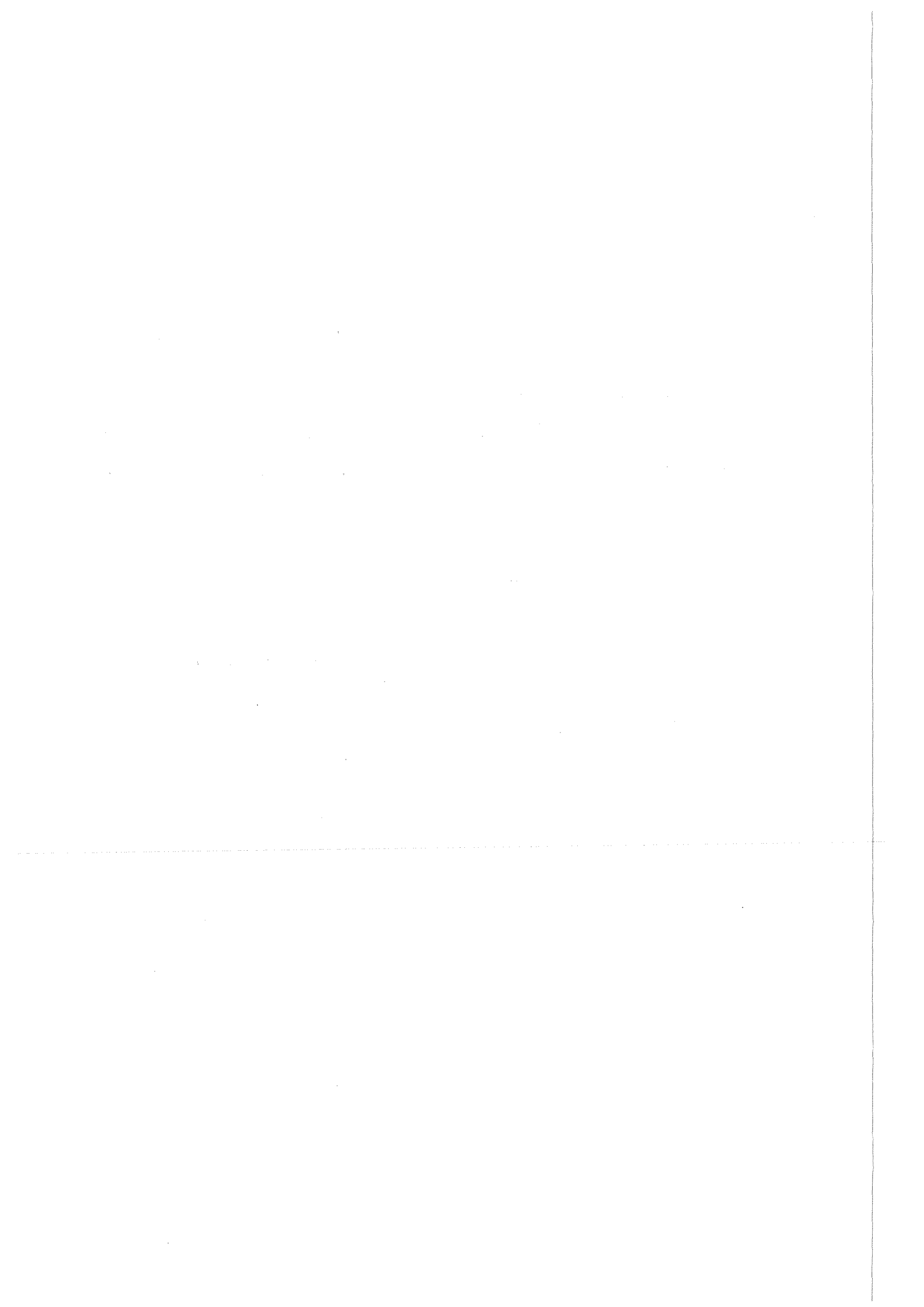
Chapter 3. Numerical Solution Scheme of CIRCE

The following convention is used for subscripts in this chapter: index i (MX1≤i≤MX2) refers to the space variable, index k (1≤k≤MDIR) to the angular variable and index j (1≤j≤MNG) to the energy variable. Unlike the other variables, energy is indexed from the highest (E_0) to the lowest (E_c) energy. Superscript n is used to distinguish between different time levels. In the remainder of this chapter, noncentered subscripts will be dropped for brevity except when a particular coordinate dependence is to be emphasized. However, it is to be understood that, in general, the quantities depend upon the full range of subscripts. ψ is the spectral density of the angular flux.

3.1 Time Discretization

Given two time levels t^{n-1} and t^n ($t^n = t^{n-1} + \Delta t^n$), Eq. [1] is discretized in the following, fully implicit, way:

$$\frac{1}{q\Delta t}\,\psi^n + \vec{\Omega} \cdot \nabla\psi^n = \frac{1}{q\Delta t}\,\frac{V^{n-1}}{V^n}\,\psi^{n-1} + \frac{\partial}{\partial E}\,(S^n + F^n)\psi^n$$
$$+ T_k^n D_\mu \psi^n + \frac{\partial}{\partial \mu}\,(1 - \mu^2)G^n \psi^n + Q^n \qquad [27]$$

The discussion of the inertia terms, $\dfrac{\partial}{\partial E}\,F\psi$ and $\dfrac{\partial}{\partial \mu}\,(1 - \mu^2)G\psi$, will be postponed until "Discretization of Inertia Terms" on page 14 for simplicity.

3.2 Angular Discretization

The angular variable is treated by the conventional Discrete Ordinate Method. The angular mesh is chosen according to Figure 1 on page 12 to be equidistant, leading to integration weights $w_k = \Delta\mu_k$. To apply the Discrete Ordinate scheme, we evaluate Eq. [1] at the points μ_k. The angular derivative term $\dfrac{\partial}{\partial\mu}(1 - \mu^2)\psi$ is replaced by

$$\frac{\partial}{\partial \mu}\,(1 - \mu^2)\psi_{|\mu = \mu_{k+\frac{1}{2}}} = \frac{2}{w_k}\,(a_{k+\frac{1}{2}}\,\psi_{k+\frac{1}{2}} - a_{k-\frac{1}{2}}\,\psi_{k-\frac{1}{2}}) \qquad [28]$$

The coefficients a are determined by the requirement that Eq. [28] should be exact whenever $\dfrac{\partial}{\partial\mu}\psi = 0$. This criteria leads to the recurrence relation

$$a_{k+\frac{1}{2}} = a_{k-\frac{1}{2}} - \mu_k w_k \qquad k = 1, \dots, MDIR \qquad [29]$$

$a_{\frac{1}{2}} = 0$ is then used as a starting value for the recurrence Eq. [29.] One may show that if M is an even number than this yields $a_{M+\frac{1}{2}} = 0$.
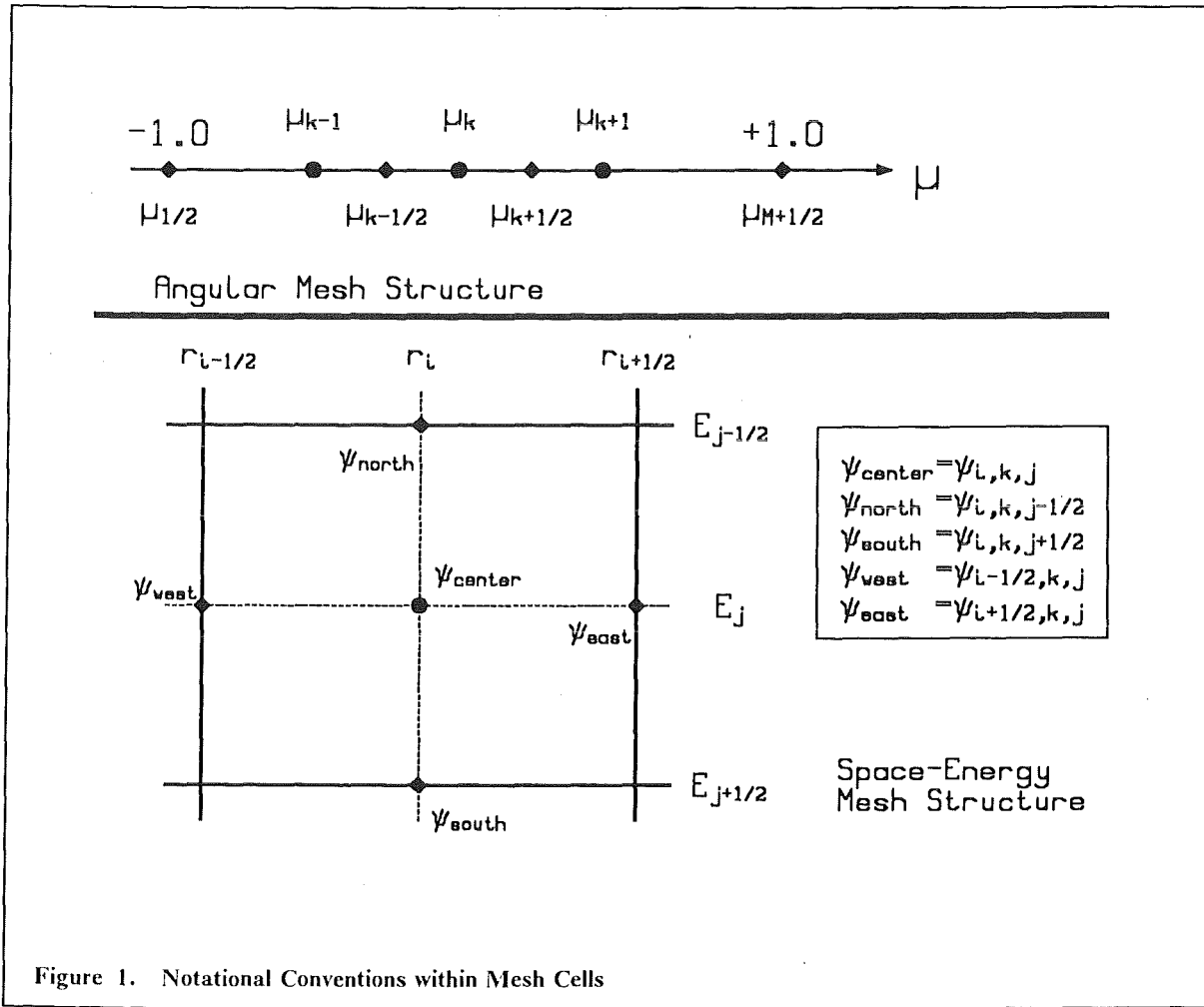
Figure 1. Notational Conventions within Mesh Cells

The operator D_μ of Eq. [2] is evaluated at $\mu_{k+\frac{1}{2}}$ using Eq. [28] and then replacing $\frac{\partial}{\partial \mu} \psi_{k \pm \frac{1}{2}}$ by central differences This leads to the discrete formulation

$$\frac{\partial}{\partial \mu} \psi_{|\mu = \mu_{k+\frac{1}{2}}} = T_k^n \frac{2}{w_k} (a_{k+\frac{1}{2}} \frac{\psi_{k+1}^n - \psi_k^n}{\mu_{k+1} - \mu_k} - a_{k-\frac{1}{2}} \frac{\psi_k^n - \psi_{k-1}^n}{\mu_k - \mu_{k-1}})$$
[30]

Taken together, Eq. [27] now has the following semidiscrete form :

$$\frac{1}{q\Delta t} \psi^n + \frac{\mu_k}{r^{g-1}} \frac{\partial}{\partial r} (r^{g-1} \psi_k^n) + \frac{g-1}{r} \frac{2}{w_k} (a_{k+\frac{1}{2}} \psi_{k+\frac{1}{2}} - a_{k-\frac{1}{2}} \psi_{k-\frac{1}{2}})$$

$$= \frac{\partial}{\partial E} S_k^n \psi_k^n + T_k^n \frac{2}{w_k} (a_{k+\frac{1}{2}} \frac{\psi_{k+1}^n - \psi_k^n}{\mu_{k+1} - \mu_k} - a_{k-\frac{1}{2}} \frac{\psi_k^n - \psi_{k-1}^n}{\mu_k - \mu_{k-1}})$$

$$+ \frac{1}{q\Delta t} \frac{V^{n-1}}{V^n} \psi_k^{n-1} + Q_k^n$$
[31]

where spatial and energy variable are still continuous.

3.3 Coupled Space-Energy Discretization

The energy derivative term $\dfrac{\partial}{\partial E}(S\psi)$ in Eq. [1] enforces a coupled space-energy discretization because the more conventional multigroup approach is too inaccurate /4/ for the Fokker-Planck equation. If we later use the term energy "level" it has to be kept in mind that no averaging of coefficients or physical constants over the energy interval is performed; energy is treated just as an additional independent variable.

Consider a cell in the (r,E) space defined by the nodes $(r_{i-\frac{1}{2}}, E_{j+\frac{1}{2}})$, $(r_{i+\frac{1}{2}}, E_{j+\frac{1}{2}})$, $(r_{i+\frac{1}{2}}, E_{j-\frac{1}{2}})$, $(r_{i-\frac{1}{2}}, E_{j-\frac{1}{2}})$ as shown in Figure 1 on page 12. The space region limited by $r_{i+\frac{1}{2}}$ and $r_{i-\frac{1}{2}}$ has a geometric volume W_i and left and right surface areas $A_{i-\frac{1}{2}}$ and $A_{i+\frac{1}{2}}$ (note that cylindrical geometry is not handled since it would require treatment of two angular variables):

	Slab	Sphere
W_i	$r_{i+\frac{1}{2}} - r_{i-\frac{1}{2}}$	$\dfrac{1}{3}(r_{i+\frac{1}{2}}^3 - r_{i-\frac{1}{2}}^3)$
$A_{i-\frac{1}{2}}$	1	$r_{i-\frac{1}{2}}^2$
$A_{i+\frac{1}{2}}$	1	$r_{i+\frac{1}{2}}^2$

Table 1.   Definition of Volume and Surface Coefficients

Then the following difference approximations are used:

$$
\begin{aligned}
\frac{1}{r^{g-1}} \frac{\partial}{\partial r}(r^{g-1}\psi)|_{r=r_i} &= \frac{(A_{i+\frac{1}{2}}\psi_{\text{east}} - A_{i-\frac{1}{2}}\psi_{\text{west}})}{W_i} \\[2mm]
\frac{g-1}{r}\psi|_{r=r_i} &= \frac{(A_{i+\frac{1}{2}} - A_{i-\frac{1}{2}})\psi_{\text{center}}}{W_i} \\[2mm]
\frac{\partial}{\partial E}(S\psi)|_{E=E_j} &= \frac{(S_{j-\frac{1}{2}}\psi_{\text{north}} - S_{j+\frac{1}{2}}\psi_{\text{south}})}{\Delta E_j}
\end{aligned}
\qquad [32]
$$

The parameter g in Eq. [32] depends on the geometry: $g = 1$ for slab and $g = 3$ for spherical geometry. To close the set of equations we use diamond differencing formulas for the (r,E) space:

$$\psi_{\text{south}} = 2\psi_{\text{center}} - \psi_{\text{north}} \qquad [33]$$

$$\psi_{\text{east}} = 2\psi_{\text{center}} - \psi_{\text{west}} \qquad \text{if } \mu > 0 \qquad [34]$$

$$\psi_{\text{west}} = 2\psi_{\text{center}} - \psi_{\text{east}} \qquad \text{if } \mu < 0 \qquad [35]$$

The two alternative forms of extrapolation in Eq. [34] and Eq. [35] arise as a consequence of the mesh sweeping technique; for positive μ, ψ_{west} is known from the boundary conditions whereas for negative μ, ψ_{east} is known from the previous solution steps.

3.4 Discretization of Inertia Terms

The term $\dfrac{\partial}{\partial \mu}(1 - \mu^2)G\psi$ is discretized using Eq. [28] with ψ replaced by $G\psi$.

The term $\dfrac{\partial}{\partial E}(F\psi)$ has to be treated in a special way because F may take both, positive and negative values. F is split in its accelerating (negative) part,

$$F_{i,k,j}^{-} = \min(F_{i,k,j\pm\frac{1}{2}}, 0) \tag{36}$$

and its decelerating (positive) part,

$$F_{i,k,j\pm\frac{1}{2}}^{+} = F_{i,k,j\pm\frac{1}{2}} - F_{i,k,j}^{-} \tag{37}$$

Fluxes of the previous time step are used to treat F^{-} and fluxes of the actual time step are used to treat F^{+}. Thus, numerical stability is improved. The formula to discretize the term in F in Eq. [1] reads as follows:

$$\frac{\partial}{\partial E}F\psi_{|E=E_j} = \frac{(F_{j-\frac{1}{2}}^{+}\psi_{j-\frac{1}{2}}^{n} - F_{j+\frac{1}{2}}^{+}\psi_{j+\frac{1}{2}}^{n})}{(E_{j-\frac{1}{2}} - E_{j+\frac{1}{2}})} + \frac{F_j^{-}(\psi_j^{n-1} - \psi_{j+1}^{n-1})}{(E_j - E_{j+1})} \tag{38}$$

A discussion of the justification of Eq. [38] may be found in reference /4/ .

3.5 Iterative Solution Scheme

Discretizing the Fokker-Planck equation in the manner described above, the following system of linear equations is obtained (for simplicity, the terms concerned with the treatment of inertia are omitted again):

$$\frac{1}{q\Delta t}\psi_{i,k,j}^{n} + \frac{\mu_k}{W_i}(A_{i+\frac{1}{2}}\psi_{i+\frac{1}{2},k,j}^{n} - A_{i-\frac{1}{2}}\psi_{i-\frac{1}{2},k,j}^{n}) + \frac{1}{W_i}\frac{2}{w_k}(a_{k+\frac{1}{2}}\psi_{i,k+\frac{1}{2},j}^{n} - a_{k-\frac{1}{2}}\psi_{i,k-\frac{1}{2},j}^{n})$$

$$= \frac{S_{i,j-\frac{1}{2}}\psi_{i,k,j-\frac{1}{2}}^{n} - S_{i,j+\frac{1}{2}}\psi_{i,k,j+\frac{1}{2}}^{n}}{\Delta E_j} + \frac{1}{q\Delta t}\frac{V_i^{n-1}}{V_i^{n}}\psi_{i,k,j}^{n-1} + Q_{i,k,j}^{n} \tag{39}$$

$$+ T_k^{n}\frac{2}{w_k}(a_{k+\frac{1}{2}}\frac{\psi_{i,k+1,j}^{n} - \psi_{i,k,j}^{n}}{\mu_{k+1} - \mu_k} - a_{k-\frac{1}{2}}\frac{\psi_{i,k,j}^{n} - \psi_{i,k-1,j}^{n}}{\mu_k - \mu_{k-1}})$$

All physical coefficients are precalculated. The noncentered stopping powers are obtained by linear interpolation. Eq. [39] is solved for the fluxes using the following steps :

(a) For a given energy level j CIRCE starts from the outer boundary $r = R_{outer}$ and sweeps the space mesh to the inner boundary $r = R_{inner}$. Only directions $k = 1,...,MDIR/2$ (negative μ) are considered in this step. Now $\psi_{i+\frac{1}{2},k,j}^{n}$ and $\psi_{i,k,j-\frac{1}{2}}^{n}$ are known from boundary conditions or previous steps and $\psi_{i,k,j+\frac{1}{2}}^{n}$ and $\psi_{i-\frac{1}{2},k,j}^{n}$ can be eliminated using Eq. [33] and Eq. [35] thus yielding the banded system

$$a\psi_{i,k-1,j}^{n} + b\psi_{i,k,j}^{n} + c\psi_{i,k+1,j}^{n} + d\psi_{i,k+\frac{1}{2},j}^{n} + e\psi_{i,k-\frac{1}{2},j}^{n} = RHS_{i,k,j}^{n} \tag{40}$$

To eliminate the fluxes $\psi^n_{i,k+\frac{1}{2},j}$ and $\psi^n_{i,k-\frac{1}{2},j}$ at the interfaces of the angular cell, a "flat flux approximation" is used:

$$\psi^n_{i,k+\frac{1}{2},j} = \psi^n_{i,k,j} \qquad [41]$$

Assuming $\psi^n_{i,MDIR/2+1,j}$ to be known from the previous iteration or (initially) from the previous timestep, Eq. [40] is a tridiagonal system which is solved by a rapid version of Gauss elimination. Next, Eq. [33] and Eq. [35] are used to calculate the fluxes $\psi^n_{i-\frac{1}{2},k,j}$ and $\psi^n_{i,k,j+\frac{1}{2}}$ at the interfaces which are needed as $\psi^n_{i+\frac{1}{2},k,j}$ and $\psi^n_{i,k,j-\frac{1}{2}}$ at the next spatial cell and next energy level, respectively.

(b) Once the inner boundary is reached, the boundary conditions are applied.

(c) Next CIRCE starts from the inner boundary $r = R_{inner}$ and sweeps the space mesh to the outer boundary $r = R_{outer}$. Only directions $k = MDIR/2 + 1, ..., MDIR$ (positive μ) are considered in this step. $\psi^n_{i-\frac{1}{2},k,j}$ and $\psi^n_{i,k,j-\frac{1}{2}}$ are known from boundary conditions or previous steps and $\psi^n_{i,k,j+\frac{1}{2}}$, $\psi^n_{i+\frac{1}{2},k,j}$ can be eliminated using Eq. [33] and Eq. [34] and $\psi^n_{i,k+\frac{1}{2},j}$ and $\psi^n_{i,k-\frac{1}{2},j}$ are eliminated using Eq. [41] as in step (a). $\psi^n_{i,MDIR/2-1,j}$ is known from step (a). Thus, for positive μ, Eq. [39] is a real tridiagonal system which again is solved by Gauss elimination.

(d) At the outer boundary the boundary conditions are applied again.

(e) Steps (a) to (d) are repeated until convergence in fluxes is obtained. Convergence is surveyed using the relative pointwise differences of fluxes in consecutive iterations.

(d) This completes a computational cycle at energy level j. Before going to the next energy, angular fluxes are saved on disk files or computer memory for the next time step calculation.

3.6 Negative Flux Fix-Up

It is obvious from the diamond relationships, Eq. [33 - 35], that positivity of fluxes cannot be guaranteed. The fix-up procedure used in CIRCE for this problem consists of two steps. First, the fluxes at the interfaces are set to zero whenever they are found to be negative. The second step consists of applying the wellknown "fine mesh rebalancing" technique /9/ to preserve energy balance. With this approach, a space dependent scaling factor, f_i, is introduced for the angular fluxes at each energy level. Multiplying Eq. [1] with E (the energy) and integrating over the angular domain, a tridiagonal system of equations for the scaling factors f_i is obtained, which is solved in each iteration.

3.7 Energy Deposition Rate Calculation

Once the angular fluxes $\psi^n_{i,k,j}$ have been obtained, energy deposition can easily be calculated using Eq. [22] along with the numerical integration scheme

$$\phi(i,j) \; = \; \sum_{k=1}^{MDIR} w_k \psi_{i,k,j} \qquad\qquad\qquad\qquad \text{(\emph{scalar particle flux})} \quad [42]$$

$$E_{ion}(i) \; = \; \sum_{j=1}^{MNG} S_{ion}(i,j) \; \phi(i,j) \; \Delta E_j + E_{MNG} \; S_{ion}(i,MNG) \; \phi(i,MNG)$$

$$\text{(\emph{deposited energies})} \quad [43]$$

$$E_{elec}(i) \; = \; \sum_{j=1}^{MNG} S_{elec}(i,j) \; \phi(i,j) \; \Delta E_j + E_{MNG} \; S_{elec}(i,MNG) \; \phi(i,MNG)$$

A similar term appears in the energy balance if inertia terms are included:

$$E_{inert}(i) \; = \; \sum_{j=1}^{MNG} F(i,j) \; \phi(i,j) \; \Delta E_j + E_{MNG} \; F(i,MNG) \; \phi(i,MNG) \qquad\qquad [44]$$

as a consequence from the transition from a resting frame to an accelerating one. For details how to interpret this term see /8/ . In total the energy balance for a meshcell is given by (see Eq. [26]) :

$$E_{supra}(i) + E_{leak}(i) + E_{ion}(i) + E_{elec}(i) + E_{inert}(i) = E_{input}(i) \qquad\qquad [45]$$

Integrated over space, this relation serves as a check of the accuracy reached in the numerical solution (see "Interpretation of Sample Output" on page 29).

3.8 Mass and Momentum Calculations

Additional sources for the hydrodynamics equations used in MEDUSA-KA arise from the mass and momentum exchange rates due to the charged particle transport. As shown in /11/, inclusion of these terms is negligible for burn phase calculations in inertial confinement fusion. Since presently this is the main application area of the coupled system CIRCE and MEDUSA-KA, no provision is made up to now to calculate mass and momentum exchange rates due to the charged particle transport though it is fairly straightforward to extend the code in this respect once the angular fluxes are known.

PART B : Code Documentation

Chapter 4. Code Description

4.1   The Karlsruhe Target Code KATACO

This part serves as a short introduction to the new code system KATACO /15/ which is still under development at KfK.

To model the physics of high energy ion (or laser) beam interaction with targets a complex code system KATACO /1/ has been set up during the last years at KFK. Several stand alone codes are contained in this modular system and may be called and interact dynamically. Figure 2 shows the basic structure of KATACO, stressing the underlying shell structure.

The basis is the modular KSSK (= KAPROS-Subsystemkern) system kernel. Its main task are management and coordination of the central data base of the system (usually a very large COMMON-block) and of the dynamics of module calls. It is a purely FORTRAN77 system kernel providing the most important features of the KAPROS /12/ system which is in use at KFK since 1974 for reactor physics design and evaluation calculations. Using KSSK, any module of the central module library can be called much like a subroutine at any place of the module. The system manages all neccessary coordination and any data transfer. Moreover, the system kernel provides functions allowing dynamic array extension.

The plasma hydrodynamics code MEDUSA-KA /2/ , based on a MEDUSA version originally provided by Culham Laboratory, is used in KATACO to perform most of the hydrodynamics steps including atomic physics of the target. The program EDEPOS /14/ , jointly developed with University of Wisconsin, has been integrated to handle the coupling of an external particle beam energy into the target.

The transport code CIRCE /4/ is used after target fusion ignition to handle the slowing down of α particles. The Los Alamos code TIMEX /13/ treats timedependent neutron transport, primarily to model the interaction of 14 MeV fusion neutrons with the target (scattering, (n-2n)- and absorption). It uses an own time scale and is synchronized with MEDUSA-KA after some timesteps.

Within KATACO, the mutligroup radiation diffusion code MULRAD is an extension of MEDUSA-KA rather than a separate module. This has been done because it is strongly coupled with the equations solved in MEDUSA-KA.

The last component of KATACO is the INTERFAC module /10/ . It supports evaluation and plotting of the vast amount of data usually generated during a simulation run.
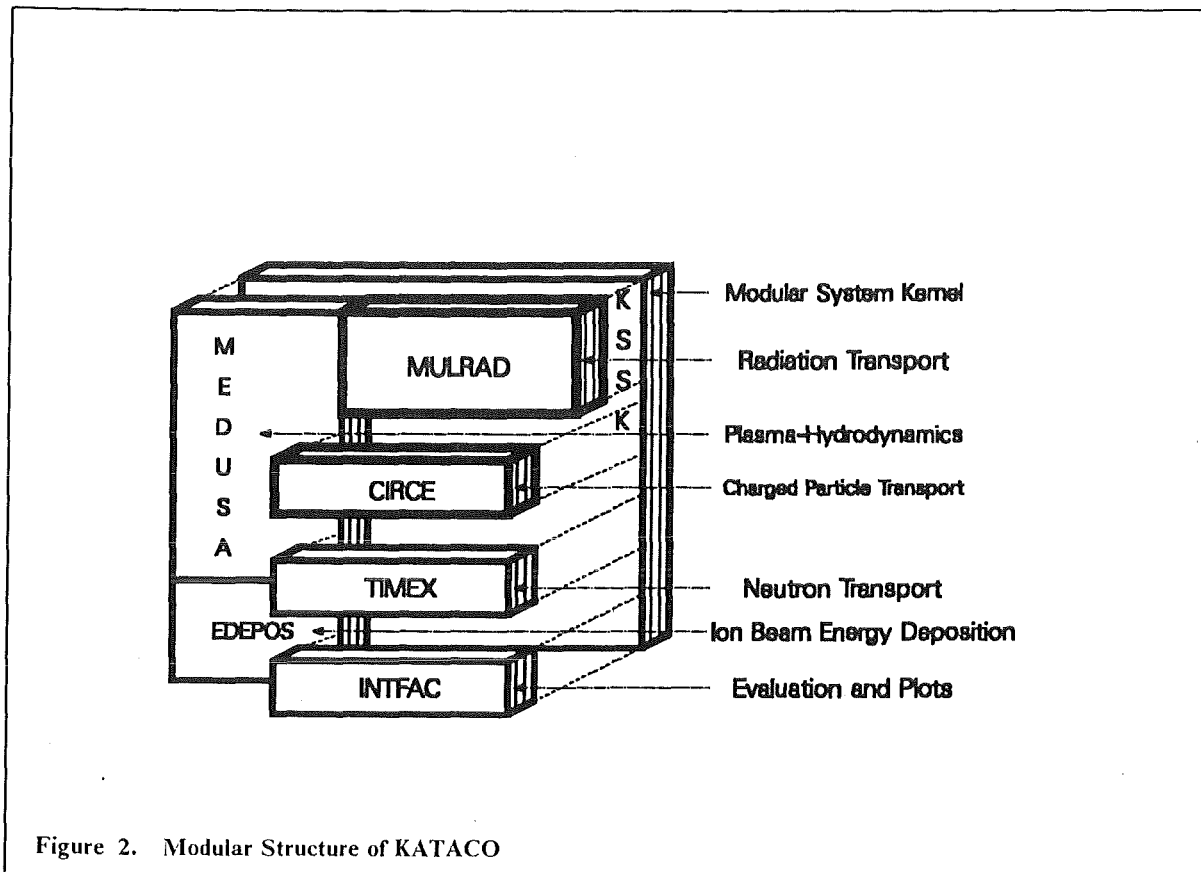
Figure 2. Modular Structure of KATACO

4.2 Code Structure of CIRCE

The Fokker-Planck transport calculation is invoked by calling the driver CIRCE. The calling list and a description of the parameters on input and output, respectively, may be found in "CIRCE Calling List" on page 49. Depending on the input value KMODE, this subroutine performs an initialization (KMODE = 0) or transports one kind of fast ions for one timestep per call. A simplified diagram showing the logical flow of control is given in Figure 3 on page 21.

In order to treat time dependent particle transport, CIRCE has to store angular fluxes from the previous timestep. For that purpose there are two possibilities implemented: the first option - the faster one - is to store fluxes in a container array located in common block /COMWOR/. If the storage place provided there is not sufficient, the code automatically switches to a storing mode using external disc data sets. Note that this option will increase computing times, computing costs and turn-around times.

A list of subroutines called by CIRCE along with a short description of their function is given in "Index of Subroutines" on page 49. In "COMMON Block Structure" on page 51, a detailed description of the COMMON block variables used by CIRCE is listed.
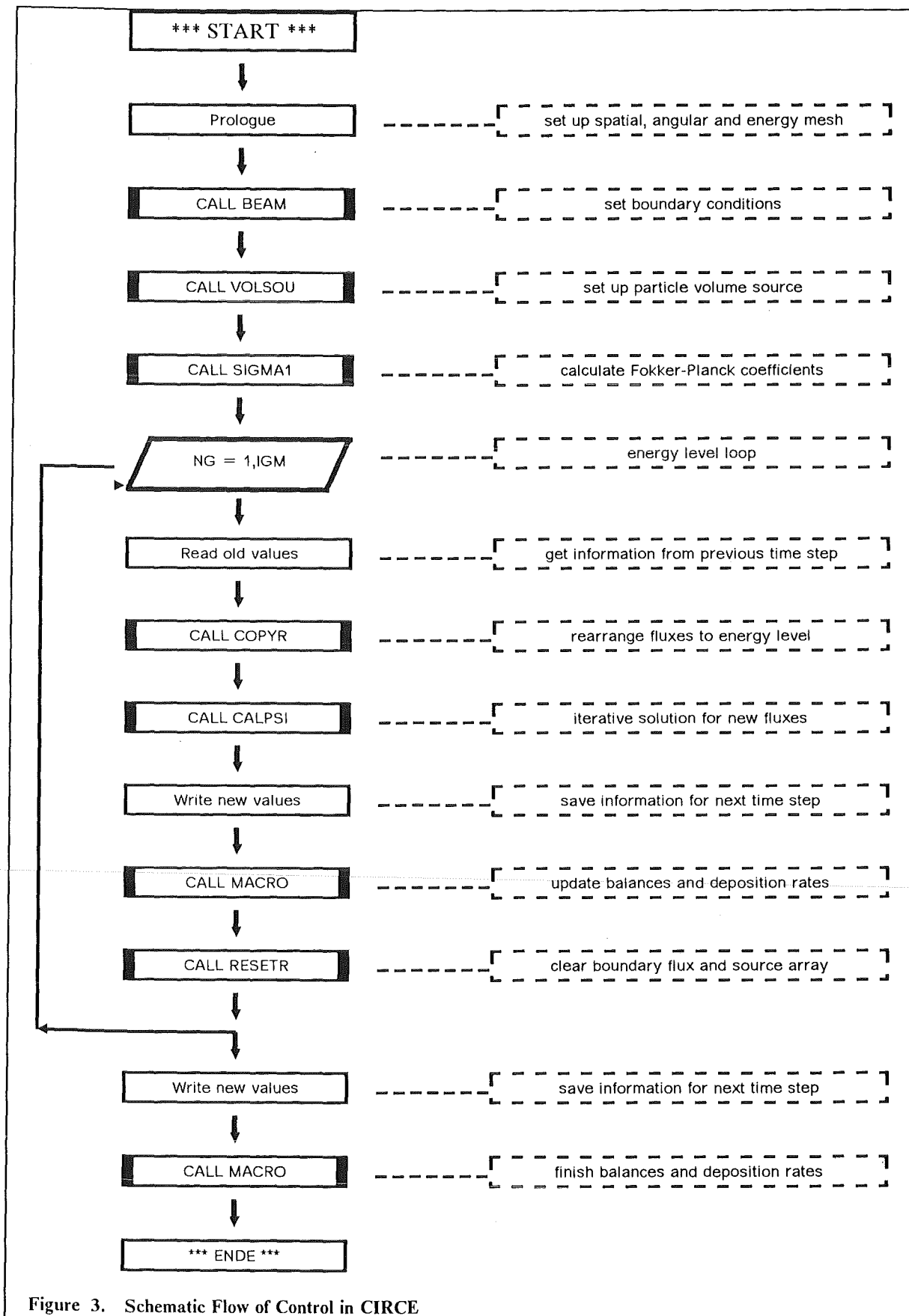
Figure 3. Schematic Flow of Control in CIRCE

The flowchart depicts the following sequence:

- ***** START *****
- **Prologue** — set up spatial, angular and energy mesh
- **CALL BEAM** — set boundary conditions
- **CALL VOLSOU** — set up particle volume source
- **CALL SIGMA1** — calculate Fokker-Planck coefficients
- **NG = 1,IGM** — energy level loop
  - **Read old values** — get information from previous time step
  - **CALL COPYR** — rearrange fluxes to energy level
  - **CALL CALPSI** — iterative solution for new fluxes
  - **Write new values** — save information for next time step
  - **CALL MACRO** — update balances and deposition rates
  - **CALL RESETR** — clear boundary flux and source array
- **Write new values** — save information for next time step
- **CALL MACRO** — finish balances and deposition rates
- ***** ENDE *****

```
                    *** START ***
                         │
                         ▼
                   KSTEP = 1,..          ─ ─ ─ ─ ─ ─    time step loop
                         │
                         ▼
              non-iterative quantities
                         │
                         ▼
                   ITER = 1,MAXIT        ─ ─ ─ ─ ─ ─    temperature iteration
                         │
                         ▼
                   State of system
                         │
                         ▼
                  particle processes     ─ ─ ─ ─ ─ ─    ** changed by the coupling of CIRCE **
                         │
                         ▼
               solve temperature eqt.
                         │
                         ▼
                 calculate pressures
                         │
                         ▼
                   CFL criterion         ─ ─ ─ ─ ─ ─    determine size of next time step
                         │
                         ▼
                 hydrodynamic state      ─ ─ ─ ─ ─ ─    ** changed by the coupling of CIRCE **
                         │
                         ▼
                 check convergence       ─ ─ ─ ─ ─ ─    ** changed by the coupling of CIRCE **
                         │
                         ▼
                diagnostic quantities
                         │
                         ▼
                   CALL SHIFT            ─ ─ ─ ─ ─ ─    adjust quantities to next time level
                         │
                         ▼
                   *** ENDE ***
```

Figure 4.   Schematic Flow of Control in the MEDUSA-KA Code

4.3 Using CIRCE within the KATACO System

Given the hydro state of the plasma in a certain time interval, a transport calculation for the ions created during that time step can be done by CIRCE. The primary result of that calculation (as far as the energy equation is concerned) are the energy deposition rates to electrons and ions. These serve as source terms in the energy equation of MEDUSA-KA.

The energy equation used in MEDUSA-KA is :

$$C_v \frac{dT}{dt} + B_T \frac{d\rho}{dt} + p \frac{dV}{dt} = S \qquad [46]$$

where S is the rate per unit mass at which energy enters the subsystem of electrons and ions, respectively. T stands for ion and electron temperature, respectively, ρ is the density, V the (Lagrangian) volume, p the hydrodynamic pressure and C and B are physical constants. The source terms S in Eq. [46] are defined as the sum of

$$S_{ion} = H_{ion} - K + E_{ion} + Q \quad \text{and} \quad S_{elec} = H_{elec} + K + E_{elec} + J + X \qquad [47]$$

where H represents the flow of heat due to thermal conduction; K is the rate of exchange of energy between ions and electrons; J is the rate of Bremsstrahlung emission; X is the rate of absorbtion of beam energy; Q is the rate of viscuous shock heating; E is the rate of thermonuclear energy release. These are all expressed in W/kg and if subscript ion or elec is omitted the expression concerned applies to both.

In MEDUSA-KA, charged reaction products are assumed to deposit their energy to ions and electrons instantaneously at the place of their birth (local deposition) using ratios p and 1-p which depend on the temperature of the electron system.

If E_{DT}, E_{DD} and E_{D^3He} denote the energies of the charged particels resulting from the DT, DD and ^3He reaction

$$E_{ion} = p_{DD} E_{DD} R_{DD} + p_{DT} E_{DT} R_{DT} + p_{D^3He} E_{D^3He} R_{D^3He} \qquad [48]$$

with a similar expression for E_{elec} where 1-p replaces p.

Upon discretization of Eq. [46] in time (supscript n) and space (subscript ℓ) a tridiagonal linear system is obtained for the temperature of each subsystem (ions and electrons):

$$A_\ell^n T_{\ell-1}^n + B_\ell^n T_\ell^n + C_\ell^n T_{\ell+1}^n = (E_\ell^n + D_\ell^n) c^n + G_\ell^{n-1} \qquad [49]$$

where E_ℓ^n and D_ℓ^n are dependent on the yet unknown temperature and G_ℓ^{n-1} is not. Therefore, this equation has to be solved iteratively. Since doing a transport calculation at each iteration would be prohibitively expensive in computing times, the following procedure is used for the coupling: Let

$$E_\ell^n = E_{\ell, DD}^n + E_{\ell, DT}^n + E_{\ell, D^3He}^n \qquad [50]$$

where all deposition rates are calculated using the standard local deposition. Then iterate Eq. [49] until temperature converges. Upon convergence the α-particle source production rate for the time [t^n , t^{n+1}] has been calculated. Assuming local approximation to be enough to obtain an accurate source rate, this

is now used to perform a CIRCE calculation over the same time interval which in turn gives an accurate energy production rate term $E_{\vartheta,DT}$ for $[\ t^n,\ t^{n+1}\ ]$. Then fix in Eq. [50] $E_{\vartheta,DT}$ using the newly calculated profile and iterate Eq. [49] again until convergence of temperatures.

Note that there are three basic assumptions involved using that approach: (1) the α-particle source is neither changed too much by transport effects nor by the different partitioning of energy to electrons and ions used in CIRCE. (2) the change in temperature during the additional iterations does not change too much the stopping power coefficients used in CIRCE. Typically, only one or two additional MEDUSA-KA iteration were needed for convergence in the examples given in "Chapter 6. Effects of α-Particle Transport" on page 33. (3) The contributions of charged fusion reaction products other than α-particles are sufficiently well described by local deposition (otherwise transport calculations had to be performed for them too).

Note also that for the fully time dependent transport solution CIRCE has to store the space-angle-energy dependent α-particle fluxes at time t^n which are used as additional sources in the next time step calculation.

From the angular flux of the α-particles the momentum and mass transfer due to slowing down and transport can be calculated and added to the equations of motion and mass as source terms. Presently this is not done in this implementation. As shown in /11/ including these terms does not change results significantly in the applications of the type given in "Chapter 6. Effects of α-Particle Transport" on page 33.

4.4 Coding Details of the Coupling of CIRCE and MEDUSA-KA

A schematic of the flow of control in MEDUSA-KA is shown in Figure 4 on page 22 .

Additions have been made in subroutines DATA and PRESET of KATACO, because there the input is read and default values are set. An additional namelist, &CPATR (for Charged Particle Transport), is used to trigger the application of CIRCE.

In MEDUSA-KA, EXPERT is called at several strategic points. In the standard version, EXPERT simply executes a RETURN statement after a call to it. To change the normal proceeding, this subroutine has been reprogrammed to call the coupling subroutine MEDCIR at appropriate places.

Calls to EXPERT are modified at the following places in MEDUSA-KA ((1) in subroutine INITAL, all others in subroutine MOTION) :

(1) after return from SUBROUTINE START (CALL EXPERT(1, 8, 4));

at this stage, the CIRCE package is initialized.

(2) after return from SUBROUTINE CVRGE (CALL EXPERT(2, 2,20));

At this place, the temperature iteration - using the standard local deposition model - has converged. Using this plasma state an α particle transport calculation is performed with CIRCE for the actual time

interval. After that the (local) deposition contributions of charged particles other than a are calculated in subroutine FUSIO2 and added to the CIRCE deposition rates. Keeping now the deposition profiles (to ions and electrons) fixed, MEDUSA-KA re-iterates on temperatures. Typically only 1 or 2 additional iterations are required.

(3) after return from SUBROUTINE FUSION (CALL EXPERT(2, 2, 8));

At place (3), the standard MEDUSA-KA energy deposition rates for the DT reaction are replaced by those changed by CIRCE and the coupling procedure.

(4) after return from SUBROUTINE BNDY (CALL EXPERT(2, 2,16));

At place (4), $\frac{\partial}{\partial r}u$, $D_i u$ and u/r are calculated at each space point. These values are needed to include the inertia term treatment in the CIRCE solution.

A detailed diagnostic package has been developed showing how much energy is deposited and where it is deposited in the model. An example output of that printout is shown in "Output of Sample Calculation" on page 61.

Subroutine HDCOPY and the corresponding input value of NHDCPY are newly defined in order to provide interface files in a structure usable for the evaluation module INTERFAC /10/. As long as CIRCE is switched on, the printing frequency of KATACO is changed to the input value defined in Namelist &CAPTR.

4.5 Coupling the Transport Module CIRCE to KATACO

Basically, the coupling described above may be used for both, MEDUSA-KA and KATACO. In order to use CIRCE as a separate module as shown in Figure 2 on page 20 a somewhat different implementation has to be used.

In KATACO, the individual modules do not share arrays but they rather access interfaces, called datablocks, provided in a central database and managed by the system kernel. Therefore, the interfacing routine MEDCIR mentioned above (which still is a part of MEDUSA-KA) simply sets up datablocks containing the same information as given in the coupling above. The execution of CIRCE is then started by issuing a KSEXEC call to KSSK.

Two advantages are gained by modularity. First of all, CIRCE is used then much like a library subroutine, thereby decreasing the chance of unwanted side-effects if one of the other modules is changed. Secondly, since CIRCE has its own environment it is possible on future computers to run CIRCE in parallel with other modules, e.g. TIMEX.
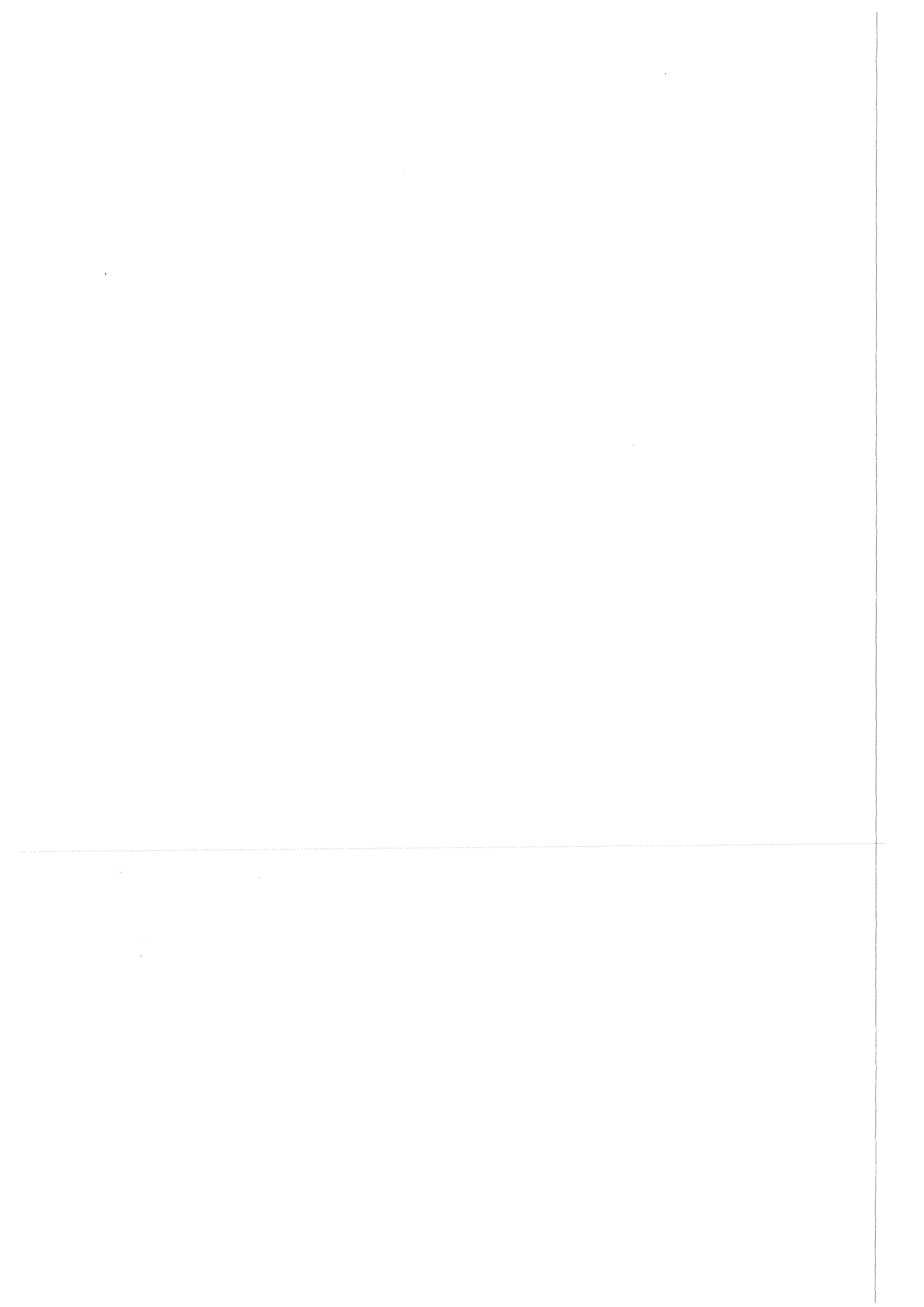
Chapter 5. Input Description and User Information

5.1 Namelist Input for Charged Particle Transport

The input is handled in CIRCE by namelist &CPATR. It has to be provided in the input stream right after the KATACO input namelist &NEWRUN. Be cautious not to use card numbering in columns 73-80 of the input cards. In the following we provide a complete alphabetical list of the input variables along with their type (I = Integer, R = Real, L = Logical), default values set in the code and their function.

Variable	Type	Default	Function
MDIR	I	8	number of angular directions to be used (see remark below)
MNG	I	15	number of energy levels to be used (see remark below)
MODE	I	1	specify mode of operation. = 1: time dependent calculation for volume source; = 11: adiabatic calculation;
MINER	I	20	maximum number of inner iterations
MX1	I	1	inner boundary cell number for transport calculation
MX2	I	91	outer boundary cell number for transport (see remark below)
MFREQ	I	1	do a transport calculation every MFREQ-th hydro time step
NLALTR	L	.TRUE.	use CIRCE for transport if .TRUE.; use local deposition otherwise
NPRCPT	I	100	frequency of printed output during a transport calculations. If NPRCPT $<$ 0 : only summary information every (-NPRCPT)-th time step; NPRCPT $>$ 0 : detailed information.
ZAION	R	4.0	mass number of fast ion (in amu)
ZCUT	R	0.01	ratio of cut off energy over starting energy of fast ion
ZDPSI	R	0.001	maximum relative deviation of angular flux allowed
ZEION	R	3.5E6	starting kinetic energy of fast ion (in eV)
ZZION	R	2.0	charge number of fast ion (in emu)

Note: The values of MDIR, MNG and MX2 are limited to 30, 30 and 100 respectively. All these maximum values are set by means of a PARAMETER statement and can easily be changed.

Table 2. Function and Default Values of Input Variables

MNG	MDIR	Gain	TImax	TEmax	$E_{ion,max}$	$E_{elec,max}$	Effort
0	0	165.5	366.0	148.5	5.897	2.442	1.0
8	4	168.9	328.5	144.7	2.999	1.434	2.0
15	4	169.3	329.1	144.7	2.932	1.422	3.0
15	*8*	*167.4*	*326.6*	*144.7*	*2.981*	*1.403*	*3.4*
20	8	167.6	326.5	144.7	2.994	1.401	4.8
20	16	168.5	323.8	144.4	2.935	1.393	8.0
25	**16**	**168.6**	**323.3**	**144.4**	**2.953**	**1.394**	**9.8**

Note:

MNG is the number of energy levels used (MNG = 0 means local deposition), **MDIR** the number of discrete directions used and **Gain** as calculated by KATACO at approximately 100 ps burnup time

TImax(t_0) given in KeV is defined as : max { $T_{ion}(r,t)$, $R_{inner} \leq r \leq R_{outer}$, $t_{start} \leq t \leq t_0$ } where T_{ion} is the ion temperature.

TEmax(t_0) given in KeV is defined as : max { $T_{elec}(r,t)$, $R_{inner} \leq r \leq R_{outer}$, $t_{start} \leq t \leq t_0$ } where T_{elec} is the electron temperature.

$E_{ion,max}(t_0)$ given in W/kg*1.0E24 is defined as : max { $E_{ion}(r,t)$, $R_{inner} \leq r \leq R_{outer}$, $t_{start} \leq t \leq t_0$ } where E_{ion} is the energy deposition rate due to collisions with ions.

$E_{elec,max}(t_0)$ given in W/kg*1.0E24 is defined as : max { $E_{elec}(r,t)$, $R_{inner} \leq r \leq R_{outer}$, $t_{start} \leq t \leq t_0$ } where E_{elec} is the energy deposition rate due to collisions with electrons.

Effort defined as ratio of CPU times used for a whole simulation run using the coupled version over CPU time needed with KATACO (local deposition)

Table 3.   Computational Effort for Different Input Parameters

5.2   Computational Efficency

Computing time and accuracy in CIRCE is directly affected by the input numbers of spatial meshes, directions and energy levels. As an example Table 3 gives results for the compression and burnup of the 4 mg HIBALL target /5/. The CIRCE transport calculations used the 45 innermost spatial mesh cells, 5 cells extending beyond the fuel region of the pellet. Burnup starts at a plasma temperature of T = 4.6E7 Kelvin. The values obtained with MDIR = 16 and MNG = 25 are regarded as reference. 8

directions and 15 energy levels seem to be sufficient to get a good accuracy in that case (deviation from the reference solution < 1% in all variables considered).

If 1.0 is assigned to the average computer time needed for one KATACO time step with local deposition, the solution of the Fokker-Planck equation with the above mentioned input numbers needs 7 units. Since the transport module is active only in approximately 1500 out of 9000 time steps (the remaining steps treating implosion and disassembly process), the relative computational burden of CIRCE compared to local deposition becomes 3.4 This means that computing times on an IBM3090 computer rise from $\simeq 3$ minutes to $\simeq 10$ minutes for a whole pellet simulation.

5.3 Interpretation of Sample Output

This chapter describes the output shown in "Output of Sample Calculation" on page 61 . The first few pages show a reproduction of the input namelists in a readable form. This should enable a user to check whether input has been correct or not. After that the usual KATACO output is given for the first timestep and the timestep just at ignition. It is that point of time when CIRCE starts its regular operation.

We will concentrate on the interpretation of the CIRCE diagnostic output triggered by the input value of variable NPRCPT of namelist &CPATR. In the appendix the output corresponds to a negative value of NPRCPT (only summary information; see input description above). Note that not the complete output is shown but only a few characteristic time steps have been selected.

The first few lines of the CIRCE output contain timestep numbers, elapsed simulation time since ignition and elapsed time since start of the simulation. The 'SUMMARY ENERGY BALANCES' contain information contain a global energy balance allowing for a quick check. Note that the value of 'NEUTRON ENERGY / DEPOSITED ENERGY' should approach the value of 14.08MeV/3.52MeV = 4 at the end of the simulation whenever inertia contributions and leakage are negligible.

The next table gives the individual terms of the energy balance as described in "Energy Deposition Rate Calculation" on page 15. Also shown are the values obtained from the local deposition model and the share of ions other than a to the deposition. All values are given for the actual timestep as well as time integrated. Following this, the next table shows the same information expressed in percentages.

The last table gives an impression of the distribution of deposited energy on the burning part of the pellet, the fuel zone, the leakage outside the burning part and the leakage outside the fuel zone, again expressed as rates and time integrated.

The last line gives some statistical values obtained by timing the CIRCE code.

PART C : Application to the HIBALL Target
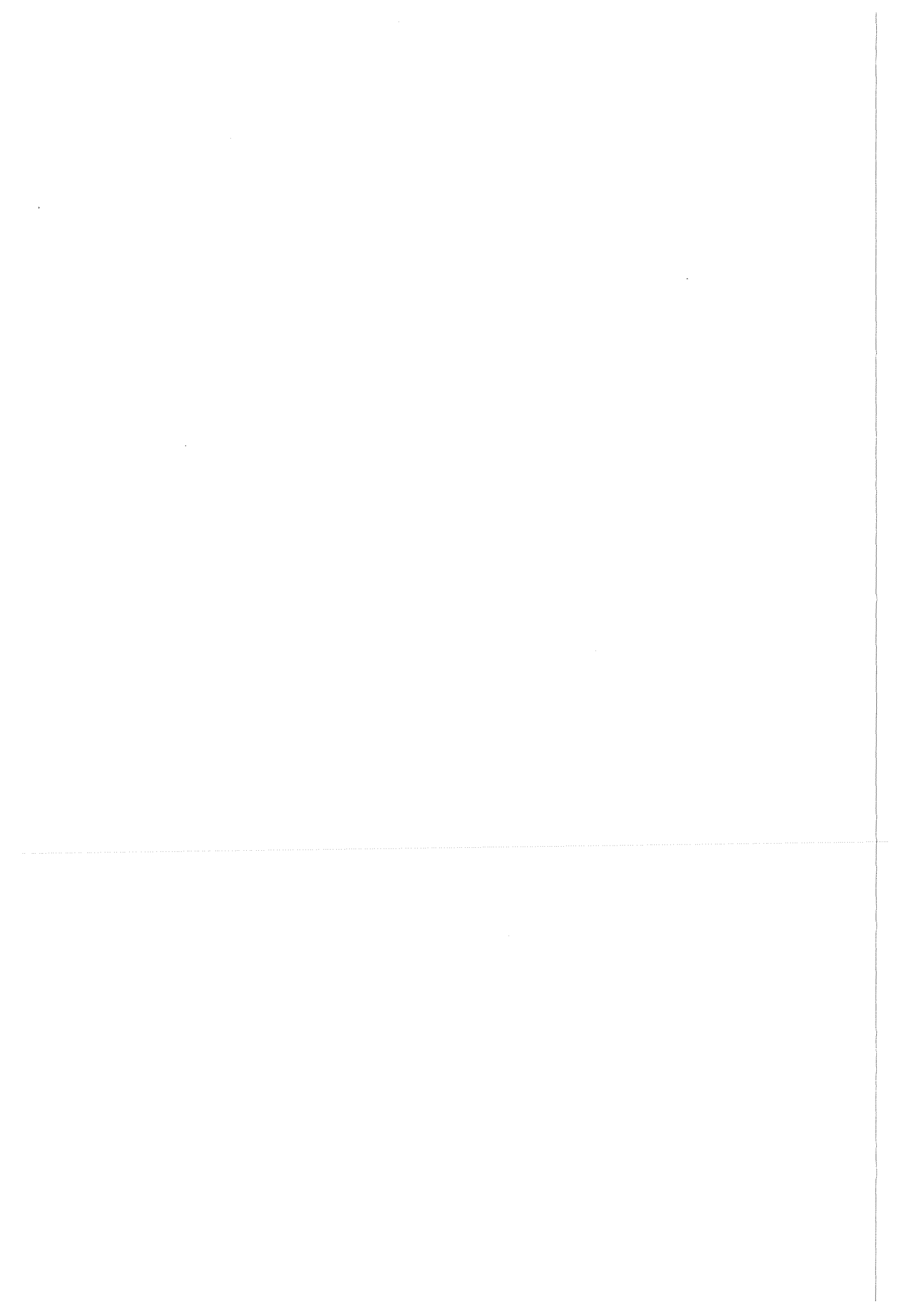
Chapter 6. Effects of α-Particle Transport

As a first test of the coupled KATACO-CIRCE system, the compression, ignition and burnup of a HIBALL pellet /5/ has been investigated. This pellet is a hollow sphere built up of 3 concentric zones, an outer Pb shell, followed by a LiPb pusher and a 4 mg inner shell of frozen DT. The discussion is concentrated on effects of α-particle transport during burnup.

6.1 Local Deposition vs. Fully Time Dependent Fokker-Planck Solution

The curves shown in Figure 5 on page 34 demonstrate that there is little effect of a detailed treatment of α-particle transport on the final gain factor if compared to local α-particle energy deposition. But burn propagation is somewhat (approximately 10 ps) retarded compared to local deposition.

As shown in Table 4 on page 36, ion temperature and deposition rates are strongly affected by the solution method chosen. Maximum deposition rates are almost a factor 2 higher in the local deposition model. The peak averaged ion temperature (averaged over the whole fuel zone) drop from 202 keV (local) to 183 (CIRCE) (see Figure 6 on page 34). The time integrated fraction of α-particle energy escaping the burning fuel varies from 2 to 3 percent during burn wave propagation. At the time when the burn wave reaches the outer fuel boundary (65 ps), the average fuel temperature is well above 50 keV and much more energy leaks out of the fully burning fuel (finally nearly 14 percent) since the fuel zone is much more transparent to the particles. The inclusion of inertia terms amounts to approximately 2 percent of the energy balance during the first 65 ps. As the disassembly of the pellet progresses, this part goes up to some 7 percent. Naturally, local deposition does not account for these effects. Results similar to this study have been obtained by Honrubia et al. /11/ .

One should keep in mind that though the effect of exact treatment of α-particle transport is rather small for this highly optimized pellet, it may be crucial for only marginally burning targets.

6.2 Adiabatic vs. Fully Time Dependent Fokker-Planck Solution

One approximation to particle transport is to neglect the time dependence of slowing down, i.e. in each time step the whole energy of the particles is deposited according to a space dependent distribution. This might be better than local deposition which neglects both, time and space dependence. Calculations have been done to check the validity of this adiabatic deposition in the present example.

Figure 5.   Pellet Gain: Local Deposition Option vs. CIRCE Transport Solution

Figure 6.   Ion Temperature: Local Deposition Option vs. CIRCE Transport Solution

Figure 7.   Pellet Gain: CIRCE Adiabatic vs. CIRCE Fully Time Dependent

Figure 8.   Ion Temperature: CIRCE Adiabatic vs. CIRCE Fully Time Dependent
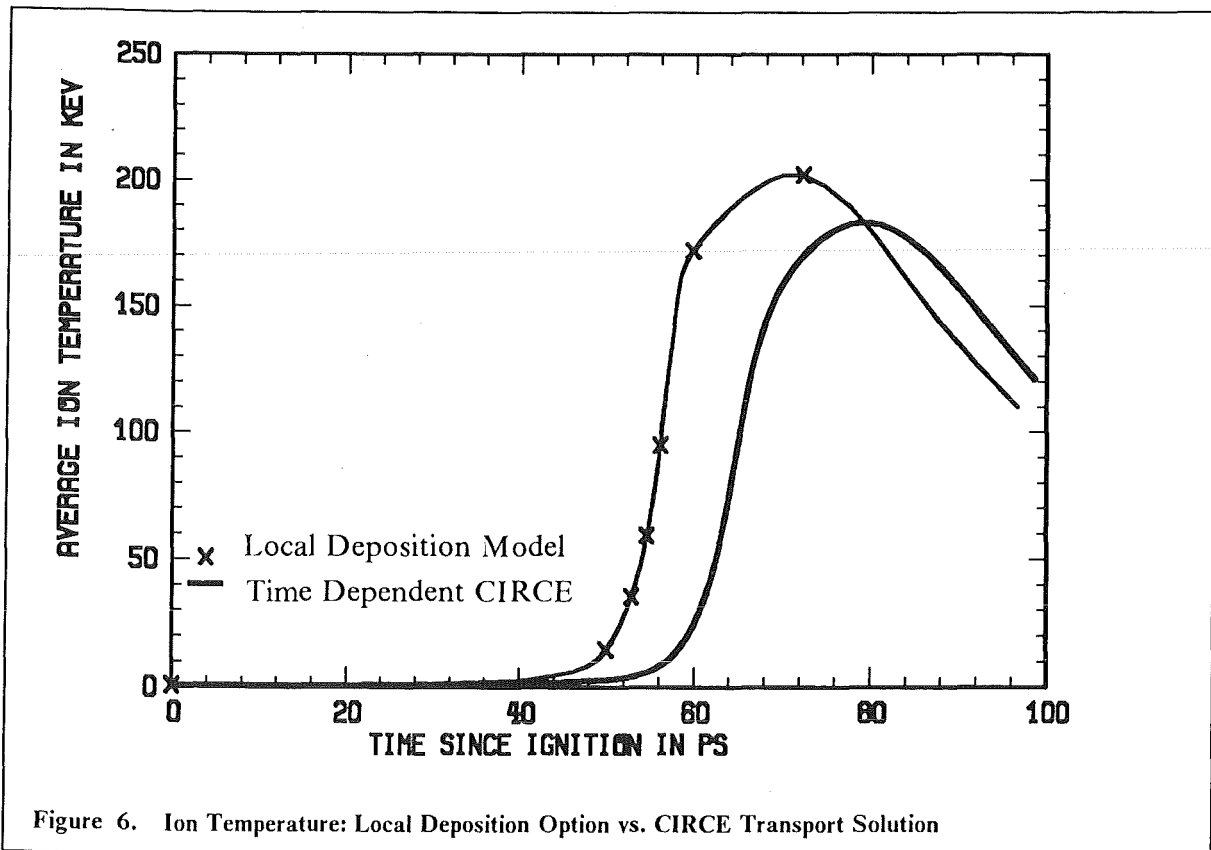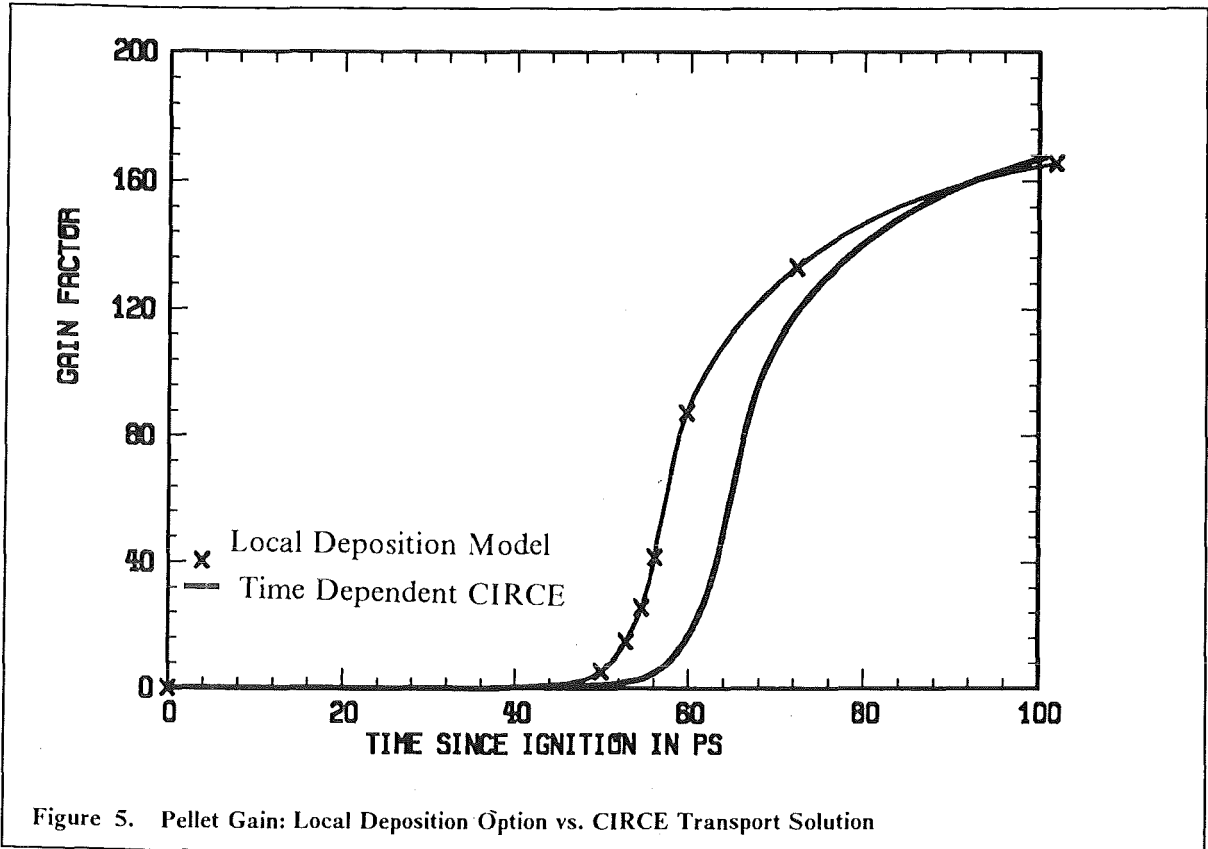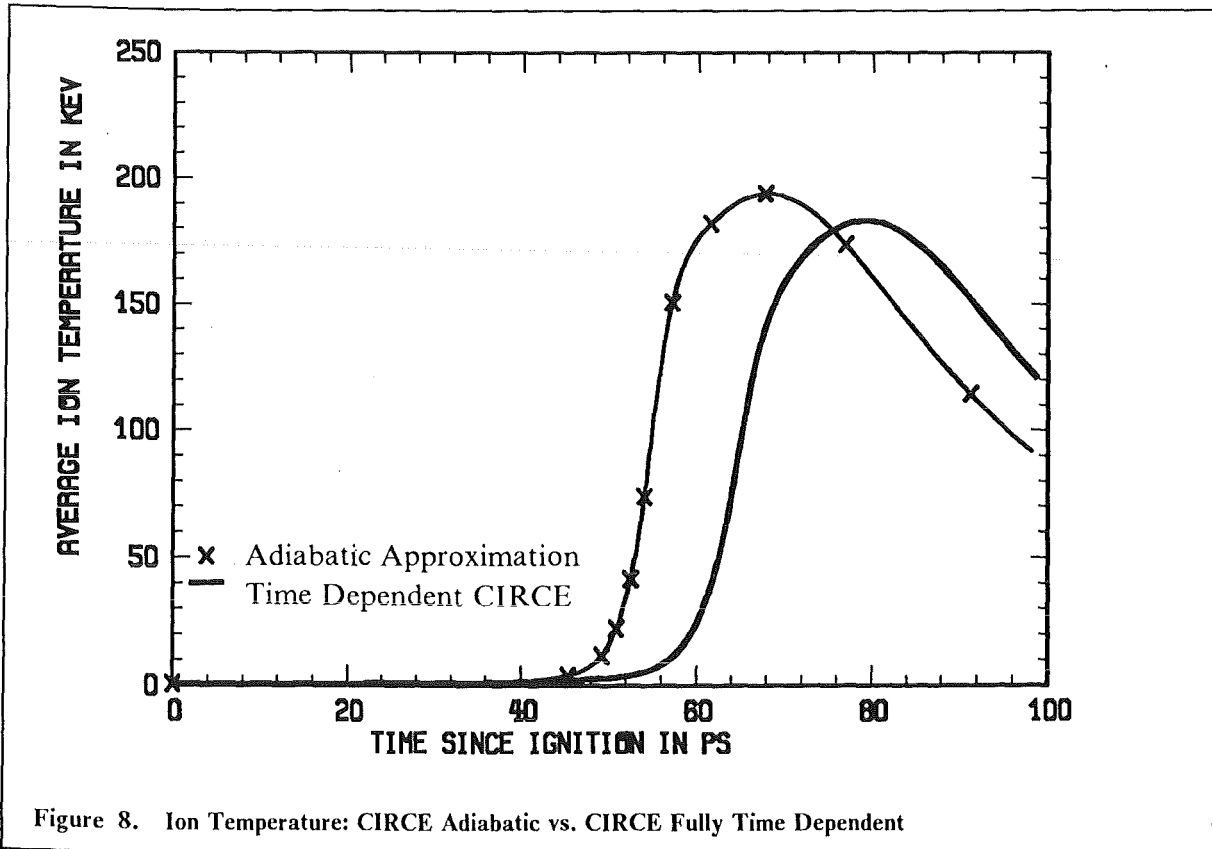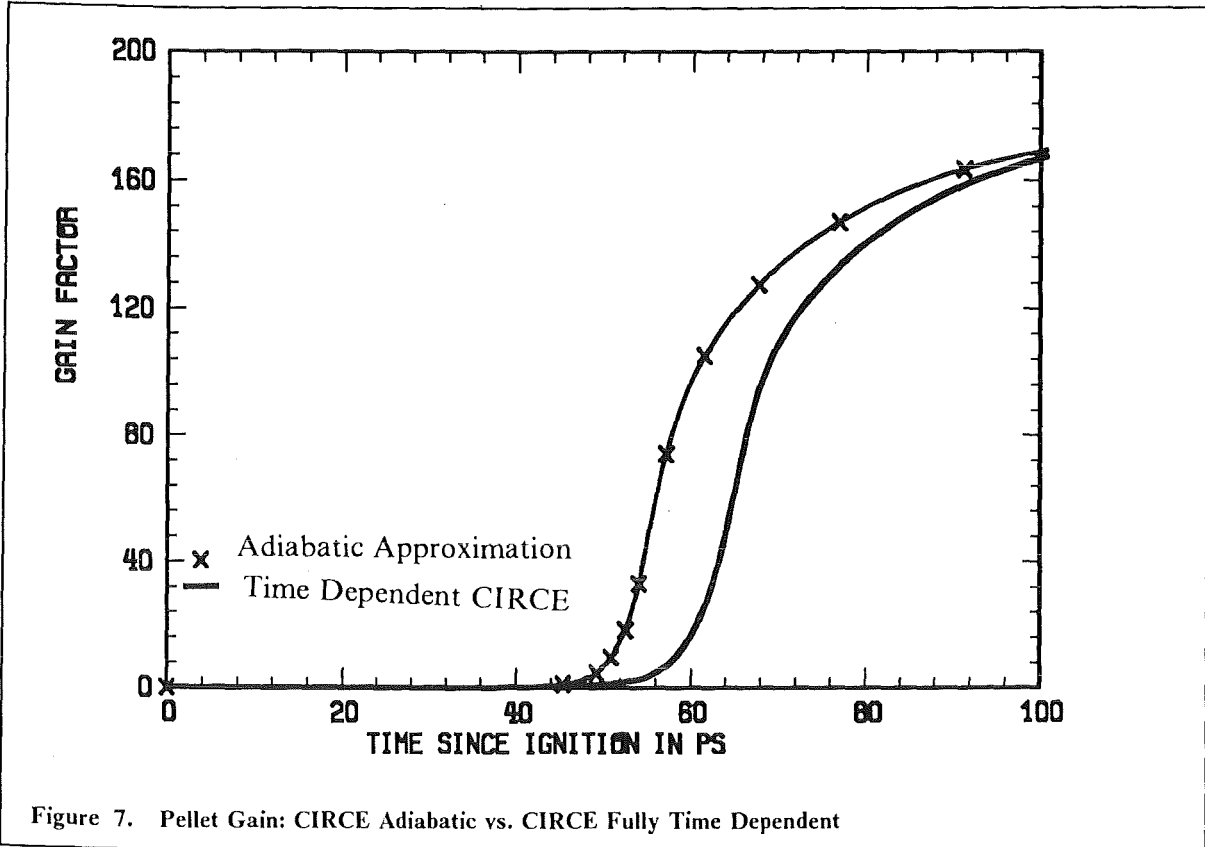
Approximation	Gain	TImax	TEmax	$E_{ion,max}$	$E_{elec,max}$	twave
Reference	181.3	325.4	144.6	2.969	1.404	64.5
	Relative deviations from reference in %					
local	-3.7	12.4	2.7	98.6	73.9	-12.4
adiabatic	-1.8	11.0	1.4	72.2	111.	-17.1
no inertia	0.8	10.4	1.5	53.1	6.9	-1.9
no deflection	1.0	10.9	1.3	59.5	6.4	-1.9

Note:

Reference = full time dependent CIRCE calculation with 8 directions and 15 energy levels.

Remaining rows given as relative deviations from the reference solution expressed in percent.

local = standard KATACO calculation using local deposition model.
adiabatic = CIRCE calculation with 8 directions and 15 energy levels where all α-particles thermalize within each time step.
no inertia = time dependent CIRCE calculation with 8 directions and 15 energy levels with inertia terms excluded.
no deflection = time dependent CIRCE calculation with 8 directions and 15 energy levels with inertia and deflection terms excluded.
twave = time after ignition when burn wave reaches outer fuel boundary.

For an explanation of the remaining variables see Table 3 on page 28

Table 4. Influence of Various Approximations on Selected Results

Figure 7 on page 35 and Figure 8 on page 35 make apparent that the adiabatic approximation is not able to account for the effects seen in fully time dependent calculations even for averaged variables. Especially the time retardation of burn wave propagation does not show up. The deviations from the reference solution given in Table 4 stress, that local deposition and adiabatic Fokker-Planck approach have a similar lack to describe correctly pointwise details.

We may conclude that the adiabatic approximation is too inaccurate to justify its usage (at least in the present calculation). Moreover, there are no savings in computing time: the numbers given in Table 3 on page 28 in column 'Effort' remain almost unchanged.

Figure 9. Comparison of Electron and Ion Temperatures
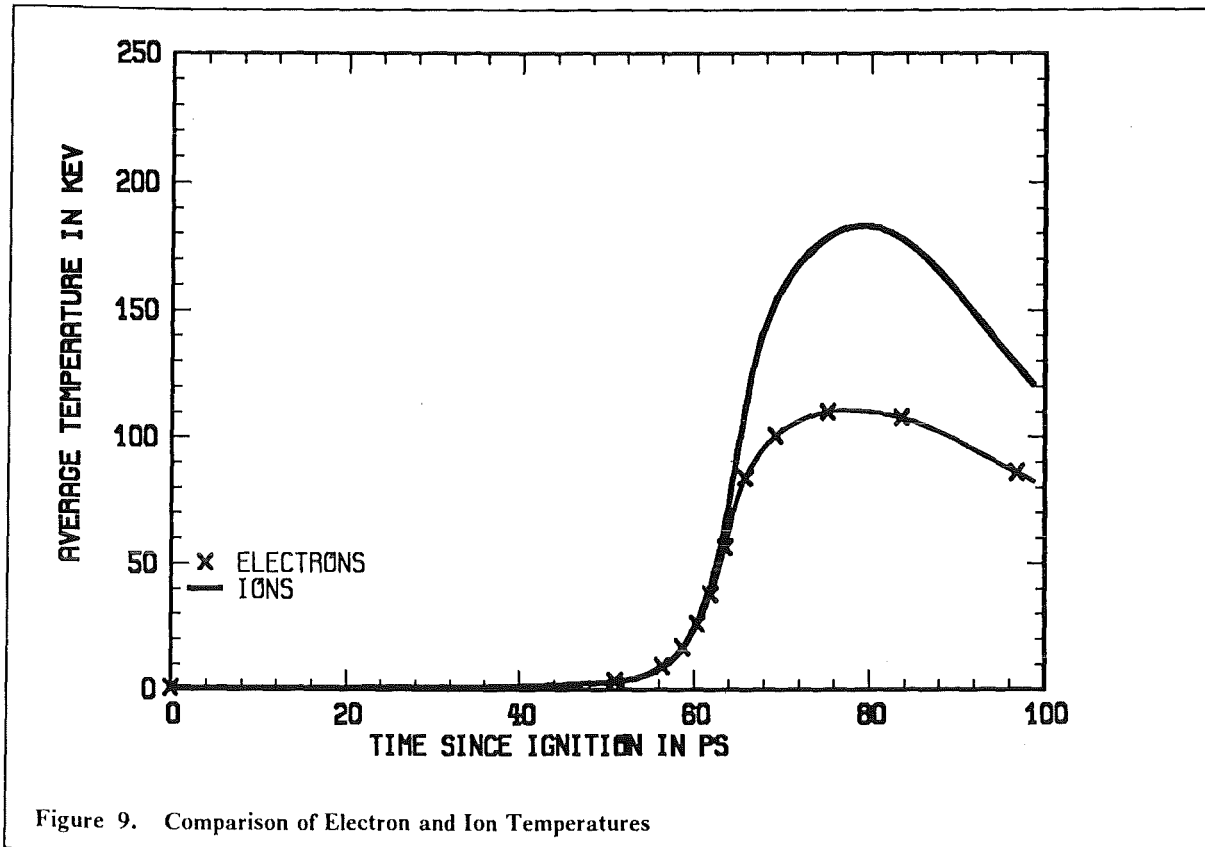
6.3 Influence of the Inertia and Deflection Terms

The two other possibilities mentioned in "Simplifiying Approximations to Fokker-Planck Equation" on page 9 , namely neglecting the inertia terms in Eq. [1] or both inertia and deflection terms, have also been investigated. Table 4 shows that the gain factor is sligthly increased due to absence of dissipative terms. This effect also shows up in the temperatures. The time retardation of burn wave propagation is described, in contrast, as accurately as in the reference solution.

Again it is not recommended to make these simplifications especially since, as before, no computational effort is saved by this.
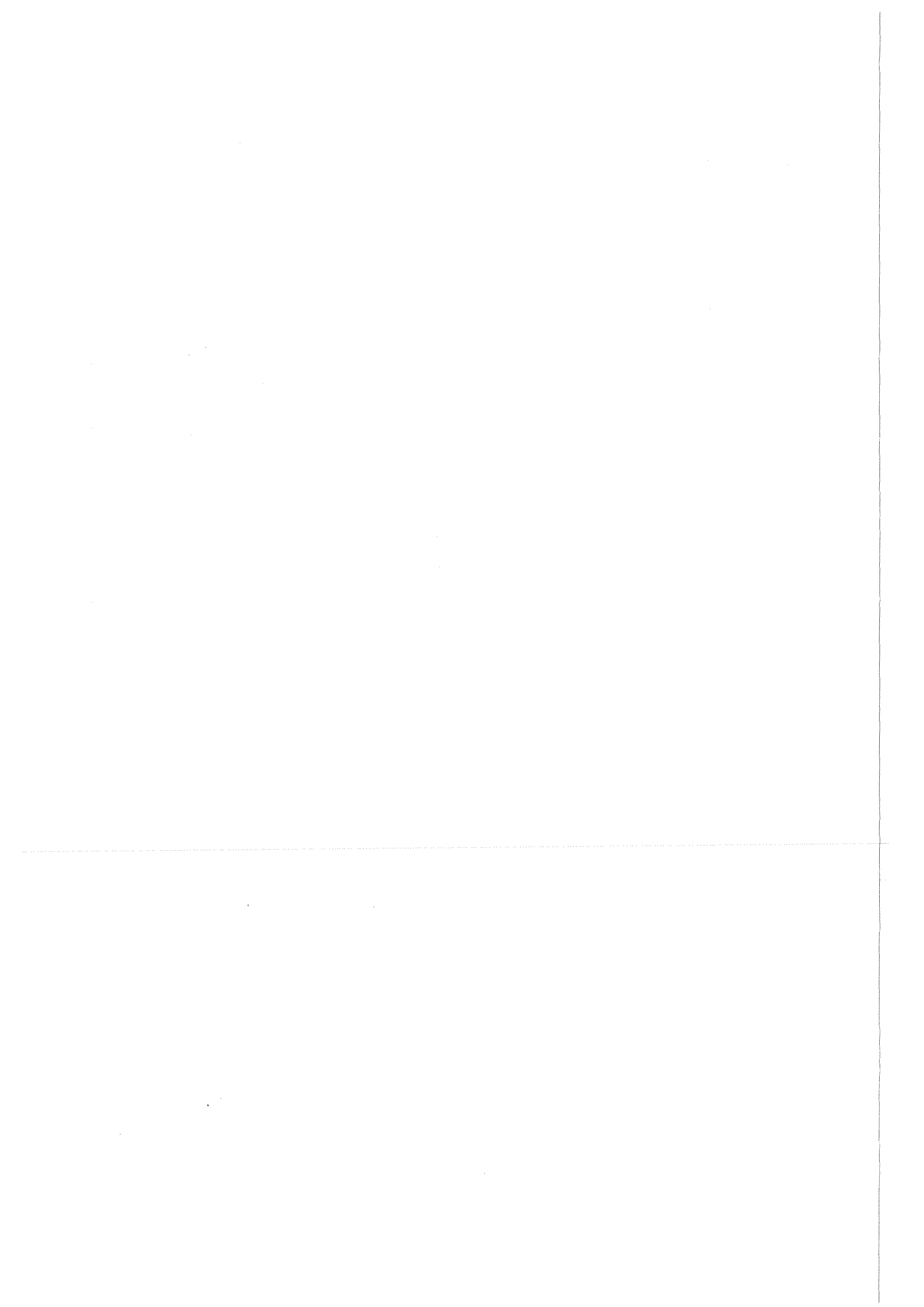
Chapter 7. Time Dependent Particle Tracking

7.1 Particle Tracking Theory

For simplicity only the time independent particle tracking method is decribed in this section to provide an introduction into the basic ideas involved. This description is based on the original paper of G.A.Moses /6/. Assuming that fast ions to move along straight lines during slowdown, the range-velocity equation in a thermal plasma is given for each line by

$$- dv = (A + \frac{B}{v^3}) \, ds \qquad [51]$$

where

$$A = A_0 \frac{Z^2}{m} \ln(\Lambda_e) \frac{n_e}{T_e^{3/2}} \quad \text{and} \quad B = B_0 \frac{Z^2}{m} \ln(\Lambda_i) \sum_i \frac{Z_i^2 n_i}{\rho} \qquad [52]$$

are collision coefficients. A_0 and B_0 are constants. A describes scattering on electrons and B the scattering on ions. s and v are the distance travelled along the line and the velocity of the charged particles considered. The straight line approximation is fairly accurate as long as the slowing down is mainly due to collisions with electrons. At the end of slowdown, it is not valid, but in this regime, the energy transferred to the thermal plasma is fairly small, so one may expect, that the overall accuracy is good.

Integrating Eq. [51] along a ray one obtains :

$$\Delta s = \int_{v_0 - \Delta v}^{v_0} g(v) \, dv \, , \quad \text{where} \quad g(v) = - (A + \frac{B}{v^3})^{-1} \qquad [53]$$

Naturally the A and B terms depend on the mesh cell under consideration. Eq. [53] Using a first order Taylorexpansion for g(v):

$$g(v) = g(v_0) + (v - v_0) g'(v_0) \qquad [54]$$

in Eq. [53] results in :

$$\Delta s = g(v_0) \Delta v - 0.5 \, g'(v_0)(\Delta v)^2 \qquad [55]$$

Δs is known for each mesh cell and each ray from geometric considerations. Now, Eq. [55] is solved to second order for Δv :

$$\Delta v = \frac{\Delta s}{[g(v_0)(1 - 0.5 \frac{g'(v_0)}{g(v_0)^2} \Delta s)]} \qquad [56]$$

The total energy loss in a zone can be calculated :

$$\Delta E = 0.5m[v_0^2 - (v_0 - \Delta v)^2]N \qquad [57]$$

where N is the number of ions streaming along the ray under consideration. The fraction of this energy deposited to electrons and ions is

$$\Delta E_{elec} = A \frac{\Delta s}{\Delta v} \Delta E \text{ and } \Delta E_{ion} = \Delta E - \Delta E_{elec} \qquad [58]$$

respectively. A detailed derivation of this formalism and the generalization to the time dependent case can be found in /6/. Two main differences between the TDPT and CIRCE code should be noted: (1) the collision coefficients used by CIRCE, Eq. [8] , and TDPT Eq. [52] , are calculated differently and (2) the energy threshhold for defining 'thermal' plasma temperature has not the same meaning. CIRCE uses a global (time and space independent) 'cutoff' energy defined in the input (variable ZCUT) and assumes a-particles below this energy to have completely thermalized. TDPT uses the plasma ion temperature provided by the hydro code in each mesh as the thermalization threshhold.

7.2   Implementation of the Method

A set of subroutines implementing the TDPT method has been obtained from G.A.Moses, University of Wisconsin (Madison). This package is described in detail in /6/. It has been coupled in just the same way as CIRCE to MEDUSA-KA. Time dependent particle tracking takes the following steps:

(1) At a given point of time the hydro part of MEDUSA-KA provides the number of particles newly created; these particles are treated as if they were born at the beginning of the timestep though MEDUSA-KA generates them at the midpoint of the timestep;

(2) these particles are distributed in equal 'bunches' to the number of directions used;

(3) all particle bunches of previous time steps, which are not yet thermalized, are slowed down for the present time step; if they are still not thermalized, they have to be stored for further transport in the next time step calculation;

(4) the new particle bunches of the actual time step are transported and slowed down as far as possible during the present time step;

(5) energy deposition rates can be calculated now from the loss in velocity of each individual bunch of particle.

As can be seen from step (3), one difficulty of the TDPT method might be the amount of memory needed to store bunches of particles from previous time steps. Since there are always certain limitations on the computer memory size, particles that cannot be stored any further are slowed down adiabatically or are simply forgotten (code option). There are some code options which allow to ease that effect (e.g., a separate transport time step, number of time levels different for forward and backward directed bunches). No attempt has been made in this comparison to optimize these input parameters.

Figure 10. Pellet Gain: CIRCE vs. Particle Tracking

Figure 11. Ion Temperature: CIRCE vs. Particle Tracking
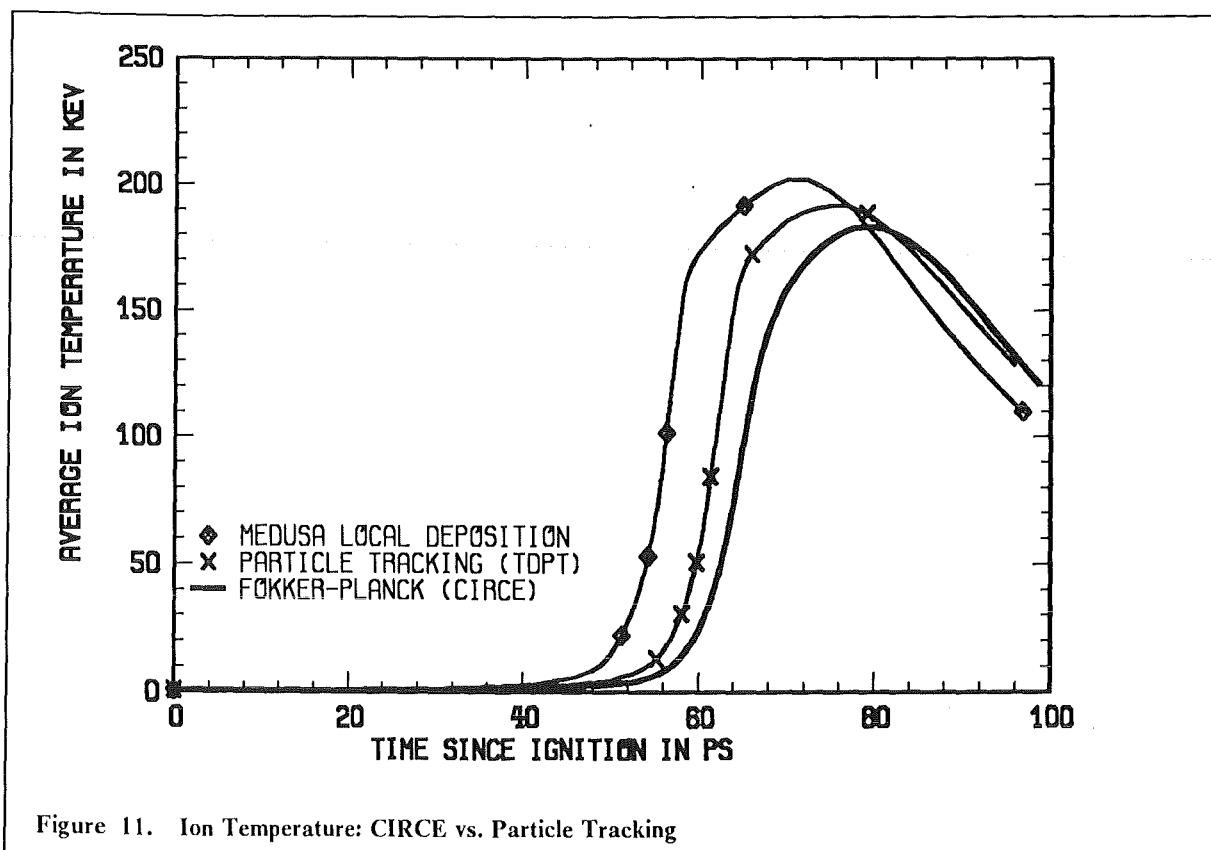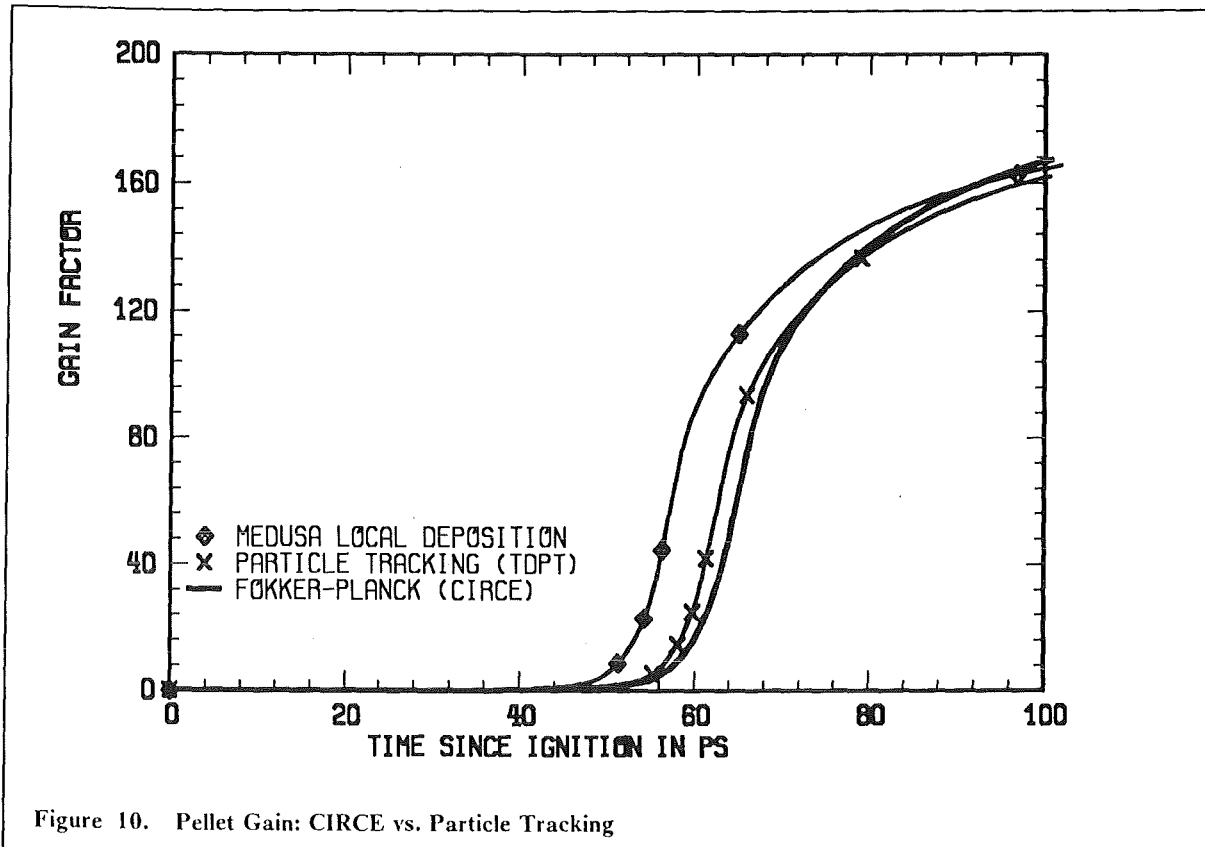
7.3 Comparison with CIRCE

A first variation of the number of directions (MDIR) and the number of time levels (NT) to be stored showed that MDIR = 16 and NT = 20 give sufficient accuracy (Table 5 on page 42), the deviation from the results using MDIR = 16 and NT = 120 is well below 1% for most of the variables displayed. Only the energy deposition rate due to collisions with electrons deviates for almost 6%.

NT	MDIR	Gain	TImax	TEmax	$E_{ion,max}$	$E_{elec,max}$	twave	Effort
0	0	165.5	366.0	148.5	2.165	0.864	56.5	1.0
8	4	162.2	316.6	151.2	1.767	1.088	60.9	1.5
16	4	162.5	320.4	151.7	1.817	1.495	61.3	1.6
16	8	162.0	319.7	151.3	1.806	1.522	62.5	2.0
20	16	161.8	323.4	151.7	1.835	1.056	62.6	3.0
26	16	161.6	323.5	151.5	1.869	1.007	62.8	3.3
120	16	161.8	322.3	151.5	1.842	1.122	62.5	6.9
CIRCE	Ref.	167.4	327.0	144.6	1.351	0.851	64.5	3.4

Note:

NT is the number of time levels to be stored (NT = 0 means local deposition), **MDIR** the number of discrete directions used and **Gain** as calculated by KATACO at approximately 100 ps burnup time

TImax(t_0) given in KeV is defined as : max { T_{ion}(r,t), $R_{inner} \le r \le R_{outer}$, $t_{start} \le t \le t_0$ } where T_{ion} is the ion temperature.

TEmax(t_0) given in KeV is defined as : max { T_{elec}(r,t), $R_{inner} \le r \le R_{outer}$, $t_{start} \le t \le t_0$ } where T_{elec} is the electron temperature.

$E_{ion,max}$(t_0) given in W/kg*1.0E24 is defined as : max { E_{ion}(r,t), $R_{inner} \le r \le R_{outer}$, $t_{start} \le t \le t_0$ } where E_{ion} is the energy deposition rate due to collisions with ions.

$E_{elec,max}$(t_0) given in W/kg*1.0E24 is defined as : max { E_{elec}(r,t), $R_{inner} \le r \le R_{outer}$, $t_{start} \le t \le t_0$ } where E_{elec} is the energy deposition rate due to collisions with electrons.

twave = time after ignition when burn wave reaches outer fuel boundary.

Effort defined as ratio of CPU times used for a whole simulation run using the coupled version over CPU time needed with MEDUSA-KA (local deposition)

Table 5. **Sensitivity of Particle Tracking on Input Specification**
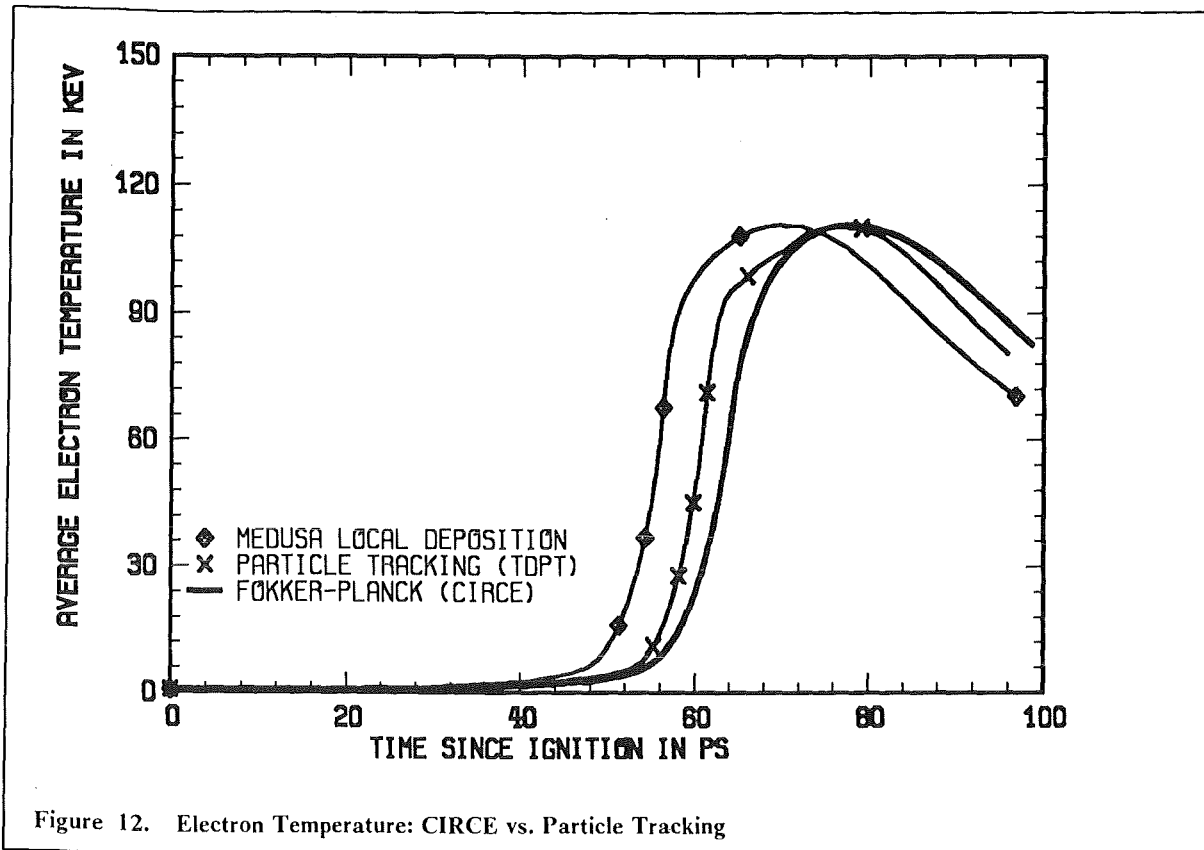
Figure 12.   Electron Temperature: CIRCE vs. Particle Tracking

Comparing the results of CIRCE with those of particle tracking (see Figure 10, Figure 11 , Figure 12 and Table 5, row 5 and last row) clearly shows that particle tracking indicates the same trends as the Fokker-Planck method. The time retardation (indicated by the time twave when the burn wave reaches the outer fuel boundary) is by some 3% smaller than calculated by CIRCE, the remaining variables are in between the values of local deposition option and of Fokker-Planck treatment but tend to be closer to the latter. One remarkable exception are the deposition rates showing a much larger deviation.

The main effect responsible for the deviations between the two codes are the different slowing down coefficients (see Eq. [52] and Eq. [8]). The energy of a-particles is deposited much faster by TDPT, during burn wave propagation some 90% of the total a-particle energy released are already deposited whereas the CIRCE code deposits only 60 to 70%. Naturally, at the end of the simulation, these ratios are almost equal, 94% for the particle tracking and 96% for the Fokker-Planck method. The second effect results from the definition of 'thermal'; whereas the particle tracking code uses the ion plasma temperature of each mesh cell as the cutoff energy, CIRCE uses a fixed (time independent) cutoff energy for all mesh cells and during the whole calculation (the reference calculation used a threshold of 35 KeV).

The increase of CPU time over that of the local deposition option is comparable in both codes (see Table 5 on page 42 , column Effort). The amount of computer memory needed can be roughly estimated by

Storage (TDPT) = NZ * MDIR * NT * 4
Storage (CIRCE) = NZ * MDIR * MNG

where NZ is the total number of meshcells used in the transport calculation, MDIR the number of angles (or of rays) used, MNG the number of energy levels used in CIRCE, and NT the number of time levels to be stored in TDPT. From this estimate, one sees that the tracking code needs at least 4 times more memory than CIRCE does. In the example compared above, comparable accuracy has been achieved with $MDIR = 8$ and 16 and $MNG = 16$ and $NT = 20$, therefore particle tracking needs even more than 4 times the memory size than CIRCE. (Moreover, there is a code option in CIRCE allowing a reduction of this amount by a factor of MNG at the cost of using more CPU time).

One should keep in mind, however, that no attempt has been made to optimize the input values of TDPT responsible for the amount of memory need. Moreover, with present day computer systems, main memory is no longer a critical resource for such spatially one dimensional problems.

In conclusion: the comparison of the Fokker-Planck code CIRCE with the time dependent particle tracking code TDPT shows sufficient agreement of results to consider CIRCE as verified. The differences found can be explained by differences in the methods, especially in the calculation of slowing down coefficients and the treatment of the energy variable. Both codes run roughly at the same speed in the example calculation (HIBALL-I pellet simulation).

Chapter 8. Conclusions

A method to be used as charged (a-) particle transport module has been coupled to the Lagrangian hydro code KATACO. The module, CIRCE, solves the time dependent Fokker-Planck equation. Sample calculations have been done for a-particle transport in the heavy ion driven 4 mg HIBALL target /5/, therefore the conclusions are valid for similar applications of the code. Inclusion of the transport module increased the computing time by a factor of 3 to 4 for the complete simulation. Thus an accurate treatment of transport seems to be quite affordable without too big a penalty.

The adiabatic approximation to a-particle transport, that is, using instantaneous but space dependent a-particle energy deposition, did not substantially improve the results of local deposition. Therefore it is not recommended to use this for realistic target calculations.

A comparison with a different method, the time dependent particle tracking method, showed sufficient agreement of results. The differences found thereby can be explained by differences in the method, especially in the calculation of slowing down coefficients and the treatment of the energy variable. Both methods need comparable computing times to achieve the same accuracy level, but particle tracking requires more computer memory.

Chapter 9. Acknowledgements and References

References

/1/   B.Kiefer, B.Goel, W.Höbel, K.Küfner, "An Updated Version of the MEDUSA Code for Lagrangian Simulation of Hydro- and Thermodynamics of Ion Beam Irradiated Plasmas", unpublished

/2/   J.P.Christiansen et al., "MEDUSA - A One Dimensional Laser Fusion Code", Comp.Phys.Comm., 7 (1974) p.271

       and N.A.Tahir, K.A.Long, "MEDUSA-KA: A One-Dimensional Computer Code for ICF Target Design", Report KfK 3454, Karlsruhe (1983)

/3/   T.M.Tran, J.Ligou, "An Accurate Numerical Method to Solve the Linear Fokker-Planck Equation Characterizing Charged Particle Transport in Spherical Plasmas", Nucl. Sci. Eng., 79 (1981) p.269

       and T.M.Tran, J.Ligou, "Application of the Fokker-Planck Equation to Pellet Ignition Analysis", Trans. ANS, 43 (1982) p.388

/4/   T.M.Tran, "Contribution a l'Etude Theoretique et Numerique de la Fusion par Confinement Inertiel", Ph.D. Thesis, Ecole Polytechnique Federale de Lausanne, Switzerland (1983)

/5/   B.Badger et al., "HIBALL - A Conceptual Heavy Ion Beam Driven Fusion Reactor Study", Report KfK 3202, Karlsruhe (1981)

/6/   G.A.Moses, "Laser Fusion Hydrodynamics Calculations", Nucl. Sci. Eng., 64 (1977) p.49

/7/   P.A.Haldy, J.Ligou, "A Moment Method for Calculating the Transport of Energetic Charged Particles in Hot Plasmas", Nuclear Fusion, 17 (1977), p.1225

/8/   J.Ligou, "The Boltzmann-Fokker-Planck Equation", Transport Theory and Statistical Physics, 15 (1936)

/9/   J.J.Duderstadt, W.R.Martin, "Transport Theory", Wiley Intern. Pub. (1979)

/10/   K.Küfner, "INTERFAC", report in preparation

/11/   J.J.Honrubia, J.M.Aragones, "Finite Element Method for Charged-Particle Calculations", Nucl.Sci.Eng. 93, pp. 386-402, 1986

/12/ G.Buckel, W.Höbel, "Das Karlsruher Programmsystem KAPROS, Teil 1", Report KfK 2253, Karlsruhe, 1976

/13/ T.R.Hill, "TIMEX - A Time-Dependent Explicit Discrete Ordinates Program", LANL-Bericht LA-6201-MS, Los Alamos, 1976

/14/ B.Goel, G.A.Moses, R.R.Peterson, "Proton Stopping in Thin Aluminum Slabs", Laser und Particle Beams, Vol.5, Part 1, 1987

/15/ W.Höbel, K.Küfner, "Numerische Simulation von Teilchen- und Strahlungstransportprozessen", KfK-Nachrichten 3/88, Karlsruhe, 1988, p.169

Appendix A. Code Interfaces

A.1 Index of Subroutines

```
          SUBROUTINES OF THE CIRCE PACKAGE
CIRCE     FORTRAN MAIN SUBROUTINE
A1A2A3    OBTAIN TIME AND SPACE DERIVATIVES OF VELOCITY
BEAM      DEFINE BOUNDARY CONDITIONS FOR INCOMING BEAM
VOLSOU    DEFINE VOLUMIC PARTICLE SOURCE
SIGMA1    CALCULATE THE COLLISION COEFFICIENTS S AND T
CALPSI    CALCULATE THE ANG. FLUX FOR ENERGY GROUP JGRP
MACRO     ENERGY AND POWER BALANCE EQUATIONS
GH        CALCULATE THE FUNCTION G AND H (USED IN SIGMA1
SOLVE     SOLVE A TRIDIAGONAL SYSTEM OF EQUATIONS
MWRITi    AUXILIARY I/O-ROUTINES
MREADi    AUXILIARY I/O-ROUTINES
MREWIi    AUXILIARY I/O-ROUTINES

          ADDITIONAL SERVICE SUBROUTINES FROM KATACO
RESETR    CLEARS A REAL ARRAY TO ZERO
COPYR     COPIES A REAL ARRAY INTO ANOTHER REAL ARRAY
MESAGE    PRINTS OUT MESSAGES

          ADDITIONAL SUBROUTINES TO PERFORM THE COUPLING
MEDCIR    REALIZES THE COPULING BETWEEN KATACO AND CIRCE
CIRDIA    CALCULATES AND PRINTS DIAGNOSTIC QUANTITIES
ENDEPO    CALCULATES ENERGY DEPOSITION IN DIFFERENT REGIONS
```

A.2 CIRCE Calling List

The sequence of arguments for calling CIRCE is the same as indicated in the following two tables, first the input, afterwards the output variables. There are only two exceptions, KXP1 and KNGP1, which are the second-last and last parameters in the calling list. The arrays (Type = RA = REAL Arrays) are dimensioned as follows: PRAD(KXP1), PRHO(KX), PV(KX), PDU1(KX), PDU2(KX), PDU3(KX), PTE(KX), PTI(KX), PMIEFF(KX), PEFFZ(KX), PSOUR(KX), PYE(KX), PYI(KX), PYTH(KX), PEG(KNGP1), PJOUT(KNG), PJEOUT(KNG).

Argument	Description	Unit	Type
KMODE	SPECIFY MODE OF OPERATION		I
KTRANS	FAST ION NUMBER		I
KKDIR	NUMBER OF DIRECTIONS		I
KNG	NUMBER OF ENERGY GROUPS		I
KNGP1	KNG + 1		I
KFREQ	REPETITION RATE OF TRANSPORT CALCULATIONS		I
KINER	NUMBER OF INNER ITERATIONS		I
NGEOM	GEOMETRY INDEX (= 1:SLAB, = 3:SPHERE)		I
KX	NUMBER OF CELL BOUNDARIES (HOST MEDIUM)		I
KXP1	KX + 1		I
KX1	INNER BOUNDARY CELL NUMBER		I
KX2	OUTER BOUNDARY CELL NUMBER		I
PCUT	CUT OFF ENERGY / MAXIMUM ENERGY		R
PDPSI	MAX. DEVIATION FOR ANGULAR FLUX		R
PTIME	PROBLEM TIME		R
PKHI	TIME DEPENDENT NORMALIZATION FACTOR		R
PKHIP	RATIO OF PKHI(LEVEL n-1) / PKHI(LEVEL n)		R
PRAD	COORDINATES OF CELL BOUNDARIES (HOST MEDIUM)		RA
PRHO	DENSITY OF HOST MEDIUM		RA
PV	SPECIFIC VOLUME OF HOST MEDIUM		RA
PDU1	TIME DERIVATIVE OF HOST VELOCITY		RA
PDU2	GRADIENT OF HOST VELOCITY		RA
PDU3	HOST VELOCITY / SPACE		RA
PTE	ELECTRON TEMPERATURE		RA
PTI	ION TEMPERATURE		RA
PMIEFF	AVERAGE HOST ION MASS NUMBER		RA
PEFFZ	AVERAGE HOST ION CHARGE NUMBER		RA
PSOUR	DISTRIBUTION OF ISOTROPIC VOLUME SOURCE		RA
PBEAM	POWER OF INCOMING BEAM		R
PBMU	DIRECTION OF INCOMING BEAM		R
PSINT	INTEGRATED VOLUME SOURCE		R
PAION	MASS NUMBER OF FAST ION	amu	R
PZION	CHARGE NUMBER OF FAST ION		R
PEION	MAX. KINETIC ENERGY OF FAST ION	eV	R
Note: SI units used unless mentioned explicitly			

Table 6.   **Input Arguments for CIRCE Calling List**

Argument	Description	Unit	Type
PYE	VOLUMIC POWER DEPOSITION TO ELECTRONS	W/kg	RA
PYI	VOLUMIC POWER DEPOSITION TO IONS	W/kg	RA
PYTH	RATE OF THERM. ION PRODUCTION IN EACH CELL	1./s	RA
PEG	PARTICLE ENRGIES	eV	RA
PJOUT	PARTICLE CURRENT LEAKAGE SPECTRUM (NORMALIZED)		RA
PJEOUT	ENERGY CURRENT LEAKAGE SPECTRUM (NORMALIZED)		RA
PEDEPO	DEPOSITED ENERGY	J	R
PEINER	INERTIA TERM	J	R
PEINPT	TOTAL INPUT ENERGY	J	R
PELEAK	LEAKAGE ENERGY	J	R
PESUPR	SUPRATHERMAL ION ENERGY	J	R
PEEROR	ERROR IN ENERGY BALANCE	J	R
PPDEPO	DEPOSITED POWER	W	R
PPINER	INERTIA TERM	W	R
PPINPT	TOTAL INPUT POWER	W	R
PPLEAK	LEAKAGE POWER	W	R
PPSUPR	SUPRATHERMAL ION POWER	W	R
PPEROR	ERROR IN POWER BALANCE	W	R
Note: SI units used unless mentioned explicitly			

Table 7.   Output Arguments for CIRCE Calling List

A.3 COMMON Block Structure

All COMMON variables use SI units unless mentioned explicitly. Angular fluxes are used in $1/(m^2 \ \text{eV s ster})$

The array CONTAI in COMMON block /COMWOR/ is used to store the information from the previous time step calculation. It is used to avoid external I/O, CIRCE switches automatically to disk storage should the length of CONTAI be to small to hold this information. CONTAI is dimensioned by a PARAMETER statement.

A.3.1 COMMON-Block Usage Ordered by Subroutines

SUBROUTINE	USES COMMON BLOCKS
A1A2A3	COMCI2, COMCI3, COMTIM
BEAM	COMCI2, COMCI3, COMTIM
CALPSI	COMCI2, COMCI3, COMTIM
CIRCE	COMCI2, COMCI3, COMTIM, COMWOR
CIRDIA	COMADM, COMBAS, COMCI4, COMCON, COMCPT, COMDDP, COMEN, COMFUS, COMHYD, COMIE, COMLAS, COMNC, COMNUM, COMOUT, COMTH, COMTIM
FUSIO2	COMADM, COMCON, COMDDP, COMFUS, COMHYD, COMIE, COMNUM, COMTH
GH	COMTIM
MACRO	COMCI2, COMCI3, COMTIM
MEDCIR	COMADM, COMBAS, COMCI4, COMCON, COMCPT, COMDDP, COMEN, COMFUS, COMHYD, COMIE, COMLAS, COMNC, COMNUM, COMOUT, COMTH, COMTIM
MREAD1	COMWOR
MREAD2	COMWOR
MREAD3	COMWOR
MREAD4	COMWOR
MREWI1	COMWOR
MREWI2	COMWOR
MWRIT1	COMWOR
MWRIT2	COMWOR
MWRIT3	COMWOR
MWRIT4	COMWOR
SIGMA1	COMCI2, COMCI3, COMTIM
SOLVE	COMCI3, COMTIM
VOLSOU	COMCI2, COMCI3, COMTIM

A.3.2 COMMON-Block Usage Ordered by COMMON-Names

COMMON	USED IN SUBROUTINE
COMADM	CIRDIA, FUSIO2, MEDCIR
COMBAS	CIRDIA, MEDCIR
COMCI2	A1A2A3, BEAM, CALPSI, CIRCE, MACRO, SIGMA1, VOLSOU
COMCI3	A1A2A3, BEAM, CALPSI, CIRCE, MACRO, SIGMA1, SOLVE, VOLSOU
COMCI4	CIRDIA, MEDCIR
COMCON	CIRDIA, FUSIO2, MEDCIR
COMCPT	CIRDIA, MEDCIR
COMDDP	CIRDIA, FUSIO2, MEDCIR
COMEN	CIRDIA, MEDCIR
COMFUS	CIRDIA, FUSIO2, MEDCIR
COMHYD	CIRDIA, FUSIO2, MEDCIR
COMIE	CIRDIA, FUSIO2, MEDCIR
COMLAS	CIRDIA, MEDCIR
COMNC	CIRDIA, MEDCIR
COMNUM	CIRDIA, FUSIO2, MEDCIR
COMOUT	CIRDIA, MEDCIR
COMTH	CIRDIA, FUSIO2, MEDCIR
COMTIM	A1A2A3, BEAM, CALPSI, CIRCE, CIRDIA, GH, MACRO, MEDCIR, SIGMA1, SOLVE, VOLSOU
COMWOR	CIRCE, MREAD1, MREAD2, MREAD3, MREAD4, MREWI1, MREWI2, MWRIT1, MWRIT2, MWRIT3, MWRIT4

A.3.3 Index of COMMON Variables

Variable	Description	Unit	Type
A1	TIME DERIVATIVE OF IMPULSION	eV/m	RA
A2	GRADIENT OF IMPULSION	$eV\text{*}s/m^2$	RA
A3	IMPULSION / SPACE	$eV\text{*}s/m^2$	RA
AION	MASS NUMBER OF FAST IONS		R
ALPHAK	DIRECTION REDISTRIBUTION TERM		RA
AMU	PITCH ANGLE COSINE		RA
AREA	AREA OF CELLS		RA
CENT	WORKING ARRAYS		RA
DPSIMX	MAX. DEVIATION FOR ANGULAR FLUX		R
DT0,DT1	OLD (NEW) TRANSPORT TIMESTEP		R
EDEPO	DEPOSITED ENERGY		R
EEROR	ERROR IN ENERGY BALANCE		R
EG	ENERGY GROUP BOUNDARIES	eV	RA
EINER	INERTIA TERM	J	R
EINPT	TOTAL INPUT ENERGY		R
EION	MAX. KINETIC ENERGY OF FAST IONS	eV	R
ELEAK	LEAKAGE ENERGY		R
ESUPR0	SUPRATHERMAL ION ENERGY (LEVEL n-1)	J	R
ESUPR1	SUPRATHERMAL ION ENERGY (LEVEL n	J	R
FA	COEFFICIENT IN FMR EQUATION		RA
FB	COEFFICIENT IN FMR EQUATION		RA
FC	COEFFICIENT IN FMR EQUSTION		RA
FD	COEFFICIENT IN FMR EQUATION		RA
FIX	FMR PARAMETERS		RA
KHI	TIME DEPENDENT NORMALIZATION FACTOR		R
KHIPRI	RATIO OF KHI(LEVEL n-1) / KHI(LEVEL n)		R
PDEPO0	RATE OF ENERGY DEPOSITION (LEVEL n-1)		R
PDEPO1	RATE OF ENERGY DEPOSITION (LEVEL n)		R
PEROR	ERROR IN POWER BALANCE		R
PINER0	INERTIA TERM AT LEVEL n-1	W	R
PINER1	INERTIA TERM AT LEVEL n	W	R
PINPT0	INPUT POWER AT LEVEL n-1		R
PINPT1	INPUT POWER AT LEVEL n		R
PLEAK0	LEAKAGE POWER AT LEVEL n-1		R
PLEAK1	LEAKAGE POWER AT LEVEL n		R
PSIBND	INCOMING ANGULAR FLUX		RA
PSICEN	ANGULAR FLUX AT THE CENTER OF (R,E) CELL (LEVEL n)		RA

Variable	Description	Unit	Type
PSINOR	ANGULAR FLUX AT THE NORTH FACE OF (R,E) CELL (LEVEL n)		RA
PSIOLC	ANGULAR FLUX AT THE CENTER OF (R,E) CELL (LEVEL n-1)		RA
PSIOLN	ANGULAR FLUX AT THE NORTH FACE OF (R,E) CELL (LEVEL n-1)		RA
PSIOLS	ANGULAR FLUX AT THE SOUTH FACE OF (R,E) CELL (LEVEL n-1)		RA
PSISTH	ANGULAR FLUX AT THE SOUTH FACE OF (R,E) CELL (LEVEL n)		RA
PSUPR0	SUPRATHERMAL ION POWER (LEVEL n-1)	W	R
PSUPR1	SUPRATHERMAL ION POWER (LEVEL n)	W	R
SEG	STOPPING POWER BY ELECTRONS	eV/m	RA
SIG	STOPPING POWER BY IONS	eV/m	RA
SOURCE	VOLUMIC PARTICLE SOURCE	$1/(sm^3eV)$	RA
T0	SIMULATION TIME AT LEVEL n-1		R
T1	SIMULATION TIME AT LEVEL n		R
TA	COEFFICIENT IN ANGULAR FLUX EQUATION		RA
TB	COEFFICIENT IN ANGULAR FLUX EQUATION		RA
TC	COEFFICIENT IN ANGULAR FLUX EQUATION		RA
TD	COEFFICIENT IN ANGULAR FLUX EQUATION		RA
TDEFL	ANGULAR DEFLECTION TERM	1/m	RA
VOL0,1	VOLUME OF SPATIAL CELL AT LEVEL n-1 and n, respectively		RA
WMU	ANGULAR WEIGTHING FACTOR		RA
YDEPE	VOLUMIC POWER DEPOSITION TO ELECTRONS	W/m^3	RA
YDEPI	VOLUMIC POWER DEPOSITION TO IONS	W/m^3	RA
YTHERM	RATE OF THERMALIZED PARTICLE PRODUCTION	$1/(sm^3)$	RA
ZION	CHARGE NUMBER OF FAST IONS		R
JGRP	CURRENT ENERGY GROUP NUMBER		I
ISTEP	STEP NUMBER OF TRANSPORT CALCULATION		I
KDIR	NUMBER OF DIRECTIONS		I
KDIRN	NUMBER OF NEGATIVE-MU DIRECTIONS		I
KDIRP	NUMBER OF POSITIVE-MU DIRECTIONS		I
MMESH	NUMBER OF SPACE CELLS		I
NFREQ	REPETITION RATE OF TRANSPORT CALCULATIONS		I
KGEOM	GEOMETRY FACTOR (= 1:SLAB, = 3:SPHERE)		I
NGRP	NUMBER OF ENERGY GROUPS		I
NPT	TOTAL NUMBER OF DIRECTION-SPACE CELLS		I
NINER	NUMBER OF MAX. INNER ITERATIONS		I
NLBEAM	SWITCH FOR INCOMING BEAM B.C.		L
NLSOUR	SWITCH FOR ISOTROPIC VOLUME SOURCE		L
NLSTAT	SWITCH FOR ADIABATIC TRANSPORT		L

Table 8.   /COMCI2/ - Variables for Internal Use in CIRCE

Variable	Description	Unit	Type
NPERM	SCRATCH FILE PARAMETER		IA
NSAVE	SCRATCH FILE CHANNEL NUMBER		IA
NWRITE	SCRATCH FILE CHANNEL NUMBER		IA

Table 9. /COMCI3/ - File Numbers for Disk Storage Option

Variable	Description	Unit	Type
CONTAI	CONTAINER ARRAY USED TO STORE INTERMEDIATE DATA		RA
LREC1	POINTER TO CONTAI FOR READING		I
LREC2	POINTER TO CONTAI FOR WRITING		I
NSAVEI	DISK UNIT NUMBER FOR READING		I
NWRITI	DISK UNIT NUMBER FOR WRITING		I
LIO	USE EXTERNAL I/O OR ARRAY CONTAI FOR STORING		L

Table 10. /COMWOR/ - Array Used to Store Information between Timesteps

Variable	Description	Unit	Type
MODE	SPECIFY MODE OF OPERATION		I
MDIR	NUMBER OF DIRECTIONS		I
MNG	NUMBER OF ENERGY GROUPS		I
MFREQ	REPETITION RATE OF TRANSPORT CALCULATIONS		I
MINER	NUMBER OF INNER ITERATIONS		I
MX1	INNER BOUNDARY CELL NUMBER		I
MX2	OUTER BOUNDARY CELL NUMBER		I
NLALTR	=T IF ALPHA TRANSPORT IS TO BE DONE USING CIRCE		L
NLCIRC	=T DURING ADDITIONAL MEDUSA ITERATIONS		L
NLENTR	=F IF ALPHA SOURCE IS TOO SMALL		L
NLPREX	CONTROLS THE FREQUENCY OF DIAGNOSTIC CIRCE OUTPUT		L
ZCUT	CUT OFF ENERGY / MAXIMUM ENERGY		R
ZAMU	DIRECTION OF INCOMING BEAM		R
ZAION	MASS NUMBER OF FAST ION	amu	R
ZZION	CHARGE NUMBER OF FAST ION		R
ZEION	MAX. KINETIC ENERGY OF FAST ION		R
ZDPSI	MAX. DEVIATION FOR ANGULAR FLUX		R
RALPH1	INTEGRATED ION SOURCE AT TIME T1		R
RALPH3	INTEGRATED ION SOURCE AT TIME T3		R

Table 11. /COMCPT/ - Input Variables from Namelist &CPATR

Variable	Description	Unit	Type
ICNT	COUNTS THE NUMBER OF CALLS TO CIRCE		I
BUF10	AUXILIARY STORAGE ARRAY		RA
BUF11	AUXILIARY STORAGE ARRAY		RA
BUF12	AUXILIARY STORAGE ARRAY		RA
BUF13	AUXILIARY STORAGE ARRAY		RA
BUF14	AUXILIARY STORAGE ARRAY		RA
BUF15	AUXILIARY STORAGE ARRAY		RA
BUF16	AUXILIARY STORAGE ARRAY		RA
BUF17	AUXILIARY STORAGE ARRAY		RA
BUF18	AUXILIARY STORAGE ARRAY		RA
BUF19	AUXILIARY STORAGE ARRAY		RA
BUF20	AUXILIARY STORAGE ARRAY		RA
BUF21	AUXILIARY STORAGE ARRAY		RA
DU1	TIME DERIVATIVE OF HOST VELOCITY		RA
DU2	GRADIENT OF HOST VELOCITY		RA
DU3	HOST VELOCITY / SPACE		RA
ZEINPT	INPUT ENERGY	J	R
ZEDEPO	RATE OF ENERGY DEPOSITION	J	R
ZESUPR	SUPRATHERMAL ION ENERGY	J	R
ZELEAK	LEAKAGE ENERGY	J	R
ZEINER	INERTIA TERM	J	R
ZEEROR	ERROR IN ENERGY BALANCE		R
ZPINPT	INPUT POWER	W	R
ZPDEPO	RATE OF POWER DEPOSITION	W	R
ZPSUPR	SUPRATHERMAL ION POWER	W	R
ZPLEAK	LEAKAGE POWER	W	R
ZPINER	INERTIA TERM	W	R
ZPEROR	ERROR IN POWER BALANCE		R

Table 12. /COMCI4/ - Auxiliary Arrays Used in MEDUSA-KA for the Coupling

Variable	Description	Unit	Type
KCPU	TOTAL CPU TIME USED BY CIRCE		I
KCPU1	TOTAL CPU TIME USED BY A1A2A3		I
KCPU2	TOTAL CPU TIME USED BY BEAM		I
KCPU3	TOTAL CPU TIME USED BY VOLSOU		I
KCPU4	TOTAL CPU TIME USED BY SIGMA1		I
KCPU5	TOTAL CPU TIME USED BY CALPSI		I
KCPU6	TOTAL CPU TIME USED BY MACRO		I
KCPU7	TOTAL CPU TIME USED BY GH		I
KCPU8	TOTAL CPU TIME USED BY SOLVE		I

Table 13.   /COMTIM/ - CIRCE Internal Time Measurement Variables
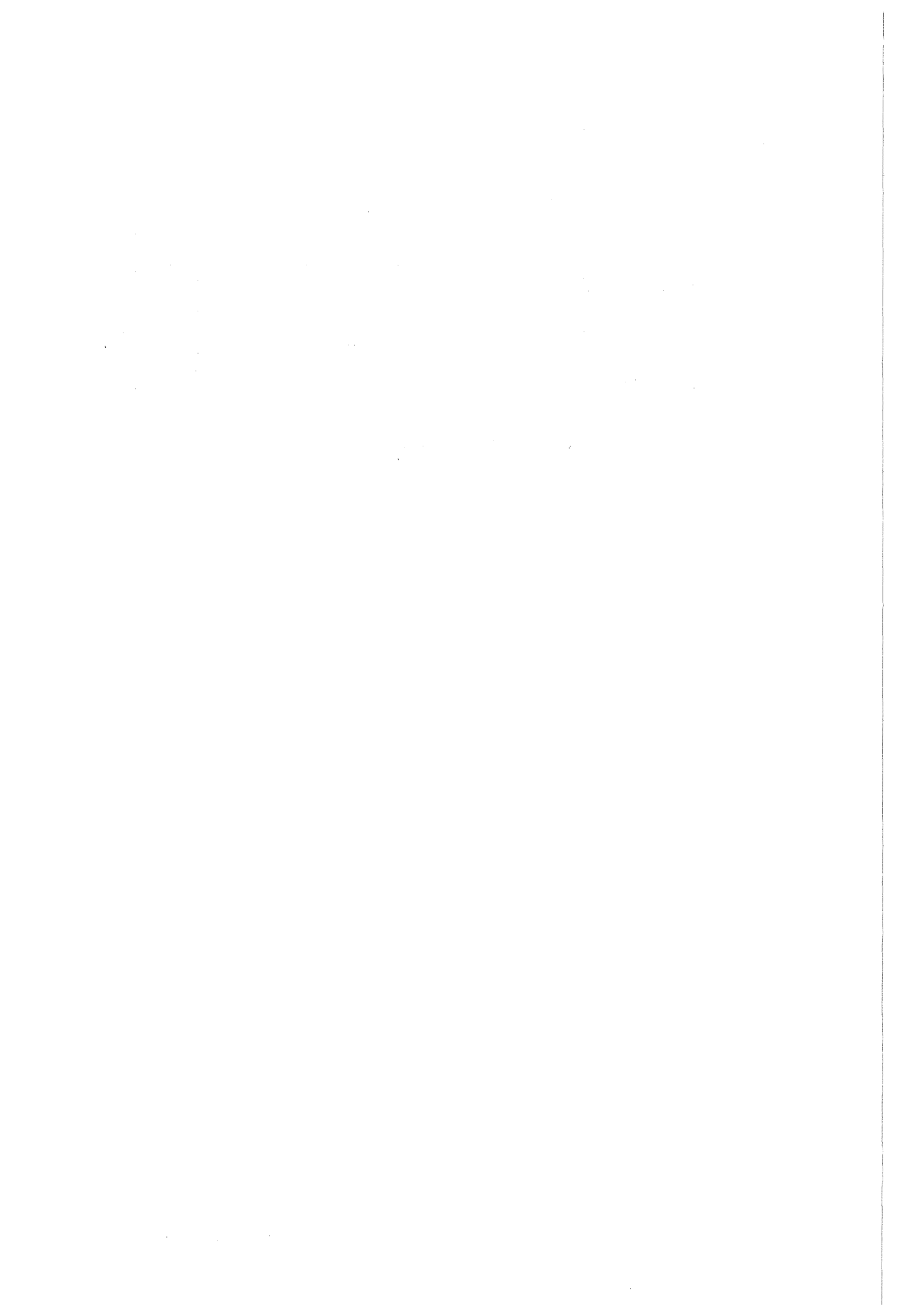
Appendix B. Sample Calculation

B.1 Input for Sample Calculation

```
TEST CASE : HIBALL TARGET

COUPLED MEDUSA - CIRCE - VERSION

&NEWRUN
 NDUMP=400, NLHCPY=.TRUE.,NHDCPY=10,MESH= 90,
 DELTAT=1.0E-18,NRUN=9000,PIQ(70)=1.,
 LASER1(21)=1.97,LASER1(22)=0.5,LASER1(23)=1.5E-8,LASER1(24)=2.1E-8,
 LASER1(25)=2.4E-8,LASER1(26)=3.10E-8,LASER1(27)=1.90E11,NPRNT=100,
 LASER1(28)=2.39E12,LASER1(29)=3.98E13,
 PIQ(71)=1.0,PIQ(72)=1.0,SAHA=1.0,NLPFE=F,STATE=3.0,
 TINUCL=3.5E7,TEINI=500.0,TIINI=500.0,NLBRMS=F,
 LASER1(4)=2.4E-8,LASER1(5)=1.0,LASER1(6)=1.4E13,NP3=1,
&END
&CPATR
 NLALTR=T,NPRCPT=-100,
 MDIR=4,MNG=4,MODE=1,MX1=1,MX2=45,
 ZDPSI=1.0E-1,ZCUT=0.1,
&END
&BMPAR
 IBOPT=4, NBEAM=1, IBPRNT=1,
 BEAMA=1., BEAMZ=1., ANGLE=16.,
 BEAMT=0.0, 10.0E-9, 16.0E-9, 20.0E-9, 28.0E-9, 32.0E-9,
        42.0E-9, 48.0E-9, 54.0E-9, 74.0E-9, 90.0E-9,
 BEAMV(1,1)= 0.3E3,  1.0E3,  1.35E3, 1.25E3, 1.5E3,  1.35E3,
        1.51E3,  1.3E3,  1.25E3,  0.6E3,  0.0,
 BEAMC(1,1)= 0.0,  0.13E10,  0.165E10,  0.265E10, 0.33E10,
        0.4E10,  0.465E10,  0.5E10,  0.51E10,  0.43E10,  0.4E10,
&END
&TARGET
 NZONE=4,
 RINI=0.0,
 NCEL= 1,39, 35, 15,
 THICK=0.302E-2,0.15E-3, 0.37E-3, 0.14E-3,
 RHO= 0.1E-11,224., 1.26E3, 1.13E4,
```

```
MISCH=1,2, 1, 1,
ATW(1,1)=1.,ATW(2,1)=2., ATW(2,2)=3.,ATW(3,1)=16.48,
ATW(4,1)=207.12,
ZN(1,1)=1.,ZN(2,1)=1.,ZN(2,2)=1.,ZN(3,1)=7.,ZN(4,1)=82.,
FRC(1,1)=1.,FRC(2,1)=0.5, FRC(2,2)=0.5,FRC(3,1)=1.,
FRC(4,1)=1.,
&END
```

C I R C E   INITIALISED FOR ALPHA TRANSPORT AT TIME = 0.0000000E+00

```
MASS NUMBER OF ION  . . . . . . . . . . .   4.000E+00
MAXIMUM KINETIC ENERGY  . . . . . . . . .   3.520E+06
CHARGE NUMBER OF ION  . . . . . . . . . .   2.000E+00
DIRECTION OF INCOMING BEAM  . . . . . . . -1.000E+00
MAXIMUM DEVIATION FOR ANGULAR FLUX  . . .   1.000E-03
NUMBER OF SN-DIRECTIONS . . . . . . . . .           8
NUMBER OF ENERGY GROUPS . . . . . . . . .          15
INNER BOUNDARY CELL NUMBER  . . . . . . .           1
OUTER BOUNDARY CELL NUMBER  . . . . . . .          40
MAXIMUM NUMBER OF INNER ITERATIONS  . . .          20
MODE OF OPERATION . . . . . . . . . . . .           1
REPETITION RATE OF TRANSPORT CALCULATIONS           1
CUT OFF ENERGY / MAXIMUM ENERGY . . . . .   1.000E-02
```

TIMESTEP NUMBER   0   TIME =   0.0000000E+00   DELTA T =   1.0000001E-18
--------------------   ---------------------   -------------------------

BOUNDARY :   R = 3.6800E-03   U =   0.0000E+00   P = 1.0000E-60   TI = 0.0000E+00   TE = 0.0000E+00   SOUND SPEED = 1.2146E+02

ENERGIES :   THERMAL -7.53801E+01   KINETIC 0.00000E+00   NUCLEAR 0.00000E+00   ERROR 0.00000E+00   RHO R 3.29772E+01

LASER POWER :   1.90000E+11 WATTS   TOTAL ENERGY INPUT FROM LASER 0.00000E+00 JOULE   ABSORPTION AT R = 3.2281E-03

CELL NO	COORDINATES M	HYDRODYNAMIC VELOCITY	HYDRODYNAMIC PRESSURE	DENSITY	TEMPERATURE (KEV) ION	TEMPERATURE (KEV) ELECTRON	AVERAGE CHARGE
1	0.0000E+00	0.0000E+00	8.2776E-06	1.0000E-12	4.3103E-05	4.3103E-05	1.0000
2	3.0200E-03	0.0000E+00	1.0001E+08	2.2400E+02	4.3103E-05	4.3103E-05	1.0000
3	3.0238E-03	0.0000E+00	1.0001E+08	2.2400E+02	4.3103E-05	4.3103E-05	1.0000
4	3.0277E-03	0.0000E+00	1.0001E+08	2.2400E+02	4.3103E-05	4.3103E-05	1.0000
5	3.0315E-03	0.0000E+00	1.0001E+08	2.2400E+02	4.3103E-05	4.3103E-05	1.0000
6	3.0354E-03	0.0000E+00	1.0001E+08	2.2400E+02	4.3103E-05	4.3103E-05	1.0000
7	3.0392E-03	0.0000E+00	1.0001E+08	2.2400E+02	4.3103E-05	4.3103E-05	1.0000
8	3.0431E-03	0.0000E+00	1.0001E+08	2.2400E+02	4.3103E-05	4.3103E-05	1.0000
9	3.0469E-03	0.0000E+00	1.0001E+08	2.2400E+02	4.3103E-05	4.3103E-05	1.0000
10	3.0508E-03	0.0000E+00	1.0001E+08	2.2400E+02	4.3103E-05	4.3103E-05	1.0000
11	3.0546E-03	0.0000E+00	1.0001E+08	2.2400E+02	4.3103E-05	4.3103E-05	1.0000
12	3.0585E-03	0.0000E+00	1.0001E+08	2.2400E+02	4.3103E-05	4.3103E-05	1.0000
13	3.0623E-03	0.0000E+00	1.0001E+08	2.2400E+02	4.3103E-05	4.3103E-05	1.0000
14	3.0662E-03	0.0000E+00	1.0001E+08	2.2400E+02	4.3103E-05	4.3103E-05	1.0000
15	3.0700E-03	0.0000E+00	1.0001E+08	2.2400E+02	4.3103E-05	4.3103E-05	1.0000
16	3.0738E-03	0.0000E+00	1.0001E+08	2.2400E+02	4.3103E-05	4.3103E-05	1.0000
17	3.0777E-03	0.0000E+00	1.0001E+08	2.2400E+02	4.3103E-05	4.3103E-05	1.0000
18	3.0815E-03	0.0000E+00	1.0001E+08	2.2400E+02	4.3103E-05	4.3103E-05	1.0000
19	3.0854E-03	0.0000E+00	1.0001E+08	2.2400E+02	4.3103E-05	4.3103E-05	1.0000
20	3.0892E-03	0.0000E+00	1.0001E+08	2.2400E+02	4.3103E-05	4.3103E-05	1.0000
21	3.0931E-03	0.0000E+00	1.0001E+08	2.2400E+02	4.3103E-05	4.3103E-05	1.0000
22	3.0969E-03	0.0000E+00	1.0001E+08	2.2400E+02	4.3103E-05	4.3103E-05	1.0000
23	3.1008E-03	0.0000E+00	1.0001E+08	2.2400E+02	4.3103E-05	4.3103E-05	1.0000
24	3.1046E-03	0.0000E+00	1.0001E+08	2.2400E+02	4.3103E-05	4.3103E-05	1.0000
25	3.1085E-03	0.0000E+00	1.0001E+08	2.2400E+02	4.3103E-05	4.3103E-05	1.0000
26	3.1123E-03	0.0000E+00	1.0001E+08	2.2400E+02	4.3103E-05	4.3103E-05	1.0000
27	3.1162E-03	0.0000E+00	1.0001E+08	2.2400E+02	4.3103E-05	4.3103E-05	1.0000
28	3.1200E-03	0.0000E+00	1.0001E+08	2.2400E+02	4.3103E-05	4.3103E-05	1.0000
29	3.1238E-03	0.0000E+00	1.0001E+08	2.2400E+02	4.3103E-05	4.3103E-05	1.0000
30	3.1277E-03	0.0000E+00	1.0001E+08	2.2400E+02	4.3103E-05	4.3103E-05	1.0000
31	3.1315E-03	0.0000E+00	1.0001E+08	2.2400E+02	4.3103E-05	4.3103E-05	1.0000
32	3.1354E-03	0.0000E+00	1.0001E+08	2.2400E+02	4.3103E-05	4.3103E-05	1.0000
33	3.1392E-03	0.0000E+00	1.0001E+08	2.2400E+02	4.3103E-05	4.3103E-05	1.0000
34	3.1431E-03	0.0000E+00	1.0001E+08	2.2400E+02	4.3103E-05	4.3103E-05	1.0000
35	3.1469E-03	0.0000E+00	1.0001E+08	2.2400E+02	4.3103E-05	4.3103E-05	1.0000
36	3.1508E-03	0.0000E+00	1.0001E+08	2.2400E+02	4.3103E-05	4.3103E-05	1.0000
37	3.1546E-03	0.0000E+00	1.0001E+08	2.2400E+02	4.3103E-05	4.3103E-05	1.0000
38	3.1585E-03	0.0000E+00	1.0001E+08	2.2400E+02	4.3103E-05	4.3103E-05	1.0000
39	3.1623E-03	0.0000E+00	1.0001E+08	2.2400E+02	4.3103E-05	4.3103E-05	1.0000
40	3.1662E-03	0.0000E+00	1.0001E+08	2.2400E+02	4.3103E-05	4.3103E-05	1.0000

41	3.1700E-03	0.0000E+00	1.0001E+08	1.2600E+03	4.3103E-05	4.3103E-05	1.4101
42	3.1806E-03	0.0000E+00	1.0001E+08	1.2600E+03	4.3103E-05	4.3103E-05	1.4101
43	3.1911E-03	0.0000E+00	1.0001E+08	1.2600E+03	4.3103E-05	4.3103E-05	1.4101
44	3.2017E-03	0.0000E+00	1.0001E+08	1.2600E+03	4.3103E-05	4.3103E-05	1.4101
45	3.2123E-03	0.0000E+00	1.0001E+08	1.2600E+03	4.3103E-05	4.3103E-05	1.4101
46	3.2229E-03	0.0000E+00	1.0001E+08	1.2600E+03	4.3103E-05	4.3103E-05	1.4101
47	3.2334E-03	0.0000E+00	1.0001E+08	1.2600E+03	4.3103E-05	4.3103E-05	1.4101
48	3.2440E-03	0.0000E+00	1.0001E+08	1.2600E+03	4.3103E-05	4.3103E-05	1.4101
49	3.2546E-03	0.0000E+00	1.0001E+08	1.2600E+03	4.3103E-05	4.3103E-05	1.4101
50	3.2651E-03	0.0000E+00	1.0001E+08	1.2600E+03	4.3103E-05	4.3103E-05	1.4101
51	3.2757E-03	0.0000E+00	1.0001E+08	1.2600E+03	4.3103E-05	4.3103E-05	1.4101
52	3.2863E-03	0.0000E+00	1.0001E+08	1.2600E+03	4.3103E-05	4.3103E-05	1.4101
53	3.2969E-03	0.0000E+00	1.0001E+08	1.2600E+03	4.3103E-05	4.3103E-05	1.4101
54	3.3074E-03	0.0000E+00	1.0001E+08	1.2600E+03	4.3103E-05	4.3103E-05	1.4101
55	3.3180E-03	0.0000E+00	1.0001E+08	1.2600E+03	4.3103E-05	4.3103E-05	1.4101
56	3.3286E-03	0.0000E+00	1.0001E+08	1.2600E+03	4.3103E-05	4.3103E-05	1.4101
57	3.3391E-03	0.0000E+00	1.0001E+08	1.2600E+03	4.3103E-05	4.3103E-05	1.4101
58	3.3497E-03	0.0000E+00	1.0001E+08	1.2600E+03	4.3103E-05	4.3103E-05	1.4101
59	3.3603E-03	0.0000E+00	1.0001E+08	1.2600E+03	4.3103E-05	4.3103E-05	1.4101
60	3.3709E-03	0.0000E+00	1.0001E+08	1.2600E+03	4.3103E-05	4.3103E-05	1.4101
61	3.3814E-03	0.0000E+00	1.0001E+08	1.2600E+03	4.3103E-05	4.3103E-05	1.4101
62	3.3920E-03	0.0000E+00	1.0001E+08	1.2600E+03	4.3103E-05	4.3103E-05	1.4101
63	3.4026E-03	0.0000E+00	1.0001E+08	1.2600E+03	4.3103E-05	4.3103E-05	1.4101
64	3.4131E-03	0.0000E+00	1.0001E+08	1.2600E+03	4.3103E-05	4.3103E-05	1.4101
65	3.4237E-03	0.0000E+00	1.0001E+08	1.2600E+03	4.3103E-05	4.3103E-05	1.4101
66	3.4343E-03	0.0000E+00	1.0001E+08	1.2600E+03	4.3103E-05	4.3103E-05	1.4101
67	3.4449E-03	0.0000E+00	1.0001E+08	1.2600E+03	4.3103E-05	4.3103E-05	1.4101
68	3.4554E-03	0.0000E+00	1.0001E+08	1.2600E+03	4.3103E-05	4.3103E-05	1.4101
69	3.4660E-03	0.0000E+00	1.0001E+08	1.2600E+03	4.3103E-05	4.3103E-05	1.4101
70	3.4766E-03	0.0000E+00	1.0001E+08	1.2600E+03	4.3103E-05	4.3103E-05	1.4101
71	3.4871E-03	0.0000E+00	1.0001E+08	1.2600E+03	4.3103E-05	4.3103E-05	1.4101
72	3.4977E-03	0.0000E+00	1.0001E+08	1.2600E+03	4.3103E-05	4.3103E-05	1.4101
73	3.5083E-03	0.0000E+00	1.0001E+08	1.2600E+03	4.3103E-05	4.3103E-05	1.4101
74	3.5189E-03	0.0000E+00	1.0001E+08	1.2600E+03	4.3103E-05	4.3103E-05	1.4101
75	3.5294E-03	0.0000E+00	1.0001E+08	1.2600E+03	4.3103E-05	4.3103E-05	1.4101
76	3.5400E-03	0.0000E+00	1.0002E+08	1.1300E+04	4.3103E-05	4.3103E-05	1.8136
77	3.5493E-03	0.0000E+00	1.0002E+08	1.1300E+04	4.3103E-05	4.3103E-05	1.8136
78	3.5587E-03	0.0000E+00	1.0002E+08	1.1300E+04	4.3103E-05	4.3103E-05	1.8136
79	3.5680E-03	0.0000E+00	1.0002E+08	1.1300E+04	4.3103E-05	4.3103E-05	1.8136
80	3.5773E-03	0.0000E+00	1.0002E+08	1.1300E+04	4.3103E-05	4.3103E-05	1.8136
81	3.5867E-03	0.0000E+00	1.0002E+08	1.1300E+04	4.3103E-05	4.3103E-05	1.8136
82	3.5960E-03	0.0000E+00	1.0002E+08	1.1300E+04	4.3103E-05	4.3103E-05	1.8136
83	3.6053E-03	0.0000E+00	1.0002E+08	1.1300E+04	4.3103E-05	4.3103E-05	1.8136
84	3.6147E-03	0.0000E+00	1.0002E+08	1.1300E+04	4.3103E-05	4.3103E-05	1.8136
85	3.6240E-03	0.0000E+00	1.0002E+08	1.1300E+04	4.3103E-05	4.3103E-05	1.8136
86	3.6333E-03	0.0000E+00	1.0002E+08	1.1300E+04	4.3103E-05	4.3103E-05	1.8136
87	3.6427E-03	0.0000E+00	1.0002E+08	1.1300E+04	4.3103E-05	4.3103E-05	1.8136
88	3.6520E-03	0.0000E+00	1.0002E+08	1.1300E+04	4.3103E-05	4.3103E-05	1.8136
89	3.6613E-03	0.0000E+00	1.0002E+08	1.1300E+04	4.3103E-05	4.3103E-05	1.8136
90	3.6707E-03	0.0000E+00	1.0002E+08	1.1300E+04	4.3103E-05	4.3103E-05	1.8136

- -

TIMESTEP NUMBER 5608   TIME = 3.6295695E-08   DELTA T = 8.4149278E-13
---------------------   ---------------------   ---------------------

DELTA T DETERMINED BY CONDITION   1 AT MESHPOINT 39

BOUNDARY :   R = 5.2430E-03   U = 1.6155E+05   P = 1.0000E-60   TI = 0.0000E+00   TE = 0.0000E+00   SOUND SPEED = 4.1360E+04

ENERGIES :   THERMAL 2.82610E+05   KINETIC 6.59525E+04   NUCLEAR 2.71308E+01   ERROR -3.64308E+02   RHO R   4.38494E+00

FUSION   :   YIELD 7.69233E-05   NEUTRONS 9.63981E+12   RATE 2.27913E+25   ENERGY 2.16347E+01

*** LASER SWITCHED OFF AT STEP   0   TIME 0.0000000E+00   POWER 0.00000E+00   ENERGY 0.00000E+00   R(ABS) 0.00000E+00

CELL NO	COORDINATES M	HYDRODYNAMIC VELOCITY	PRESSURE	DENSITY	TEMPERATURE (KEV) ION	ELECTRON	AVERAGE CHARGE
1	0.0000E+00	0.0000E+00	1.5943E+17	2.0317E+05	3.9752E+00	3.9842E+00	1.0000
2	5.1321E-09	4.4139E-01	3.5776E+16	1.1590E+05	3.9885E+00	3.9975E+00	1.0000
3	5.8805E-05	-1.1865E+05	5.4876E+16	2.4589E+05	2.8307E+00	2.8308E+00	1.0000
4	6.6904E-05	-1.8138E+05	4.7820E+16	2.6042E+05	2.3079E+00	2.3080E+00	1.0000
5	7.3092E-05	-9.4422E+04	4.8025E+16	3.3167E+05	1.7793E+00	1.7796E+00	1.0000
6	7.7311E-05	-9.2530E+04	4.0996E+16	5.1356E+05	8.8248E-01	8.8229E-01	1.0000
7	7.9814E-05	-1.2069E+05	4.0776E+16	6.1702E+05	6.7898E-01	6.7832E-01	1.0000
8	8.1789E-05	-5.8755E+04	4.0566E+16	6.0804E+05	6.8897E-01	6.8885E-01	1.0000
9	8.3705E-05	-7.5622E+04	4.0109E+16	6.2399E+05	6.5334E-01	6.5341E-01	1.0000
10	8.5495E-05	-7.0140E+04	3.3647E+16	5.6613E+05	6.0247E-01	6.0248E-01	1.0000
11	8.7391E-05	-5.3029E+04	3.4025E+16	5.8633E+05	5.7954E-01	5.7949E-01	1.0000
12	8.9150E-05	-4.6515E+04	3.3100E+16	5.9106E+05	5.5178E-01	5.5177E-01	1.0000
13	9.0834E-05	-3.0369E+04	3.1612E+16	5.9594E+05	5.1183E-01	5.1182E-01	1.0000
14	9.2449E-05	-2.0812E+04	3.1034E+16	6.0180E+05	4.9109E-01	4.9108E-01	1.0000
15	9.3998E-05	-1.4110E+04	3.0639E+16	6.1916E+05	4.5984E-01	4.5983E-01	1.0000
16	9.5460E-05	-5.7865E+03	2.9678E+16	6.1591E+05	4.4343E-01	4.4343E-01	1.0000
17	9.6889E-05	4.8302E+02	2.8775E+16	6.1643E+05	4.2349E-01	4.2348E-01	1.0000
18	9.8280E-05	3.2637E+03	2.8097E+16	6.1584E+05	4.0971E-01	4.0970E-01	1.0000
19	9.9637E-05	5.5765E+03	2.7333E+16	6.1883E+05	3.8989E-01	3.8988E-01	1.0000
20	1.0096E-04	8.4633E+03	2.6699E+16	6.1699E+05	3.7848E-01	3.7848E-01	1.0000
21	1.0225E-04	9.7965E+03	2.6324E+16	6.1947E+05	3.6768E-01	3.6768E-01	1.0000
22	1.0351E-04	1.0313E+04	2.6039E+16	6.2558E+05	3.5485E-01	3.5485E-01	1.0000
23	1.0472E-04	1.0535E+04	2.5589E+16	6.2395E+05	3.4712E-01	3.4712E-01	1.0000
24	1.0592E-04	1.0618E+04	2.5220E+16	6.2886E+05	3.3409E-01	3.3408E-01	1.0000
25	1.0709E-04	9.8864E+03	2.5248E+16	6.3308E+05	3.3021E-01	3.3021E-01	1.0000
26	1.0822E-04	8.6430E+03	2.5047E+16	6.3957E+05	3.1931E-01	3.1931E-01	1.0000
27	1.0933E-04	8.8767E+03	2.4775E+16	6.4525E+05	3.0795E-01	3.0794E-01	1.0000
28	1.1040E-04	6.5962E+03	2.4965E+16	6.5353E+05	3.0357E-01	3.0357E-01	1.0000
29	1.1144E-04	4.6096E+03	2.4819E+16	6.6150E+05	2.9283E-01	2.9283E-01	1.0000
30	1.1246E-04	4.3625E+03	2.4817E+16	6.6567E+05	2.8878E-01	2.8878E-01	1.0000
31	1.1345E-04	2.7610E+03	2.4635E+16	6.7361E+05	2.7770E-01	2.7770E-01	1.0000
32	1.1442E-04	1.4880E+03	2.4657E+16	6.7177E+05	2.7985E-01	2.7985E-01	1.0000
33	1.1537E-04	-6.5850E+02	2.4635E+16	6.8431E+05	2.6784E-01	2.6784E-01	1.0000
34	1.1630E-04	-1.9110E+03	2.4722E+16	6.8519E+05	2.6871E-01	2.6871E-01	1.0000
35	1.1721E-04	-2.9902E+03	2.4338E+16	6.8380E+05	2.6254E-01	2.6254E-01	1.0000
36	1.1811E-04	-5.5182E+03	2.4731E+16	6.9737E+05	2.5792E-01	2.5792E-01	1.0000
37	1.1898E-04	-7.5653E+03	2.4310E+16	7.0438E+05	2.4385E-01	2.4385E-01	1.0000
38	1.1983E-04	-9.1857E+03	2.4253E+16	7.2771E+05	2.2318E-01	2.2318E-01	1.0000
39	1.2065E-04	-1.0409E+04	2.4340E+16	7.5070E+05	2.0632E-01	2.0632E-01	1.0000
40	1.2143E-04	-1.3533E+04	2.4124E+16	6.6428E+05	2.7633E-01	2.7633E-01	1.0000

41	1.2231E-04	-1.4527E+04	2.3816E+16	6.3532E+05	5.4810E-01	5.4818E-01	5.5421
42	1.3504E-04	-1.6014E+04	6.3573E+15	3.3946E+05	2.5241E-01	2.5202E-01	5.0127
43	1.5405E-04	-1.6798E+05	3.1666E+14	3.0821E+04	2.1726E-01	2.1724E-01	5.4543
44	2.5653E-04	-2.1500E+05	2.9621E+13	6.1762E+02	1.0493E+00	1.0494E+00	7.0000
45	8.7985E-04	-8.6214E+04	1.2107E+13	1.8969E+02	1.3941E+00	1.3927E+00	7.0000
46	1.4195E-03	-7.7122E+04	8.7507E+12	1.5820E+02	1.2093E+00	1.2085E+00	7.0000
47	1.7642E-03	-7.3719E+04	7.3428E+12	1.6178E+02	9.9372E-01	9.9372E-01	7.0000
48	2.0067E-03	-6.5020E+04	6.5547E+12	1.8121E+02	7.9415E-01	7.9440E-01	7.0000
49	2.1831E-03	-5.8659E+04	6.1274E+12	2.1323E+02	6.3341E-01	6.3360E-01	7.0000
50	2.3141E-03	-5.3268E+04	5.7941E+12	2.4890E+02	5.1557E-01	5.1568E-01	7.0000
51	2.4161E-03	-4.8385E+04	5.5412E+12	2.8217E+02	4.3697E-01	4.3702E-01	7.0000
52	2.5000E-03	-4.3543E+04	5.3332E+12	3.1061E+02	3.8371E-01	3.8373E-01	7.0000
53	2.5721E-03	-3.9805E+04	5.1404E+12	3.3469E+02	3.4462E-01	3.4463E-01	7.0000
54	2.6359E-03	-3.6415E+04	5.0084E+12	3.5776E+02	3.1528E-01	3.1529E-01	7.0000
55	2.6933E-03	-3.3281E+04	4.8662E+12	3.7801E+02	2.9099E-01	2.9099E-01	7.0000
56	2.7458E-03	-3.0728E+04	4.7262E+12	3.9633E+02	2.7052E-01	2.7053E-01	7.0000
57	2.7944E-03	-2.8076E+04	4.6256E+12	4.1490E+02	2.5377E-01	2.5378E-01	7.0000
58	2.8396E-03	-2.6124E+04	4.5243E+12	4.3204E+02	2.3917E-01	2.3917E-01	7.0000
59	2.8819E-03	-2.4778E+04	4.4315E+12	4.4843E+02	2.2644E-01	2.2645E-01	7.0000
60	2.9218E-03	-2.3245E+04	4.3399E+12	4.6372E+02	2.1514E-01	2.1514E-01	7.0000
61	2.9596E-03	-2.1798E+04	4.2267E+12	4.7655E+02	2.0457E-01	2.0458E-01	7.0000
62	2.9957E-03	-2.0484E+04	4.1136E+12	4.8824E+02	1.9498E-01	1.9498E-01	7.0000
63	3.0304E-03	-1.8972E+04	4.0146E+12	4.9986E+02	1.8647E-01	1.8647E-01	7.0000
64	3.0637E-03	-1.7485E+04	3.9153E+12	5.1055E+02	1.7864E-01	1.7864E-01	7.0000
65	3.0958E-03	-1.6126E+04	3.8204E+12	5.2070E+02	1.7146E-01	1.7146E-01	7.0000
66	3.1268E-03	-1.4683E+04	3.7440E+12	5.3146E+02	1.6514E-01	1.6514E-01	7.0000
67	3.1568E-03	-1.3077E+04	3.6799E+12	5.4250E+02	1.5948E-01	1.5948E-01	7.0000
68	3.1858E-03	-1.1673E+04	3.6114E+12	5.5249E+02	1.5414E-01	1.5414E-01	7.0000
69	3.2140E-03	-1.0259E+04	3.5589E+12	5.6331E+02	1.4940E-01	1.4940E-01	7.0000
70	3.2413E-03	-8.6679E+03	3.5179E+12	5.7469E+02	1.4514E-01	1.4514E-01	7.0000
71	3.2678E-03	-7.1400E+03	3.4719E+12	5.8510E+02	1.4107E-01	1.4107E-01	7.0000
72	3.2936E-03	-5.7171E+03	3.4297E+12	5.9526E+02	1.3734E-01	1.3734E-01	7.0000
73	3.3187E-03	-4.2504E+03	3.3971E+12	6.0481E+02	1.3419E-01	1.3419E-01	7.0000
74	3.3432E-03	-2.7467E+03	3.3624E+12	6.0744E+02	1.3242E-01	1.3242E-01	7.0000
75	3.3673E-03	-1.2160E+03	3.3278E+12	5.8565E+02	1.3561E-01	1.3562E-01	7.0000
76	3.3922E-03	3.5468E+02	3.1928E+12	1.0116E+03	1.9157E-01	1.9175E-01	24.6822
77	3.5022E-03	9.2449E+03	2.9601E+12	1.0507E+03	1.7535E-01	1.7553E-01	23.1170
78	3.6025E-03	1.7820E+04	2.7863E+12	1.0946E+03	1.6198E-01	1.6215E-01	22.4337
79	3.6942E-03	2.6379E+04	2.6199E+12	1.1218E+03	1.5142E-01	1.5157E-01	21.8442
80	3.7799E-03	3.4339E+04	2.4535E+12	1.1317E+03	1.4281E-01	1.4295E-01	20.7597
81	3.8616E-03	4.1603E+04	2.2994E+12	1.1316E+03	1.3573E-01	1.3584E-01	19.8426
82	3.9404E-03	4.8256E+04	2.0466E+12	1.0808E+03	1.2834E-01	1.2848E-01	18.8861
83	4.0201E-03	5.5620E+04	1.8228E+12	1.0260E+03	1.2198E-01	1.2214E-01	18.0121
84	4.1011E-03	6.3366E+04	1.6173E+12	9.6522E+02	1.1643E-01	1.1659E-01	17.2719
85	4.1844E-03	7.1483E+04	1.4235E+12	8.9660E+02	1.1152E-01	1.1169E-01	16.5915
86	4.2709E-03	7.9545E+04	1.2129E+12	8.0728E+02	1.0670E-01	1.0688E-01	15.9048
87	4.3635E-03	8.7564E+04	9.2757E+11	6.6438E+02	1.0056E-01	1.0078E-01	15.0338
88	4.4715E-03	9.7225E+04	6.8196E+11	5.2251E+02	9.5257E-02	9.5471E-02	14.9137
89	4.6023E-03	1.0601E+05	3.9985E+11	3.3599E+02	8.8249E-02	8.8628E-02	14.7973
90	4.7930E-03	1.2488E+05	1.2867E+11	1.2536E+02	7.7883E-02	7.8619E-02	14.6270

ALPHA TRANSPORT IS NOW SWITCHED ON
TIME   =   3.6297E-08
STEP   =   5609

D I A G N O S T I C S   F O R   T R A N S P O R T   C A L C U L A T I O N S   O F   A L P H A S

TIMESTEP= 5609 AT TIME= 36.29653E-09 ; TIME SINCE IGNITION= 0.000000E+00
    YIELD   =   7.6923E-05
SUMMARY ENERGY BALANCES:
=========================

NEUTRON ENERGY FROM DD REACTION: 2.378E-02   TIME INTEGRATED : 2.378E-02
NEUTRON ENERGY FROM DT REACTION: 2.159E+01   TIME INTEGRATED : 2.159E+01
SUM OF NEUTRON ENERGYS :   2.162E+01   TIME INTEGRATED : 2.162E+01
FUSION ION ENERGY RELEASED :   5.493E+00   TIME INTEGRATED : 5.493E+00
FUSION ION ENERGY DEPOSITED :   5.509E+00   TIME INTEGRATED : 5.509E+00
NEUTRON ENERGY / DEPOSITED ENERGY: 3.92

DISTRIBUTION OF DEPOSITED FUSION ION ENERGIES:

| | ENERGY IN TIME STEP | | | TIME INTEGRATED ENERGY | | |
	TO ELECTRONS	TO IONS	SUM	TO ELECTRONS	TO IONS	SUM
ALL IONS LOCAL	4.890E+00	6.033E-01	5.493E+00	4.890E+00	6.033E-01	5.493E+00
OTHER IONS LOCAL	9.008E-02	3.507E-03	9.358E-02	9.008E-02	3.507E-03	9.358E-02
ALPHAS TRANSPORTED	4.826E+00	5.902E-01	5.416E+00	4.826E+00	5.902E-01	5.416E+00
ENERGY LEAKAGE			0.000E+00			0.000E+00
ENERGY IN FLIGHT						5.985E+00
FUSION ENERGY DEPOSITED	4.916E+00	5.937E-01	5.509E+00	4.916E+00	5.937E-01	5.509E+00
INERTIAL TERM			-4.652E+02			-4.652E+02

DEPOSITED FUSION ION ENERGIES EXPRESSED IN PERCENT:

| | PERCENTAGE TIME STEP | | | TIME INTEGRATED PERCENTAGE | | |
	TO ELECTRONS	TO IONS	SUM	TO ELECTRONS	TO IONS	SUM
ALL IONS LOCAL	89.017	10.983	100.000	89.017	10.983	100.000
OTHER IONS LOCAL	1.640	0.064	1.704	1.640	0.064	1.704
ALPHAS TRANSPORTED	87.850	10.745	98.595	87.850	10.745	98.595
ENERGY LEAKAGE			0.000			0.000
ENERGY IN FLIGHT						108.959
FUSION ENERGY DEPOSITED	89.490	10.809	100.299	89.490	10.809	100.299
INERTIAL TERM			-8469.294			-8469.294

DISTRIBUTION OF DEPOSITED ALPHA ENERGY ON ZONES:

| | ENERGY IN TIME STEP | | | | TIME INTEGRATED ENERGY | | | |
	TO ELECTRONS	TO IONS	SUM	PERCENT	TO ELECTRONS	TO IONS	SUM	PERCENT
IN BURNING ZONE	4.743E+00	5.670E-01	5.310E+00	98.338	4.743E+00	5.670E-01	5.310E+00	98.338
IN FUEL ZONE	4.826E+00	5.902E-01	5.416E+00	100.304	4.826E+00	5.902E-01	5.416E+00	100.304
OUTSIDE BURNING ZONE			1.062E-01	1.966			1.062E-01	1.966
OUTSIDE FUEL ZONE			0.000E+00	0.000			0.000E+00	0.000

CIRCE USED TOTAL CPU (MS)   484 * AVERAGE CPU TIME PER CALL IN S: 2.420E-01 * NUMBER OF CIRCE CALLS =   2

D I A G N O S T I C S   F O R   T R A N S P O R T   C A L C U L A T I O N S   O F   A L P H A S

TIMESTEP= 6000 AT TIME= 36.35705E-09 ; TIME SINCE IGNITION= 60.52048E-12
    YIELD   = 2.4894E+01
SUMMARY ENERGY BALANCES:
===========================

```
NEUTRON ENERGY FROM DD REACTION: 1.135E+01    TIME INTEGRATED : 2.978E+03
NEUTRON ENERGY FROM DT REACTION: 2.272E+04    TIME INTEGRATED : 7.549E+06
SUM OF NEUTRON ENERGYS :         2.273E+04    TIME INTEGRATED : 7.552E+06
FUSION ION ENERGY RELEASED :     5.724E+03    TIME INTEGRATED : 1.899E+06
FUSION ION ENERGY DEPOSITED :    3.855E+03    TIME INTEGRATED : 1.247E+06
NEUTRON ENERGY / DEPOSITED ENERGY:    6.06
```

DISTRIBUTION OF DEPOSITED FUSION ION ENERGIES:

	ENERGY IN TIME STEP			TIME INTEGRATED ENERGY		
	TO ELECTRONS	TO IONS	SUM	TO ELECTRONS	TO IONS	SUM
ALL IONS LOCAL	2.142E+03	3.582E+03	5.724E+03	8.391E+05	1.060E+06	1.899E+06
OTHER IONS LOCAL	2.885E+01	1.592E+01	4.477E+01	8.162E+03	3.570E+03	1.173E+04
ALPHAS TRANSPORTED	1.896E+03	1.914E+03	3.810E+03	7.201E+05	5.148E+05	1.235E+06
ENERGY LEAKAGE			2.631E-44			4.548E-44
ENERGY IN FLIGHT						5.347E+05
FUSION ENERGY DEPOSITED	1.925E+03	1.930E+03	3.855E+03	7.283E+05	5.183E+05	1.247E+06
INERTIAL TERM			1.018E+02			3.611E+04

DEPOSITED FUSION ION ENERGIES EXPRESSED IN PERCENT:

	PERCENTAGE TIME STEP			TIME INTEGRATED PERCENTAGE		
	TO ELECTRONS	TO IONS	SUM	TO ELECTRONS	TO IONS	SUM
ALL IONS LOCAL	37.424	62.576	100.000	44.188	55.812	100.000
OTHER IONS LOCAL	0.504	0.278	0.782	0.430	0.188	0.618
ALPHAS TRANSPORTED	33.117	33.442	66.558	37.921	27.108	65.029
ENERGY LEAKAGE			0.000			0.000
ENERGY IN FLIGHT						28.155
FUSION ENERGY DEPOSITED	33.621	33.720	67.340	38.351	27.296	65.647
INERTIAL TERM			1.779			1.902

DISTRIBUTION OF DEPOSITED ALPHA ENERGY ON ZONES:

	ENERGY IN TIME STEP				TIME INTEGRATED ENERGY			
	TO ELECTRONS	TO IONS	SUM	PERCENT	TO ELECTRONS	TO IONS	SUM	PERCENT
IN BURNING ZONE	1.830E+03	1.906E+03	3.736E+03	65.770	6.807E+05	5.074E+05	1.188E+06	62.954
IN FUEL ZONE	1.896E+03	1.914E+03	3.810E+03	67.083	7.201E+05	5.148E+05	1.235E+06	65.433
OUTSIDE BURNING ZONE			7.458E+01	1.313			4.679E+04	2.479
OUTSIDE FUEL ZONE			2.631E-44	0.000			4.548E-44	0.000

CIRCE USED TOTAL CPU (MS)   140456 * AVERAGE CPU TIME PER CALL IN S: 3.570E-01 * NUMBER OF CIRCE CALLS =   393

TIMESTEP NUMBER 6000   TIME = 3.6357054E-08   DELTA T = 1.2451767E-14
--------------------   ---------------------   -----------------------
                    DELTA T DETERMINED BY CONDITION   4 AT MESHPOINT 25

BOUNDARY : R = 5.2522E-03 U = 1.6184E+05 P = 1.0000E-60 TI = 0.0000E+00 TE = 0.0000E+00 SOUND SPEED = 4.1303E+04

ENERGIES : THERMAL 1.38285E+06   KINETIC 1.24254E+05   NUCLEAR 8.80677E+06   ERROR -8.83096E+04   RHO R 4.51653E+00

FUSION   : YIELD 2.49696E+01   NEUTRONS 3.35756E+18   RATE 8.11407E+29   ENERGY 7.56028E+06

***   LASER SWITCHED OFF AT STEP   0   TIME 0.0000000E+00   POWER 0.00000E+00   ENERGY 0.00000E+00   R(ABS) 0.00000E+00

CELL NO	COORDINATES M	HYDRODYNAMIC VELOCITY	PRESSURE	DENSITY	TEMPERATURE (KEV) ION	ELECTRON	AVERAGE CHARGE
1	0.0000E+00	0.0000E+00	3.0884E+18	1.9960E+05	8.7470E+01	7.4504E+01	1.0000
2	5.1623E-09	6.7575E-01	7.3352E+17	1.2708E+05	8.7443E+01	7.4504E+01	1.1184
3	5.6201E-05	-7.0099E+05	1.2343E+18	2.0389E+05	9.6867E+01	7.2582E+01	1.1152
4	6.6086E-05	-9.5774E+05	1.4105E+18	2.4582E+05	9.0555E+01	7.1052E+01	1.1263
5	7.2476E-05	-5.8453E+05	1.5412E+18	2.7788E+05	8.7248E+01	6.9833E+01	1.1366
6	7.7308E-05	-3.5694E+05	1.6258E+18	3.0306E+05	8.3561E+01	6.8630E+01	1.1396
7	8.1267E-05	-1.7903E+05	1.7688E+18	3.3808E+05	8.1206E+01	6.7398E+01	1.1420
8	8.4520E-05	-4.1712E+03	1.9356E+18	3.7866E+05	7.9082E+01	6.6150E+01	1.1429
9	8.7232E-05	1.9948E+05	2.0854E+18	4.1770E+05	7.6716E+01	6.4901E+01	1.1402
10	8.9562E-05	3.9372E+05	2.2287E+18	4.5710E+05	7.4226E+01	6.3626E+01	1.1346
11	9.1598E-05	5.5678E+05	2.3896E+18	5.0195E+05	7.1718E+01	6.2297E+01	1.1271
12	9.3386E-05	6.8522E+05	2.5470E+18	5.5037E+05	6.8746E+01	6.0888E+01	1.1186
13	9.4967E-05	8.0955E+05	2.7068E+18	6.0315E+05	6.5590E+01	5.9397E+01	1.1087
14	9.6373E-05	9.4631E+05	2.9048E+18	6.6651E+05	6.2718E+01	5.7841E+01	1.0973
15	9.7619E-05	1.1103E+06	3.1509E+18	7.4299E+05	6.0188E+01	5.6258E+01	1.0849
16	9.8718E-05	1.3008E+06	3.4605E+18	8.3477E+05	5.8200E+01	5.4682E+01	1.0711
17	9.9684E-05	1.4792E+06	3.6165E+18	8.9915E+05	5.5444E+01	5.3078E+01	1.0558
18	1.0057E-04	1.4615E+06	3.2312E+18	8.6686E+05	4.8519E+01	5.1153E+01	1.0405
19	1.0148E-04	1.2286E+06	2.6478E+18	8.0175E+05	3.9087E+01	4.8533E+01	1.0272
20	1.0246E-04	9.7547E+05	2.1729E+18	7.5729E+05	3.0578E+01	4.5052E+01	1.0165
21	1.0347E-04	7.7755E+05	1.7785E+18	7.2983E+05	2.3288E+01	4.0607E+01	1.0086
22	1.0451E-04	6.0746E+05	1.4184E+18	7.1497E+05	1.6872E+01	3.4929E+01	1.0034
23	1.0556E-04	4.6602E+05	1.0343E+18	7.0124E+05	1.1077E+01	2.7287E+01	1.0007
24	1.0661E-04	3.0747E+05	5.4151E+17	6.8567E+05	5.5929E+00	1.4761E+01	1.0000
25	1.0767E-04	1.0411E+05	7.8637E+16	6.6680E+05	1.1340E+00	1.5662E+00	1.0000
26	1.0873E-04	4.2503E+03	2.7539E+16	6.7611E+05	3.3198E-01	3.3223E-01	1.0000
27	1.0977E-04	4.3154E+02	2.7557E+16	6.8732E+05	3.2126E-01	3.2126E-01	1.0000
28	1.1077E-04	1.9822E+03	2.7939E+16	6.9882E+05	3.1731E-01	3.1731E-01	1.0000
29	1.1174E-04	3.3568E+03	2.7714E+16	7.0624E+05	3.0598E-01	3.0598E-01	1.0000
30	1.1269E-04	5.6466E+03	2.7648E+16	7.0991E+05	3.0129E-01	3.0129E-01	1.0000
31	1.1361E-04	6.0800E+03	2.7406E+16	7.1747E+05	2.8981E-01	2.8981E-01	1.0000
32	1.1452E-04	8.1497E+03	2.6887E+16	7.0743E+05	2.8942E-01	2.8942E-01	1.0000
33	1.1542E-04	8.9610E+03	2.6778E+16	7.1887E+05	2.7698E-01	2.7698E-01	1.0000
34	1.1630E-04	9.5003E+03	2.6139E+16	7.0831E+05	2.7464E-01	2.7464E-01	1.0000
35	1.1719E-04	1.1425E+04	2.6000E+16	7.1120E+05	2.6947E-01	2.6947E-01	1.0000
36	1.1805E-04	1.2243E+04	2.5560E+16	7.1123E+05	2.6125E-01	2.6125E-01	1.0000
37	1.1891E-04	1.3803E+04	2.5049E+16	7.1708E+05	2.4669E-01	2.4669E-01	1.0000
38	1.1975E-04	1.5461E+04	2.4794E+16	7.3722E+05	2.2521E-01	2.2521E-01	1.0000
39	1.2056E-04	1.5091E+04	2.4242E+16	7.4760E+05	2.0702E-01	2.0702E-01	1.0000
40	1.2134E-04	1.7144E+04	2.3907E+16	6.6072E+05	2.7536E-01	2.7536E-01	1.0000

41	1.2222E-04	1.8157E+04	2.0573E+16	5.8337E+05	5.1826E-01	5.1826E-01	5.4886
42	1.3600E-04	3.6372E+04	1.6512E+16	5.3567E+05	4.3902E-01	4.3901E-01	5.3470
43	1.4845E-04	-7.5915E+03	4.5986E+14	3.6460E+04	2.6528E-01	2.6423E-01	5.7192
44	2.4358E-04	-1.9767E+05	3.0357E+13	6.2656E+02	1.0596E+00	1.0600E+00	7.0000
45	8.7465E-04	-8.0050E+04	1.2252E+13	1.9114E+02	1.4000E+00	1.3986E+00	7.0000
46	1.4148E-03	-7.4075E+04	8.8214E+12	1.5903E+02	1.2128E+00	1.2118E+00	7.0000
47	1.7596E-03	-7.1743E+04	7.3733E+12	1.6217E+02	9.9518E-01	9.9550E-01	7.0000
48	2.0026E-03	-6.3617E+04	6.5749E+12	1.8149E+02	7.9511E-01	7.9564E-01	7.0000
49	2.1795E-03	-5.7758E+04	6.1370E+12	2.1335E+02	6.3383E-01	6.3425E-01	7.0000
50	2.3108E-03	-5.2483E+04	5.7965E+12	2.4885E+02	5.1564E-01	5.1602E-01	7.0000
51	2.4131E-03	-4.7733E+04	5.5305E+12	2.8175E+02	4.3666E-01	4.3686E-01	7.0000
52	2.4973E-03	-4.2985E+04	5.3233E+12	3.1019E+02	3.8342E-01	3.8358E-01	7.0000
53	2.5696E-03	-3.9257E+04	5.1279E+12	3.3414E+02	3.4426E-01	3.4439E-01	7.0000
54	2.6336E-03	-3.6022E+04	4.9925E+12	3.5703E+02	3.1486E-01	3.1496E-01	7.0000
55	2.6912E-03	-3.2850E+04	4.8525E+12	3.7733E+02	2.9063E-01	2.9073E-01	7.0000
56	2.7439E-03	-3.0281E+04	4.7095E+12	3.9545E+02	2.7011E-01	2.7021E-01	7.0000
57	2.7927E-03	-2.7756E+04	4.6132E+12	4.1419E+02	2.5347E-01	2.5355E-01	7.0000
58	2.8379E-03	-2.5794E+04	4.5168E+12	4.3156E+02	2.3902E-01	2.3905E-01	7.0000
59	2.8804E-03	-2.4456E+04	4.4203E+12	4.4772E+02	2.2622E-01	2.2625E-01	7.0000
60	2.9203E-03	-2.2924E+04	4.3286E+12	4.6297E+02	2.1492E-01	2.1495E-01	7.0000
61	2.9582E-03	-2.1396E+04	4.2158E+12	4.7578E+02	2.0437E-01	2.0439E-01	7.0000
62	2.9944E-03	-2.0070E+04	4.0996E+12	4.8723E+02	1.9472E-01	1.9474E-01	7.0000
63	3.0292E-03	-1.8607E+04	3.9996E+12	4.9874E+02	1.8620E-01	1.8622E-01	7.0000
64	3.0625E-03	-1.7115E+04	3.9009E+12	5.0943E+02	1.7837E-01	1.7839E-01	7.0000
65	3.0947E-03	-1.5764E+04	3.8048E+12	5.1943E+02	1.7118E-01	1.7120E-01	7.0000
66	3.1258E-03	-1.4382E+04	3.7251E+12	5.2989E+02	1.6481E-01	1.6482E-01	7.0000
67	3.1559E-03	-1.2831E+04	3.6621E+12	5.4096E+02	1.5917E-01	1.5919E-01	7.0000
68	3.1851E-03	-1.1402E+04	3.5937E+12	5.5091E+02	1.5384E-01	1.5385E-01	7.0000
69	3.2133E-03	-1.0041E+04	3.5378E+12	5.6138E+02	1.4905E-01	1.4906E-01	7.0000
70	3.2407E-03	-8.5050E+03	3.4976E+12	5.7278E+02	1.4481E-01	1.4482E-01	7.0000
71	3.2673E-03	-6.9524E+03	3.4527E+12	5.8323E+02	1.4077E-01	1.4077E-01	7.0000
72	3.2932E-03	-5.5413E+03	3.4099E+12	5.9328E+02	1.3703E-01	1.3703E-01	7.0000
73	3.3184E-03	-4.1116E+03	3.3766E+12	6.0272E+02	1.3387E-01	1.3388E-01	7.0000
74	3.3429E-03	-2.6009E+03	3.3411E+12	6.0520E+02	1.3210E-01	1.3210E-01	7.0000
75	3.3672E-03	-1.0681E+03	3.2928E+12	5.8200E+02	1.3508E-01	1.3509E-01	7.0000
76	3.3922E-03	4.8308E+02	3.1710E+12	1.0066E+03	1.9129E-01	1.9147E-01	24.6555
77	3.5027E-03	9.3769E+03	2.9363E+12	1.0444E+03	1.7503E-01	1.7524E-01	23.0891
78	3.6035E-03	1.7924E+04	2.7613E+12	1.0874E+03	1.6166E-01	1.6185E-01	22.4198
79	3.6958E-03	2.6482E+04	2.5954E+12	1.1140E+03	1.5110E-01	1.5127E-01	21.8073
80	3.7820E-03	3.4446E+04	2.4307E+12	1.1240E+03	1.4251E-01	1.4267E-01	20.7241
81	3.8641E-03	4.1704E+04	2.2992E+12	1.1315E+03	1.3592E-01	1.3584E-01	19.8422
82	3.9429E-03	4.8436E+04	2.0266E+12	1.0732E+03	1.2808E-01	1.2819E-01	18.8467
83	4.0230E-03	5.5780E+04	1.8064E+12	1.0194E+03	1.2176E-01	1.2189E-01	17.9781
84	4.1044E-03	6.3520E+04	1.6008E+12	9.5819E+02	1.1618E-01	1.1632E-01	17.2358
85	4.1881E-03	7.1620E+04	1.4084E+12	8.8979E+02	1.1126E-01	1.1142E-01	16.5528
86	4.2751E-03	7.9700E+04	1.2010E+12	8.0163E+02	1.0647E-01	1.0664E-01	15.8704
87	4.3682E-03	8.7791E+04	9.1739E+11	6.5916E+02	1.0031E-01	1.0053E-01	14.9997
88	4.4768E-03	9.7427E+04	6.7601E+11	5.1927E+02	9.5080E-02	9.5275E-02	14.9104
89	4.6081E-03	1.0626E+05	3.9484E+11	3.3288E+02	8.8010E-02	8.8392E-02	14.7933
90	4.8000E-03	1.2514E+05	1.2724E+11	1.2432E+02	7.7708E-02	7.8441E-02	14.6239

DIAGNOSTICS FOR TRANSPORT CALCULATIONS OF ALPHAS

TIMESTEP= 6700 AT TIME= 36.39482E-09 ; TIME SINCE IGNITION= 98.28227E-12
     YIELD   =   1.6299E+02
SUMMARY ENERGY BALANCES:
===========================

```
NEUTRON ENERGY FROM DD REACTION: 4.359E+01      TIME INTEGRATED : 4.281E+04
NEUTRON ENERGY FROM DT REACTION: 4.612E+04      TIME INTEGRATED : 4.851E+07
SUM OF NEUTRON ENERGYS :         4.617E+04      TIME INTEGRATED : 4.856E+07
FUSION ION ENERGY RELEASED :     1.171E+04      TIME INTEGRATED : 1.230E+07
FUSION ION ENERGY DEPOSITED :    8.300E+03      TIME INTEGRATED : 9.341E+06
NEUTRON ENERGY / DEPOSITED ENERGY:    5.20
```

DISTRIBUTION OF DEPOSITED FUSION ION ENERGIES:

| | ENERGY IN TIME STEP | | | TIME INTEGRATED ENERGY | | |
	TO ELECTRONS	TO IONS	SUM	TO ELECTRONS	TO IONS	SUM
ALL IONS LOCAL	3.472E+03	8.236E+03	1.171E+04	3.868E+06	8.432E+06	1.230E+07
OTHER IONS LOCAL	9.986E+01	7.547E+01	1.753E+02	9.310E+04	7.665E+04	1.698E+05
ALPHAS TRANSPORTED	3.047E+03	5.077E+03	8.124E+03	3.593E+06	5.579E+06	9.171E+06
ENERGY LEAKAGE			2.713E+03			1.492E+06
ENERGY IN FLIGHT						3.617E+05
FUSION ENERGY DEPOSITED	3.147E+03	5.153E+03	8.300E+03	3.686E+06	5.655E+06	9.341E+06
INERTIAL TERM			2.414E+03			6.488E+05

DEPOSITED FUSION ION ENERGIES EXPRESSED IN PERCENT:

| | PERCENTAGE TIME STEP | | | TIME INTEGRATED PERCENTAGE | | |
	TO ELECTRONS	TO IONS	SUM	TO ELECTRONS	TO IONS	SUM
ALL IONS LOCAL	29.655	70.345	100.000	31.448	68.552	100.000
OTHER IONS LOCAL	0.853	0.645	1.497	0.757	0.623	1.380
ALPHAS TRANSPORTED	26.024	43.366	69.390	29.209	45.355	74.563
ENERGY LEAKAGE			23.172			12.127
ENERGY IN FLIGHT						2.941
FUSION ENERGY DEPOSITED	26.877	44.010	70.887	29.966	45.978	75.944
INERTIAL TERM			20.618			5.275

DISTRIBUTION OF DEPOSITED ALPHA ENERGY ON ZONES:

| | ENERGY IN TIME STEP | | | | TIME INTEGRATED ENERGY | | | |
	TO ELECTRONS	TO IONS	SUM	PERCENT	TO ELECTRONS	TO IONS	SUM	PERCENT
IN BURNING ZONE	3.047E+03	5.077E+03	8.124E+03	70.444	3.530E+06	5.566E+06	9.097E+06	74.991
IN FUEL ZONE	3.047E+03	5.077E+03	8.124E+03	70.444	3.593E+06	5.579E+06	9.171E+06	75.607
OUTSIDE BURNING ZONE			0.000E+00	0.000			7.472E+04	0.616
OUTSIDE FUEL ZONE			2.713E+03	23.524			1.492E+06	12.297

CIRCE USED TOTAL CPU (MS)   314003 * AVERAGE CPU TIME PER CALL IN S: 2.870E-01 * NUMBER OF CIRCE CALLS =   1093

TIMESTEP NUMBER 6700   TIME = 3.6394816E-08   DELTA T = 2.0287022E-13
-------------------   --------------------   ----------------------
                            DELTA T DETERMINED BY CONDITION   1 AT MESHPOINT 27

BOUNDARY : R = 5.2573E-03 U = 1.6201E+05 P = 1.0000E-60 TI = 0.0000E+00 TE = 0.0000E+00 SOUND SPEED = 4.1267E+04

ENERGIES : THERMAL 4.29008E+06   KINETIC 4.22206E+06   NUCLEAR 5.75413E+07   ERROR -1.17623E+06   RHO R 3.35436E+00

FUSION   : YIELD 1.63145E+02   NEUTRONS 2.14566E+19   RATE 9.92770E+28   ENERGY 4.82019E+07

***   LASER SWITCHED OFF AT STEP   0   TIME 0.0000000E+00   POWER 0.00000E+00   ENERGY 0.00000E+00   R(ABS) 0.00000E+00

CELL NO	COORDINATES M	HYDRODYNAMIC VELOCITY	PRESSURE	DENSITY	TEMPERATURE (KEV) ION	ELECTRON	AVERAGE CHARGE
1	0.0000E+00	0.0000E+00	4.2987E+18	1.9468E+05	1.4308E+02	8.8018E+01	1.0000
2	5.2051E-09	1.6089E+00	9.9830E+17	1.3629E+05	1.4308E+02	8.8015E+01	1.3415
3	5.3737E-05	1.7457E+06	9.4187E+17	1.3296E+05	1.3739E+02	8.7564E+01	1.3546
4	6.7984E-05	2.0569E+06	8.9394E+17	1.2761E+05	1.3608E+02	8.7305E+01	1.3629
5	7.8301E-05	2.2203E+06	8.7718E+17	1.2558E+05	1.3664E+02	8.7028E+01	1.3714
6	8.6562E-05	2.2718E+06	8.9199E+17	1.2658E+05	1.3938E+02	8.6702E+01	1.3755
7	9.3447E-05	2.2082E+06	9.4059E+17	1.3146E+05	1.4372E+02	8.6298E+01	1.3797
8	9.9244E-05	2.0742E+06	9.9477E+17	1.3779E+05	1.4670E+02	8.5804E+01	1.3836
9	1.0421E-04	1.9817E+06	1.0132E+18	1.4100E+05	1.4643E+02	8.5247E+01	1.3859
10	1.0866E-04	1.9788E+06	1.0012E+18	1.4089E+05	1.4457E+02	8.4656E+01	1.3870
11	1.1278E-04	2.0109E+06	9.8214E+17	1.3993E+05	1.4241E+02	8.4046E+01	1.3874
12	1.1666E-04	2.0484E+06	9.6142E+17	1.3878E+05	1.4014E+02	8.3421E+01	1.3877
13	1.2033E-04	2.0873E+06	9.4001E+17	1.3754E+05	1.3777E+02	8.2784E+01	1.3876
14	1.2383E-04	2.1291E+06	9.1742E+17	1.3610E+05	1.3533E+02	8.2138E+01	1.3871
15	1.2718E-04	2.1718E+06	8.9518E+17	1.3470E+05	1.3289E+02	8.1485E+01	1.3868
16	1.3041E-04	2.2147E+06	8.7295E+17	1.3329E+05	1.3043E+02	8.0826E+01	1.3865
17	1.3353E-04	2.2573E+06	8.5087E+17	1.3186E+05	1.2795E+02	8.0163E+01	1.3863
18	1.3654E-04	2.2997E+06	8.2926E+17	1.3047E+05	1.2547E+02	7.9496E+01	1.3861
19	1.3947E-04	2.3415E+06	8.0755E+17	1.2905E+05	1.2297E+02	7.8827E+01	1.3860
20	1.4231E-04	2.3818E+06	7.8611E+17	1.2765E+05	1.2044E+02	7.8154E+01	1.3859
21	1.4509E-04	2.4215E+06	7.6480E+17	1.2626E+05	1.1788E+02	7.7478E+01	1.3860
22	1.4779E-04	2.4596E+06	7.4341E+17	1.2484E+05	1.1527E+02	7.6800E+01	1.3862
23	1.5044E-04	2.4958E+06	7.2176E+17	1.2338E+05	1.1260E+02	7.6119E+01	1.3865
24	1.5303E-04	2.5294E+06	6.9971E+17	1.2185E+05	1.0985E+02	7.5434E+01	1.3869
25	1.5557E-04	2.5602E+06	6.7710E+17	1.2025E+05	1.0701E+02	7.4744E+01	1.3875
26	1.5807E-04	2.5875E+06	6.5376E+17	1.1852E+05	1.0406E+02	7.4050E+01	1.3881
27	1.6054E-04	2.6109E+06	6.2971E+17	1.1666E+05	1.0099E+02	7.3349E+01	1.3888
28	1.6297E-04	2.6306E+06	6.0510E+17	1.1470E+05	9.7828E+01	7.2640E+01	1.3895
29	1.6538E-04	2.6472E+06	5.8030E+17	1.1265E+05	9.4589E+01	7.1923E+01	1.3902
30	1.6777E-04	2.6621E+06	5.5573E+17	1.1059E+05	9.1318E+01	7.1198E+01	1.3911
31	1.7013E-04	2.6765E+06	5.3193E+17	1.0857E+05	8.8064E+01	7.0464E+01	1.3920
32	1.7249E-04	2.6922E+06	5.0922E+17	1.0663E+05	8.4875E+01	6.9724E+01	1.3930
33	1.7482E-04	2.7101E+06	4.8791E+17	1.0482E+05	8.1786E+01	6.8977E+01	1.3940
34	1.7714E-04	2.7313E+06	4.6804E+17	1.0317E+05	7.8817E+01	6.8227E+01	1.3952
35	1.7944E-04	2.7558E+06	4.4957E+17	1.0164E+05	7.5973E+01	6.7476E+01	1.3964
36	1.8172E-04	2.7838E+06	4.3237E+17	1.0025E+05	7.3249E+01	6.6724E+01	1.3978
37	1.8398E-04	2.8147E+06	4.1625E+17	9.8957E+04	7.0640E+01	6.5975E+01	1.3991
38	1.8622E-04	2.8482E+06	4.0108E+17	9.7733E+04	6.8144E+01	6.5230E+01	1.4004
39	1.8843E-04	2.8839E+06	3.8669E+17	9.6516E+04	6.5783E+01	6.4489E+01	1.4013
40	1.9063E-04	2.9214E+06	3.7299E+17	9.5235E+04	6.3601E+01	6.3754E+01	1.4014

41	1.9281E-04	2.9602E+06	2.5155E+17	1.0072E+05	3.7114E+01	5.6543E+01	7.0000
42	2.2348E-04	3.7362E+06	1.5937E+17	7.7461E+04	2.7075E+01	4.7087E+01	7.0000
43	2.5401E-04	4.3348E+06	1.3701E+17	5.0448E+04	1.4738E+02	4.6096E+01	7.0000
44	2.9032E-04	3.4536E+06	1.8363E+14	6.3642E+02	7.2354E+00	6.1215E+00	7.0000
45	8.7453E-04	3.3732E+05	1.2497E+13	1.9267E+02	1.4409E+00	1.4116E+00	7.0000
46	1.4119E-03	-7.0102E+04	8.8675E+12	1.5957E+02	1.2148E+00	1.2140E+00	7.0000
47	1.7568E-03	-7.0459E+04	7.3956E+12	1.6241E+02	9.9630E-01	9.9702E-01	7.0000
48	2.0001E-03	-6.2720E+04	6.5905E+12	1.8168E+02	7.9600E-01	7.9670E-01	7.0000
49	2.1771E-03	-5.7175E+04	6.1449E+12	2.1344E+02	6.3435E-01	6.3479E-01	7.0000
50	2.3087E-03	-5.1978E+04	5.7999E+12	2.4883E+02	5.1606E-01	5.1634E-01	7.0000
51	2.4112E-03	-4.7299E+04	5.5241E+12	2.8142E+02	4.3673E-01	4.3685E-01	7.0000
52	2.4955E-03	-4.2632E+04	5.3162E+12	3.0981E+02	3.8345E-01	3.8351E-01	7.0000
53	2.5680E-03	-3.8906E+04	5.1195E+12	3.3371E+02	3.4422E-01	3.4426E-01	7.0000
54	2.6322E-03	-3.5767E+04	4.9822E+12	3.5650E+02	3.1475E-01	3.1478E-01	7.0000
55	2.6899E-03	-3.2577E+04	4.8419E+12	3.7675E+02	2.9051E-01	2.9053E-01	7.0000
56	2.7427E-03	-2.9996E+04	4.7002E+12	3.9489E+02	2.7003E-01	2.7005E-01	7.0000
57	2.7915E-03	-2.7556E+04	4.6036E+12	4.1360E+02	2.5337E-01	2.5339E-01	7.0000
58	2.8369E-03	-2.5594E+04	4.5112E+12	4.3113E+02	2.3899E-01	2.3899E-01	7.0000
59	2.8793E-03	-2.4243E+04	4.4122E+12	4.4715E+02	2.2612E-01	2.2612E-01	7.0000
60	2.9194E-03	-2.2720E+04	4.3192E+12	4.6231E+02	2.1479E-01	2.1480E-01	7.0000
61	2.9573E-03	-2.1143E+04	4.2074E+12	4.7516E+02	2.0425E-01	2.0426E-01	7.0000
62	2.9936E-03	-1.9799E+04	4.0890E+12	4.8646E+02	1.9456E-01	1.9456E-01	7.0000
63	3.0284E-03	-1.8372E+04	3.9881E+12	4.9789E+02	1.8601E-01	1.8601E-01	7.0000
64	3.0618E-03	-1.6883E+04	3.8912E+12	5.0868E+02	1.7822E-01	1.7822E-01	7.0000
65	3.0940E-03	-1.5529E+04	3.7930E+12	5.1850E+02	1.7099E-01	1.7099E-01	7.0000
66	3.1252E-03	-1.4188E+04	3.7135E+12	5.2894E+02	1.6462E-01	1.6462E-01	7.0000
67	3.1554E-03	-1.2673E+04	3.6495E+12	5.3989E+02	1.5897E-01	1.5897E-01	7.0000
68	3.1846E-03	-1.1234E+04	3.5833E+12	5.5000E+02	1.5367E-01	1.5367E-01	7.0000
69	3.2129E-03	-9.8944E+03	3.5236E+12	5.6012E+02	1.4882E-01	1.4882E-01	7.0000
70	3.2403E-03	-8.4070E+03	3.4863E+12	5.7173E+02	1.4463E-01	1.4463E-01	7.0000
71	3.2670E-03	-6.8243E+03	3.4363E+12	5.8168E+02	1.4051E-01	1.4051E-01	7.0000
72	3.2929E-03	-5.4376E+03	3.3980E+12	5.9214E+02	1.3684E-01	1.3684E-01	7.0000
73	3.3181E-03	-4.0167E+03	3.3598E+12	6.0105E+02	1.3361E-01	1.3361E-01	7.0000
74	3.3427E-03	-2.4813E+03	3.3158E+12	6.0262E+02	1.3171E-01	1.3171E-01	7.0000
75	3.3671E-03	-9.4475E+02	3.2680E+12	5.7950E+02	1.3468E-01	1.3469E-01	7.0000
76	3.3922E-03	5.5062E+02	3.1577E+12	1.0037E+03	1.9110E-01	1.9127E-01	24.6371
77	3.5030E-03	9.4608E+03	2.9216E+12	1.0407E+03	1.7485E-01	1.7504E-01	23.0699
78	3.6041E-03	1.7990E+04	2.7443E+12	1.0825E+03	1.6145E-01	1.6163E-01	22.4098
79	3.6967E-03	2.6547E+04	2.5790E+12	1.1090E+03	1.5090E-01	1.5106E-01	21.7807
80	3.7832E-03	3.4513E+04	2.4159E+12	1.1192E+03	1.4232E-01	1.4247E-01	20.6985
81	3.8657E-03	4.1750E+04	2.3163E+12	1.1376E+03	1.3612E-01	1.3605E-01	19.8692
82	3.9439E-03	4.8566E+04	2.0145E+12	1.0688E+03	1.2788E-01	1.2800E-01	18.8195
83	4.0243E-03	5.5879E+04	1.7965E+12	1.0156E+03	1.2157E-01	1.2172E-01	17.9558
84	4.1060E-03	6.3617E+04	1.5933E+12	9.5519E+02	1.1605E-01	1.1617E-01	17.2161
85	4.1898E-03	7.1696E+04	1.3992E+12	8.8587E+02	1.1107E-01	1.1123E-01	16.5258
86	4.2771E-03	7.9785E+04	1.1934E+12	7.9821E+02	1.0630E-01	1.0646E-01	15.8445
87	4.3705E-03	8.7917E+04	9.0943E+11	6.5524E+02	1.0007E-01	1.0031E-01	14.9960
88	4.4796E-03	9.7539E+04	6.7148E+11	5.1693E+02	9.4904E-02	9.5107E-02	14.9075
89	4.6113E-03	1.0640E+05	3.9212E+11	3.3125E+02	8.7891E-02	8.8247E-02	14.7908
90	4.8037E-03	1.2528E+05	1.2643E+11	1.2373E+02	7.7607E-02	7.8332E-02	14.6221

DIAGNOSTICS FOR TRANSPORT CALCULATIONS OF ALPHAS

TIMESTEP= 6900 AT TIME= 36.48299E-09 ; TIME SINCE IGNITION= 18.64571E-11
   YIELD   = 1.7771E+02
SUMMARY ENERGY BALANCES:
===========================

NEUTRON ENERGY FROM DD REACTION: 6.469E-01   TIME INTEGRATED : 4.560E+04
NEUTRON ENERGY FROM DT REACTION: 2.638E+03   TIME INTEGRATED : 5.302E+07
SUM OF NEUTRON ENERGYS :   2.638E+03   TIME INTEGRATED : 5.307E+07
FUSION ION ENERGY RELEASED :   6.619E+02   TIME INTEGRATED : 1.344E+07
FUSION ION ENERGY DEPOSITED :   7.297E+02   TIME INTEGRATED : 1.011E+07
NEUTRON ENERGY / DEPOSITED ENERGY: 5.25

DISTRIBUTION OF DEPOSITED FUSION ION ENERGIES:

	ENERGY IN TIME STEP			TIME INTEGRATED ENERGY		
	TO ELECTRONS	TO IONS	SUM	TO ELECTRONS	TO IONS	SUM
ALL IONS LOCAL	4.410E+02	2.209E+02	6.619E+02	4.304E+06	9.134E+06	1.344E+07
OTHER IONS LOCAL	2.206E+00	3.395E-01	2.546E+00	1.003E+05	8.072E+04	1.810E+05
ALPHAS TRANSPORTED	4.627E+02	2.644E+02	7.271E+02	3.940E+06	5.986E+06	9.926E+06
ENERGY LEAKAGE			4.070E+02			1.838E+06
ENERGY IN FLIGHT						3.175E+04
FUSION ENERGY DEPOSITED	4.649E+02	2.647E+02	7.297E+02	4.040E+06	6.067E+06	1.011E+07
INERTIAL TERM			4.849E+02			1.008E+06

DEPOSITED FUSION ION ENERGIES EXPRESSED IN PERCENT:

	PERCENTAGE TIME STEP			TIME INTEGRATED PERCENTAGE		
	TO ELECTRONS	TO IONS	SUM	TO ELECTRONS	TO IONS	SUM
ALL IONS LOCAL	66.624	33.376	100.000	32.031	67.969	100.000
OTHER IONS LOCAL	0.333	0.051	0.385	0.746	0.601	1.347
ALPHAS TRANSPORTED	69.905	39.940	109.845	29.318	44.547	73.865
ENERGY LEAKAGE			61.486			13.679
ENERGY IN FLIGHT						0.236
FUSION ENERGY DEPOSITED	70.239	39.991	110.230	30.064	45.147	75.211
INERTIAL TERM			73.250			7.504

DISTRIBUTION OF DEPOSITED ALPHA ENERGY ON ZONES:

	ENERGY IN TIME STEP				TIME INTEGRATED ENERGY			
	TO ELECTRONS	TO IONS	SUM	PERCENT	TO ELECTRONS	TO IONS	SUM	PERCENT
IN BURNING ZONE	4.627E+02	2.644E+02	7.271E+02	110.269	3.877E+06	5.974E+06	9.852E+06	74.309
IN FUEL ZONE	4.627E+02	2.644E+02	7.271E+02	110.269	3.940E+06	5.986E+06	9.926E+06	74.873
OUTSIDE BURNING ZONE			0.000E+00	0.000			7.472E+04	0.564
OUTSIDE FUEL ZONE			4.070E+02	61.723			1.838E+06	13.866

CIRCE USED TOTAL CPU (MS)   358045 * AVERAGE CPU TIME PER CALL IN S: 2.760E-01 * NUMBER OF CIRCE CALLS =   1293

TIMESTEP NUMBER 6900   TIME = 3.6482991E-08   DELTA T = 9.7272104E-13

DELTA T DETERMINED BY CONDITION   1 AT MESHPOINT   40

BOUNDARY : R = 5.2713E-03 U = 1.6244E+05 P = 1.0000E-60 TI = 0.0000E+00 TE = 0.0000E+00 SOUND SPEED = 4.1185E+04

ENERGIES : THERMAL 1.20598E+06   KINETIC 7.98761E+06   NUCLEAR 6.26832E+07   ERROR -1.26075E+06   RHO R 2.95254E+00

FUSION : YIELD 1.77724E+02   NEUTRONS 2.34010E+19   RATE 1.11481E+27   ENERGY 5.25778E+07

*** LASER SWITCHED OFF AT STEP   0 TIME 0.0000000E+00   POWER 0.00000E+00   ENERGY 0.00000E+00   R(ABS) 0.00000E+00

CELL NO	COORDINATES M	HYDRODYNAMIC VELOCITY	PRESSURE	DENSITY	TEMPERATURE (KEV) ION	ELECTRON	AVERAGE CHARGE
1	0.0000E+00	0.0000E+00	6.7168E+17	1.7340E+05	2.0877E+01	1.9511E+01	1.0000
2	5.4098E-09	2.7631E+00	7.8149E+15	5.9912E+03	2.2848E+01	1.9457E+01	1.3958
3	1.5158E-04	1.2722E+06	7.0413E+15	5.7413E+03	2.1415E+01	1.8630E+01	1.4096
4	1.9235E-04	1.5256E+06	6.1145E+15	5.2689E+03	1.9892E+01	1.8161E+01	1.4182
5	2.2294E-04	1.6971E+06	5.4881E+15	4.9746E+03	1.8597E+01	1.7729E+01	1.4266
6	2.4814E-04	1.8692E+06	5.1896E+15	4.8695E+03	1.7808E+01	1.7358E+01	1.4311
7	2.6950E-04	2.0449E+06	5.0809E+15	4.8790E+03	1.7377E+01	1.7054E+01	1.4353
8	2.8792E-04	2.2122E+06	5.0521E+15	4.9298E+03	1.7136E+01	1.6805E+01	1.4388
9	3.0411E-04	2.3626E+06	5.0321E+15	4.9718E+03	1.6958E+01	1.6595E+01	1.4408
10	3.1865E-04	2.4928E+06	4.9848E+15	4.9830E+03	1.6765E+01	1.6410E+01	1.4416
11	3.3198E-04	2.6040E+06	4.9132E+15	4.9704E+03	1.6545E+01	1.6239E+01	1.4418
12	3.4438E-04	2.7024E+06	4.8406E+15	4.9546E+03	1.6325E+01	1.6079E+01	1.4418
13	3.5601E-04	2.7944E+06	4.7812E+15	4.9464E+03	1.6128E+01	1.5926E+01	1.4415
14	3.6697E-04	2.8842E+06	4.7291E+15	4.9410E+03	1.5948E+01	1.5782E+01	1.4408
15	3.7735E-04	2.9727E+06	4.6726E+15	4.9297E+03	1.5768E+01	1.5646E+01	1.4403
16	3.8723E-04	3.0599E+06	4.6089E+15	4.9098E+03	1.5586E+01	1.5519E+01	1.4398
17	3.9670E-04	3.1452E+06	4.5364E+15	4.8794E+03	1.5400E+01	1.5399E+01	1.4393
18	4.0582E-04	3.2278E+06	4.4636E+15	4.8454E+03	1.5223E+01	1.5287E+01	1.4387
19	4.1462E-04	3.3072E+06	4.3943E+15	4.8116E+03	1.5059E+01	1.5182E+01	1.4383
20	4.2315E-04	3.3835E+06	4.3337E+15	4.7827E+03	1.4916E+01	1.5083E+01	1.4379
21	4.3142E-04	3.4565E+06	4.2785E+15	4.7563E+03	1.4786E+01	1.4991E+01	1.4376
22	4.3944E-04	3.5257E+06	4.2333E+15	4.7369E+03	1.4675E+01	1.4905E+01	1.4374
23	4.4724E-04	3.5908E+06	4.1997E+15	4.7264E+03	1.4585E+01	1.4824E+01	1.4373
24	4.5480E-04	3.6521E+06	4.1744E+15	4.7225E+03	1.4509E+01	1.4747E+01	1.4373
25	4.6215E-04	3.7094E+06	4.1614E+15	4.7289E+03	1.4451E+01	1.4675E+01	1.4374
26	4.6927E-04	3.7626E+06	4.1543E+15	4.7406E+03	1.4401E+01	1.4605E+01	1.4375
27	4.7619E-04	3.8118E+06	4.1601E+15	4.7638E+03	1.4369E+01	1.4538E+01	1.4376
28	4.8289E-04	3.8576E+06	4.1733E+15	4.7941E+03	1.4345E+01	1.4473E+01	1.4378
29	4.8939E-04	3.8998E+06	4.1939E+15	4.8317E+03	1.4328E+01	1.4409E+01	1.4380
30	4.9568E-04	3.9389E+06	4.2207E+15	4.8759E+03	1.4317E+01	1.4346E+01	1.4383
31	5.0178E-04	3.9756E+06	4.2502E+15	4.9235E+03	1.4304E+01	1.4283E+01	1.4386
32	5.0769E-04	4.0097E+06	4.2854E+15	4.9775E+03	1.4296E+01	1.4219E+01	1.4389
33	5.1342E-04	4.0421E+06	4.3206E+15	5.0327E+03	1.4282E+01	1.4156E+01	1.4392
34	5.1897E-04	4.0729E+06	4.3558E+15	5.0897E+03	1.4264E+01	1.4092E+01	1.4397
35	5.2436E-04	4.1022E+06	4.3905E+15	5.1474E+03	1.4240E+01	1.4027E+01	1.4402
36	5.2959E-04	4.1308E+06	4.4219E+15	5.2037E+03	1.4207E+01	1.3961E+01	1.4407
37	5.3468E-04	4.1582E+06	4.4524E+15	5.2611E+03	1.4167E+01	1.3893E+01	1.4413
38	5.3963E-04	4.1852E+06	4.4782E+15	5.3160E+03	1.4113E+01	1.3825E+01	1.4418
39	5.4445E-04	4.2110E+06	4.5013E+15	5.3709E+03	1.4041E+01	1.3755E+01	1.4419
40	5.4915E-04	4.2370E+06	4.5202E+15	5.4244E+03	1.3944E+01	1.3685E+01	1.4412

41	5.5373E-04	4.2626E+06	4.6573E+15	7.7313E+03	1.2482E+01	1.3146E+01	7.0000
42	6.0533E-04	4.5772E+06	3.4469E+15	6.3334E+03	1.0728E+01	1.1957E+01	7.0000
43	6.5865E-04	4.9984E+06	1.5478E+15	2.9492E+03	1.2403E+01	1.1236E+01	7.0000
44	7.5123E-04	5.4122E+06	3.9782E+14	6.4018E+02	1.5641E+01	1.3166E+01	7.0000
45	1.0211E-03	2.9247E+06	1.2804E+14	2.2555E+02	5.8286E+01	5.6871E+00	7.0000
46	1.4256E-03	6.7162E+05	1.1555E+13	1.6832E+02	2.3730E+00	1.3711E+00	7.0000
47	1.7511E-03	-3.6010E+04	7.4605E+12	1.6322E+02	1.0002E+00	1.0007E+00	7.0000
48	1.9946E-03	-6.0648E+04	6.6215E+12	1.8212E+02	7.9811E-01	7.9842E-01	7.0000
49	2.1721E-03	-5.5820E+04	6.1590E+12	2.1363E+02	6.3545E-01	6.3566E-01	7.0000
50	2.3041E-03	-5.0808E+04	5.8026E+12	2.4877E+02	5.1657E-01	5.1668E-01	7.0000
51	2.4070E-03	-4.6272E+04	5.5122E+12	2.8094E+02	4.3660E-01	4.3665E-01	7.0000
52	2.4918E-03	-4.1826E+04	5.3020E+12	3.0925E+02	3.8318E-01	3.8320E-01	7.0000
53	2.5645E-03	-3.8107E+04	5.1057E+12	3.3311E+02	3.4395E-01	3.4396E-01	7.0000
54	2.6290E-03	-3.5168E+04	4.9598E+12	3.5551E+02	3.1425E-01	3.1426E-01	7.0000
55	2.6870E-03	-3.1967E+04	4.8230E+12	3.7585E+02	2.9011E-01	2.9012E-01	7.0000
56	2.7400E-03	-2.9351E+04	4.6809E+12	3.9390E+02	2.6963E-01	2.6963E-01	7.0000
57	2.7891E-03	-2.7111E+04	4.5863E+12	4.1265E+02	2.5303E-01	2.5304E-01	7.0000
58	2.8346E-03	-2.5167E+04	4.5006E+12	4.3050E+02	2.3879E-01	2.3879E-01	7.0000
59	2.8772E-03	-2.3746E+04	4.3975E+12	4.4625E+02	2.2584E-01	2.2584E-01	7.0000
60	2.9174E-03	-2.2244E+04	4.3006E+12	4.6112E+02	2.1445E-01	2.1445E-01	7.0000
61	2.9555E-03	-2.0578E+04	4.1917E+12	4.7410E+02	2.0397E-01	2.0397E-01	7.0000
62	2.9918E-03	-1.9177E+04	4.0715E+12	4.8522E+02	1.9424E-01	1.9424E-01	7.0000
63	3.0267E-03	-1.7831E+04	3.9680E+12	4.9641E+02	1.8565E-01	1.8565E-01	7.0000
64	3.0603E-03	-1.6364E+04	3.8720E+12	5.0720E+02	1.7788E-01	1.7788E-01	7.0000
65	3.0927E-03	-1.4992E+04	3.7739E+12	5.1697E+02	1.7066E-01	1.7066E-01	7.0000
66	3.1240E-03	-1.3737E+04	3.6903E+12	5.2700E+02	1.6422E-01	1.6422E-01	7.0000
67	3.1543E-03	-1.2312E+04	3.6255E+12	5.3781E+02	1.5857E-01	1.5857E-01	7.0000
68	3.1836E-03	-1.0862E+04	3.5610E+12	5.4801E+02	1.5330E-01	1.5331E-01	7.0000
69	3.2120E-03	-9.5415E+03	3.4980E+12	5.5775E+02	1.4840E-01	1.4840E-01	7.0000
70	3.2396E-03	-8.1788E+03	3.4564E+12	5.6889E+02	1.4415E-01	1.4415E-01	7.0000
71	3.2664E-03	-6.5408E+03	3.4103E+12	5.7912E+02	1.4010E-01	1.4010E-01	7.0000
72	3.2924E-03	-5.2039E+03	3.3696E+12	5.8927E+02	1.3640E-01	1.3640E-01	7.0000
73	3.3178E-03	-3.7811E+03	3.3284E+12	5.9779E+02	1.3313E-01	1.3313E-01	7.0000
74	3.3425E-03	-2.2079E+03	3.2835E+12	5.9918E+02	1.3122E-01	1.3122E-01	7.0000
75	3.3670E-03	-6.8039E+02	3.2424E+12	5.7670E+02	1.3432E-01	1.3432E-01	7.0000
76	3.3922E-03	7.0717E+02	3.1257E+12	9.9624E+02	1.9069E-01	1.9087E-01	24.5985
77	3.5038E-03	9.6549E+03	2.8892E+12	1.0322E+03	1.7446E-01	1.7464E-01	23.0309
78	3.6057E-03	1.8144E+04	2.7097E+12	1.0725E+03	1.6104E-01	1.6121E-01	22.3900
79	3.6990E-03	2.6696E+04	2.5454E+12	1.0984E+03	1.5050E-01	1.5064E-01	21.7287
80	3.7863E-03	3.4666E+04	2.3846E+12	1.1085E+03	1.4194E-01	1.4208E-01	20.6478
81	3.8694E-03	4.1838E+04	2.2993E+12	1.1316E+03	1.3574E-01	1.3583E-01	19.8420
82	3.9478E-03	4.8881E+04	1.9860E+12	1.0578E+03	1.2747E-01	1.2761E-01	18.7657
83	4.0289E-03	5.6106E+04	1.7706E+12	1.0049E+03	1.2119E-01	1.2134E-01	17.9052
84	4.1112E-03	6.3839E+04	1.5682E+12	9.4420E+02	1.1561E-01	1.1578E-01	17.1634
85	4.1958E-03	7.1906E+04	1.3781E+12	8.7614E+02	1.1069E-01	1.1087E-01	16.4740
86	4.2838E-03	8.0019E+04	1.1752E+12	7.8935E+02	1.0592E-01	1.0610E-01	15.7941
87	4.3779E-03	8.8254E+04	8.9535E+11	6.4780E+02	9.9744E-02	9.9969E-02	14.9902
88	4.4879E-03	9.7832E+04	6.6245E+11	5.1184E+02	9.4615E-02	9.4829E-02	14.9028
89	4.6204E-03	1.0677E+05	3.8528E+11	3.2696E+02	8.7550E-02	8.7923E-02	14.7853
90	4.8144E-03	1.2566E+05	1.2441E+11	1.2224E+02	7.7352E-02	7.8078E-02	14.6178